NASA Technical Memorandum 109157

92 P

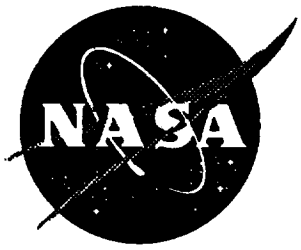

16-Foot Transonic Tunnel Test Section Flowfield Survey

J. A. Yetter and W. K. Abeyounis
Langley Research Center, Hampton, Virginia

December 1994

National Aeronautics and
Space Administration
Langley Research Center
Hampton, Virginia 23681-0001

SUMMARY

A flow survey has been made of the test section of the NASA Langley 16-Foot Transonic Tunnel at subsonic and supersonic speeds. Local test section upflow and sideflow angles and Mach number were measured to determine the flowfield characteristics of the empty test section. The survey was performed using five five-hole pyramid-head probes mounted at 14 inch intervals on a survey rake. Probes were calibrated at freestream Mach numbers from 0.50 to 0.95 and from 1.18 to 1.23. Test section flowfield surveys were made at Mach numbers from 0.50 to 0.90 and at Mach 1.20. Flowfield surveys were made at tunnel stations 130.6, 133.6 and 136.0. By rotating the survey rake through 180 degrees, a cylindrical volume of the test section 4.7 feet in diameter and 5.4 feet long centered about the tunnel centerline was surveyed.

Results show that the test section flowfield is characterized by upflow and sideflow components that diverge away from the tunnel centerline, with an apparent clockwise swirl when viewed looking upstream. The flow divergence away from the centerline is attributed to the test section slotted walls. In the survey volume, local flow angles vary little in the longitudinal axis. At subsonic speeds, in the vertical plane through the tunnel centerline, upflow angles vary from about -0.3 degree at the lower edge of the survey area to about +0.9 degree along the upper edge, with a nominal upflow angle of about +0.1 degree along the tunnel centerline. In the horizontal plane through the tunnel centerline, sideflow angles (positive toward the inner wall of the tunnel circuit) vary from about -0.7 degree on the outside edge of tunnel circuit (left side of test section) to about +0.8 degrees along the inside edge of circuit, with a sideflow angle of about +0.1 degree along the tunnel centerline.

At supersonic speeds the test section flowfield is more complex than at subsonic speeds. The flow exhibits a clockwise swirl with localized regions of larger flow angles. The overall variation in the measured upflow and sideflow angles across the entire survey area is about 1 degree. The nominal upflow and sideflow angles along the tunnel centerline are about 0.15 degrees.

The measured local Mach number distributions show a uniform Mach number distribution over the portion of the test section surveyed.

INTRODUCTION

A test section flowfield survey was performed as part of the 1991 16-Foot Transonic Tunnel calibration. Local test section flow angle and Mach number measurements were made with a set of five-hole pyramid-head flow angularity probes. The test effort consisted of individual probe calibrations, followed by flowfield surveys of the test section at three tunnel stations and Mach numbers from 0.50 to 1.20.

This report documents the survey probe calibration techniques used, summarizes the procedural problems encountered during testing, and identifies the data discrepancies observed during the post-test data analysis.

The report outlines the approaches taken to adjust the measured flow angle data for apparent data discrepancies, establishes the level of uncertainty of the data, and presents the flowfield characteristics obtained. Recommendations for ways to improve data quality by reducing the test uncertainties are provided.

Nomenclature

m	Intercept of survey probe calibration curve fit
C_{P13}	Survey probe pressure coefficient
C_{P13}	Survey probe pressure coefficient = (ΔP13) / (P5 - Pavg)
C_{P24}	Survey probe pressure coefficient = (ΔP24) / (P5 - Pavg)
C_m	Mach number coefficient = (P1 + P2 + P3 + P4) / P5
m	Slope of survey probe calibration curve fit
M_l	Local probe Mach number (from probe Mach coefficient)
M_∞	Freestream Mach number
P1	Individual probe static pressure (12 o'clock position), psia
P2	Individual probe static pressure (3 o'clock position), psia
P3	Individual probe static pressure (6 o'clock position), psia
P4	Individual probe static pressure (9 o'clock position), psia
P5	Individual probe total pressure (center of probe tip), psia
Pa	Atmospheric pressure, psia
P_{avg}	Average survey probe pressure = (P1 + P2 + P3 +P4) / 4
Pt_∞	Tunnel freestream total pressure, psia
Ptank	Tunnel freestream static (plenum) pressure, psia
P_∞	Freestream static pressure, psia
TS	Tunnel Station, feet
Xg	Distance along gravity axis in longitudinal direction, feet
Yg	Distance along gravity axis in lateral direction, feet
Zg	Distance along gravity axis in vertical direction, feet
X_W	Distance along wind axis in longitudinal direction, feet
Y_W	Distance along wind axis in lateral direction, feet
Z_W	Distance along wind axis in vertical direction, feet
V_∞	Freestream velocity, ft/sec
α	Pitch angle, deg
β	Yaw Angle, deg
α_f	Upflow angle, deg
α_R	Vertical rake misalignment, deg
ΔP13	Differential probe pressure between P_1 and P_3, psid

$\Delta P24$ Differential probe pressure between P_2 and P_4, psid

ε_{α_v} Upflow error due to vertical misalignment, deg

$\varepsilon_{\beta v}$ Sideflow error due to vertical misalignment, deg

ε_v Vertical misalignment, deg

θ Upflow angle, deg

ψ Sideflow angle, deg

ϕ Survey rake roll angle (measured from vertical axis), deg

APPARATUS AND PROCEDURES

Test Facility and Instrumentation

Wind Tunnel and Model Support This investigation was conducted in the Langley 16-Foot Transonic Tunnel. The facility is a single return, continuous flow, atmospheric wind tunnel with a test section of octagonal cross-section. To provide transonic capability the test section has slots located at the corners of the octagon that vent the test section to a plenum surrounding the test section . The test section wall divergence is adjusted as a function of airstream Mach number to minimize the longitudinal static pressure gradient in the test section. Further information on the wind tunnel can be found in References 1 and 2.

As shown in figure 1, the flowfield survey rake was attached to an adjustable support sting that was mounted off the tunnel support strut. The support sting held the survey rake at the test section centerline at all pitch angles (during probe calibrations). The offset sting allowed the rake to be manually positioned at selected tunnel stations. The tunnel support strut provided the capability to roll the rake assembly using the strut head roll mechanism.

Flow Survey Rake Local flow angle measurements were made with five-hole pyramid-head flow angularity probes. A sketch of a probe is shown in figure 2. Each probe was instrumented with four static taps, one on each face of the pyramidal tip, and a total pressure tap at the apex. As shown in figure 3, the five probes were equally spaced at 14 inch intervals along the leading edge of a survey rake, providing a maximum survey radius of 28 inches about the tunnel centerline. A photograph of the survey rake installed in the 16-Foot Transonic Tunnel is shown in figure 4.

Instrumentation A schematic of the instrumentation setup used for each probe is shown in figure 5. Individual pressure transducers were used to measure the probe static pressures at orifices 1 and 2 (P1 and P2), the pressure difference between opposing pressure orifices 1 and 3 ($\Delta P13$) and orifices 2 and 4 ($\Delta P24$), and the probe stagnation pressure at orifice 5 (P5). The absolute pressures P3 and P4 were computed from the opposing pressure and differential pressure measurements. Instrumented as such, two orthogonal flow angles were measured with each probe; the flow angles being proportional

to the pressure difference between the opposing pressure orifices. The survey probe pressure transducers were sized to provide the best accuracy at subsonic and supersonic speeds.

The survey rake was instrumented with a pitch angle transducer mounted parallel to the offset sting (i.e. horizontal when the rake is leveled) on the back of the wedge shaped forward sting strut. The survey rake pitch angle was measured in the vertical (gravity) plane. The transducer was calibrated with the rake oriented vertically and with the rake rolled to the horizontal to account for any variations that might occur as a result of rolling the rake.

Probe Calibration Procedures

Probe calibrations were performed at Mach numbers from 0.50 to 0.95 and from Mach 1.18 to 1.23. The procedure for calibrating the probes consisted of varying the rake pitch angle from at least -3 to +3 degrees while the rake was oriented vertically (as shown in figure 4). The probes were installed at fixed roll positions. The components of each probe were calibrated by rolling the individual probes in 90 degree increments relative to the rake, until each orthogonal component was run in an upright and inverted position.

A typical variation in the measured probe pressures with pitch angle is shown in figure 6. Over the pitch angle range shown, the variation in the individual static and differential static pressures are linear, with little variation in total pressure.

Probe sensitivities which relate the measured pressures to local flow angles were computed from the calibration results. The probe sensitivities are defined as:

Cp_{13} = Pressure coefficient based on probe pressures P1 & P3,

$$Cp_{13} = (\Delta P13) \; / \; (P5 - Pavg)$$

Cp_{24} = Pressure coefficient based on probe pressures P2 & P4,

$$Cp_{24} = (\Delta P24) \; / \; (P5 - Pavg)$$

where $Pavg = (P1 + P2 + P3 + P4) \; / \; 4$

With the probes properly installed in the survey rake, orifices 1 and 3 measure flow angles in the plane of the rake. Orifices 2 and 4 measure flow angles perpendicular to the rake. In the subsequent discussions, these two flow components are referred to as the "parallel" and "perpendicular" flow angles. The corresponding probe sensitivities are also referred to as "parallel" and "perpendicular" sensitivities.

Figure 7 (taken from Reference 3) shows the characteristics of the survey probe pressure coefficient as a function of probe pitch angle for a probe in an upright and inverted position. The slope and point of intersection of the two pressure coefficient (Cp) distributions determine the probe calibration sensitivities. By definition, the slope of the upright and inverted calibration curves should be equal, but opposite in sign. The point of intersection establishes the local upflow angle; the vertical offset is attributed to the probe

misalignment. An example of the probe calibration characteristics obtained for the current test is shown in figure 8. A summary of the calibration results showing the computed slopes, vertical offsets and upflow angles are presented in Tables I and II for the parallel and perpendicular components, respectively. The quantity defined as the percent difference in slope is an indication of the repeatability of the upright and inverted calibrations. A five percent difference is equivalent to an uncertainty of about 0.05 degrees at a local flow angle of 1 degree. Since the measured flow angles are typically less (smaller than 1 degree) the effect of the difference in slope is less than the measurement capability of the probe. Results obtained with probes whose difference in slope is large (i.e. probe 2 and the supersonic calibrations) have been taken into consideration as to how these results fit into the overall trends.

Local tunnel upflow and sideflow angles are presented in the wind axis convention shown in figure 9 (taken from Reference 4). All flow angle data is presented as if viewed looking downstream, with positive upflow angles directed upward and positive sideflow angles directed to the left (toward the inside of the tunnel circuit).

Survey probe Mach number coefficients (C_m) were computed from the probe calibration results and used in the table look-up routine to determine the local probe Mach number and the corresponding local flow angle.

Measurement Accuracy and Data Reduction Problems

Measurement uncertainty in the local flow angles can be attributed to the following factors:

1. Pressure measurement error
2. Rake pitch angle measurement error
3. Sting and rake misalignment
4. Rake lift induced flow angles

The significance of each of these factors and what adjustments were made during the data reduction process are addressed below.

Pressure Measurement Errors As discussed above, the local flow angles are directly proportional to the difference in pressure measured across the probe. Any uncertainty in the pressure measurements has a direct impact on flow angle uncertainty. An uncertainty analysis was performed to assess the effect of pressure measurement uncertainty on the flow angle uncertainty. The uncertainty in the pressure measurement is typically quoted at 0.5 percent of the transducer range. On this basis, the uncertainty in flow angle as a result of pressure measurement uncertainty is less than 0.03 degrees at all Mach numbers.

The most significant problem encountered during the test was the time required for the survey probe pressures to settle after a change in test condition (i.e. Mach number, angle of attack or rake roll angle). The small orifices (.020 dia.) at the tip of the survey probe and long tube runs between the tap and the pressure transducer (approximately 130 feet of tubing

increasing in size from 0.040 to 0.060 inch diameter) made the settling time of the probe pressures significant. The time required for the pressures to settle out typically ranged 4 to 5 minutes at each test point. The extent of the data base acquired was therefore limited by the available test time.

Sting Misalignments Prior to each run, the sting was leveled using an inclinometer mounted on the cylindrical portion of the sting, just behind the survey rake. Due to procedural problems in positioning the inclinometer consistently on the sting, discrepancies occurred in leveling the sting prior to each run. These discrepancies were corrected by using the pitch angle transducer as an absolute instrument.

Sting deflections during the flow survey due to aerodynamic loads were assumed to be negligible.

Calibrations of the pitch angle transducer were performed with the rake oriented vertically and while rolled to the horizontal. The two calibrations were essentially the same, indicating that the measured rake pitch angle should therefore be independent of rake roll angle.

The variation in wind-off rake pitch angle with survey rake roll angle (ϕ) is shown in figure 10. The increase in rake angle of attack at roll angles above 90^{o} suggests that the pitch angle variation is not due to the sting deflections alone. The sinusoidal variation in pitch angle indicates that the pitch angle transducer and/or the sting is not aligned with the main tunnel support strut roll axis. The result is a conical motion about the strut roll axis as the rake is rolled. An independent strut head pitch angle measurement indicated that a vertical sting misalignment and/or deflection did exist, since the main tunnel strut head had to be set at an angle of attack of about 0.19 degree to level the sting at the survey rake. This difference was originally attributed solely to sting deflections due to the weight of the survey rake. However, the variation in the measured pitch angle with roll angle suggests that this is in part a rigid misalignment problem, and not only a result of sting deflections. Sting deflections alone would not vary with roll angle, except for minor sting/strut torsional deflections which would be a maximum at a 90 degree roll angle.

The variation in the measured pitch angle (figure 10) provides information from which to estimate the misalignment characteristics. Since the sting is leveled at $\phi = 0^{o}$, the pitch angle error (in vertical direction) is assumed to be zero. The measured pitch angle at $\phi = 180^{o}$ is the error due to the vertical misalignment (~ 0.2 degree). The approach used to describe the motion of the survey rake in the vertical and lateral directions, as the rake is rolled, is shown in figure 11. Since the sting rotates about the strut centerline the apparent motion of the rake center is circular. As shown in figure 12a, applying these adjustments for a vertical misalignment to the measured pitch angle data does not fully account for apparent pitch angle error at $\phi = 90^{o}$ (rake horizontal). An additional adjustment is required.

Since the negative peak in pitch angle occurs at $\phi \approx 65^{o}$ in figure 10, the rake installation also has a lateral misalignment, the magnitude of which can be inferred from the pitch angle error remaining after the rake is rolled to the horizontal ($\phi = 90^{o}$) and the vertical misalignment adjustments are applied. The approach used to describing the motion of the rake center position as a result of a lateral misalignment is shown in figure 13. After applying adjustments for the vertical misalignments the apparent error in pitch angle due to a lateral misalignment is about 0.18 degree.

The validity of this approach is apparent when the adjustments for vertical and lateral misalignments are applied to the measured rake pitch angle. As shown in figure 12b, subtracting the adjustments due to the vertical and lateral misalignments from the measured rake pitch angle leaves a near zero condition at all roll angles. The validity of these adjustments to sideflow cannot be established since no measurements were made to check for sting misalignment in this direction. The magnitude of the corresponding lateral adjustments are shown in figure 14. The combined effect of the adjustments for vertical and lateral sting misalignment is as much as 0.2 degree at a rake roll angle of 150^{o}.

It should be noted that the discrepancies referred to as a sting misalignment is the result of numerous factors. The adjustments applied above only account for the most obvious. The inability to account for all of the discrepancies only serves to emphasize the complexity of the sting deflections and misalignments involved.

It has been shown that the measured survey rake pitch angle effectively accounts for the vertical and lateral misalignments in the vertical direction at all roll angles. In the subsequent discussions, the effect of sting misalignment on the measured upflow angle has been accounted for by subtracting the measured nonzero survey rake pitch angle from the measured upflow angle. Since direct measurement of rake lateral position was not made, the adjustments to sideflow have been made by subtracting the estimated vertical and lateral misalignment errors (figure 14) from the measured sideflow angles.

The design of the sting provides for repositioning the rake by sliding the sting forward or aft in the saddle located at the aft sting strut (see figure 1). This capability introduces the potential for variation in the sting misalignment adjustments with sting extension. A check of the misalignment characteristics at the forward survey position (TS 130.6) showed that the required adjustment did indeed change, with the discrepancies associated with the sting misalignment increasing with sting extension. The misalignment adjustments applied as a function of the tunnel station (TS) are summarized below:

Adjustments for Sting Misalignment

TS	Vertical	Lateral
130.6	0.18 deg	-0.25 deg
133.6	0.13	-0.22
136.0	0.09	-0.20

With the sting extended to the forward most survey position, and a lateral misalignment angle of 0.25 degree, the displacement in the actual center probe location from the nominal centerline location is less than 0.6 inches (1/20th of the spacing between the probes). In the subsequent discussions, since the probe displacement is relatively small, no attempt has been made to track the repositioning of the probe due to the sting misalignments. All reference to probe position are made with respect to their nominal (aligned) locations.

Adjustments for Rake Lift Previous pyramid probe calibrations performed in the NASA Langley 7 x 10 Foot Tunnel and documented in Reference 3 indicated that flow angles measured perpendicular to the rake plane of symmetry could be affected by rake lift, or by the rake inducing a flow angle at the probe tip which varies with angle of attack. A check of the effect of rake lift on the probe sensitivities was made by varying the rake pitch angle with the rake rolled to the horizontal. A comparison of the probe sensitivities (calibration slopes) obtained with the rake vertical (no lift) and with the rake horizontal (with lift) is shown in figure 15. The comparison confirms that the probe sensitivities are indeed affected by the rake lift, as evidenced by the increase in slope of the calibration curve when the rake is horizontal.

Since the lift induced flow angle increments occur only in the plane perpendicular to the rake spanwise plane of symmetry, only the perpendicular probe sensitivities need to be adjusted for rake lift effects. The probe calibration data presented in reference 3 were used to establish corrections for the perpendicular probe sensitivities. The data provided an adjustment increment as a function of Mach number and probe spanwise position on the rake. The correction for rake lift represents an increment in the probe calibration sensitivity (slope), the vertical offset not being affected. A plot of the spanwise variation in the difference between the rake vertical (no lift) and rake horizontal (with lift) probe sensitivities (calibration curve slopes) at M = 0.80 is shown in figure 16. The corresponding differences extracted from Reference 3 are also presented for comparison. The trends show a symmetric spanwise variation which is consistent with the expected survey rake lift distribution, the probe at the center of the rake requiring the largest adjustment.

During the current investigation, the data required to identify the rake lift effects on the perpendicular probe sensitivities were only obtained at Mach 0.80. As shown in figure 17, the data from Reference 3 indicates that the effect of rake lift is a function of Mach number, as well as the spanwise position. These data were therefore used to establish the necessary rake lift adjustments at other subsonic Mach numbers. Assuming spanwise symmetry, a nominal probe sensitivity increment was established from the available data base. A cross-plot of the variation in the sensitivity increment with Mach number is presented in figure 18. The trends show that at Mach numbers below about 0.7 the effect of rake lift on probe sensitivities is nearly constant. Above Mach 0.7 the effect of rake lift decreases with Mach number. The available data from the current test (symbols at M = 0.80) were used to adjust these trends and extrapolations to Mach 0.95 were made. No rake lift adjustments were made to

the supersonic calibration data. The actual increments applied to the perpendicular probe calibration slopes are listed in Table II.

It should be noted that since the measured flow angles are relatively small, the lift induced flow angles are also small. Local flow angle uncertainties introduced by the approach outline above are therefore expected to be minimal.

Rake Misalignment An example of the variation in measured upflow and sideflow angles with rake roll angle is shown in figure 19. The data are presented for the centerline probe (no. 3) at Mach 0.80 and TS 133.6. The adjustments for sting misalignment and rake lift have been applied. The dashed lines represents the nominal zero rake lift condition for each flow angle component. Since the centerline probe remains in the approximately the same position as the rake is rolled, the measured upflow and sideflow angles should be constant if the proper sting misalignment and rake lift induced flow angle adjustments have been applied. This obviously is not the case. The variation in upflow angle indicates an effective increase in the probe angle of attack as the rake rolls through $\phi = 90^{o}$. The upflow angle then returns to nearly the same flow angle at $\phi = 180^{o}$. The sideflow angle decreases as the rake rolls through $\phi = 180^{o}$. These trends are indicative of a misalignment between the probe axis and the support sting. In effect, the axis of the survey probe is not aligned with the axis of the sting.

Since the angle of attack measurement was shown to correctly account for sting misalignment in the vertical direction, and individual probe misalignments in the plane of rake spanwise symmetry were effectively accounted for with the probe calibrations, these discrepancies are attributed to a rake to sting misalignment which effectively changes the probe upflow and sideflow angle as the rake rolls. As such, the rake misalignment correction to upflow is zero when the rake is vertical. It should be noted that the relatively large magnitude of the apparent upflow discrepancy is greater than what is thought to be the capability of the flow angle measurement, and the consistent character of the upflow trends with roll angle (gradual increase and decrease) suggests that the discrepancies are not due to a random measurement error.

As noted above the survey probe calibrations account for any probe to sting misalignment in the vertical direction (in rake spanwise direction at $\phi = 0^{o}$ and 180^{o}). The effect of rake misalignment therefore exists only in the lateral direction. The approach used to correct for rake lateral misalignment is outline in figure 20. The adjustments for rake misalignment can only be obtained from the wind-on test results. The data presented in figure 19 were used to establish that the apparent magnitude of the rake misalignment, based on the upflow angle variation, is about 0.20 deg. However, as shown in figure 21, after adjustments are made for the rake lateral misalignment, the adjusted upflow and sideflow angles still exhibit some variation with rake roll angle. This suggests that the combined sting and rake misalignments are more complex that the simple misalignments assumed above. However, the necessary sting and rake alignment data needed to resolve these problems is not available.

Since no changes were made in the probe to sting installation during the test (i.e. not disassembled), the rake misalignment adjustment factor was assumed to be independent of sting extension (i.e. tunnel station).

The variation in the center probe upflow and sideflow angles after applying all adjustments for sting and rake misalignments and rake lift effects provides a level of uncertainty for the individual flow angle measurements. Based on the results shown in figure 21, the uncertainty in the measured upflow angle is less than 0.05 degree. The uncertainty in sideflow angle could be as large as 0.15 degree when the rake is oriented vertically ($\phi = 0^o$ and 180^o), but drops to less that 0.05 degree when the rake is oriented horizontally ($\phi = 90^o$), the sideflow angles actually being measured by the parallel taps.

Other Sources of Data Discrepancies In addition to the sting and rake misalignment problems discussed above, additional discrepancies in the individual probe data were encountered that can be attributed to such things as bent probes, improper probe installation, and unsettled pressures.

The characteristics of a bent probe on the individual probe calibration is shown in figure 22. The number 5 probe (at the bottom of rake) was bent when it was inadvertently bumped by a technician. The bending of a probe (after the calibration process had begun) is characterized by a shift in the calibration curves without a change in slope or indicated upflow angle. This represents a change in the probe alignment relative to the sting and is accounted for by shifting the probe calibration.

Inconsistencies in the probe calibration characteristics between individual calibration runs are attributable to an improperly installed probe. The survey rake is designed such that each probe is held in place with a set screw. If the probe is not installed properly a change in the probe alignment can occur. The effect of an improper probe installation on the probe calibration is shown in figure 23. The data show good repeatability except for Run 7. The slope and linearity of the data is nearly the same, except that Run 7 shows a small shift. Although the shift is characteristic of a bent probe, the repeatability of the runs made after Run 7 indicate that the discrepancy is not a result of the probe being bent.

As mentioned previously, the probes have small orifices in the tip and long instrumentation tubing runs (a relatively large volume) which resulted in significant settling times for the pressure measurements. The effect of taking data before the pressures were settled is shown in figure 24. The repeatability and linearity of the calibration data is adversely affected. During the post test data analysis each data point was evaluated with respect to the overall calibration trends. Data that was felt to exhibit any of the above discrepancies were deleted from the individual probe calibration data base.

Finally, it should be noted that uncertainties introduced by the apparent sting and rake misalignments affect only the absolute magnitude of the measured flow angles. This in effect is an uncertainty in the magnitude of the reference flow angle, defined as that flow angle measured along the test section

centerline. The differences between the flow angles measured on the centerline and those measured at the outboard rake locations is still indicative of the vertical and lateral variations that exist across the test section.

RESULTS AND DISCUSSIONS

Tunnel Centerline Axes Flow Angle Characteristics

Upflow Angles based of Survey Probe Calibrations As discussed in the Apparatus and Procedures section, test section upflow angles were obtained directly from the survey probe calibrations. Upflow angles measured at TS 133.6, in the vertical plane passing through the tunnel centerline, are shown in figure 25, for freestream Mach numbers from 0.50 to 1.23. Two sets of data are presented, one based on pressures P1 and P3, the other based on pressures P2 and P4 (see figure 5). In each case, the rake is vertical ($\phi = 0^o$) and the individual probes have been rolled to align the taps with the rake spanwise plane of symmetry (no rake lift effects). The data show that the upflow angles are largest at locations off the tunnel centerline. At a position 2.3 feet above the tunnel centerline the upflow angles are about +0.55 degree at Mach numbers below about 0.85, increasing to about +0.90 degree at Mach 0.95. Along the tunnel centerline the upflow angle is nearly zero at the lower subsonic Mach numbers and increases to about +0.10 degree at Mach 0.95. Below the centerline the upflow angle is about -0.20 degree at Mach numbers below 0.85, with the flow angle diverging away from the centerline at higher Mach numbers. The data show good correlation between the two probe components at all Mach numbers, providing a relative accuracy for the flow angle measurements and confidence in the probe calibrations. The differences are typically smaller than the nominal upflow angle at each spanwise location.

The flow divergence away from the tunnel centerline is attributed to the effects of the slotted test section. The increase in upflow angle at locations off the tunnel centerline at Mach numbers above 0.80 is consistent with the variation in the test section wall (flat) divergence angle at high subsonic Mach numbers. In the 16-foot tunnel, flat divergence is used at Mach numbers above 0.83 to achieve a zero centerline Mach gradient ($dM/dx = 0$). The variation in wall flat divergence with Mach number is shown in figure 26. The variation in the upflow angles with Mach number is attributed in part to the variation in tunnel wall divergence angle.

Upflow angle characteristics at supersonic speeds are also shown in figure 25. The local supersonic upflow angles varies from about +0.15 degree above the centerline to about +0.35 degree below the centerline. The predominant flow direction is towards the top of the test section. This may in part be attributable to the fact that at supersonic speeds the test section air removal system is operating and some flow asymmetry may result from the air removal process.

Flowfield Survey Locations Test section flowfield surveys were made over a circular cross section of the tunnel by rotating the survey rake from the vertical through 180 degrees. Local flow angles were measured parallel and perpendicular to the rake and then resolved to the tunnel wind axis coordinate

system. Flowfield surveys were made with the rake positioned at tunnel stations 130.6, 133.6 and 136.0. A sketch showing the rake roll angle increments used at each survey location is shown in figure 27. Tunnel station 134.0 is considered the longitudinal center of the test section. The survey at tunnel station 136.0 was limited to a maximum rake roll angle of 142° because of interference between the retracted sting and the main tunnel support strut.

Upflow Angles Based on Roll Surveys The variation in test section upflow angles along the vertical centerline at TS 130.6, 133.6 and 136.0 and Mach 0.80 are shown in figure 28. The upflow angles were measured with the parallel taps (P1 and P3). The comparison of local upflow angles obtained with the rake at $\phi = 0^{o}$ and rolled to $\phi = 180^{o}$ shows that the flow angle resolution procedure correctly accounts for the probes being inverted. The comparison shows good agreement between the measured flow angles at either rake roll angle. The flow angles measured at TS 133.6 show good agreement between the probe calibration results presented in figure 25.

The variation in the test section upflow angles with Mach number at TS 130.6, 133.6, and 136.0 are shown in figure 29. The upflow data are those measured along the vertical centerline with the rake positioned at $\phi = 0^{o}$ and $\phi = 180^{o}$. In general, the upflow angles trends at all tunnel stations are similar to those obtained with the probe calibrations. Along the centerline, the local upflow angle is typically about 0.10 degree, increasing to about +0.40 degree 1.2 feet above the centerline, and -0.20 degree 1.2 feet below the centerline. At all tunnel stations, the local upflow angles at a distance of 2.3 feet from the centerline exhibit an increase in the flow divergence away from the test section centerline at Mach numbers above 0.80. The apparent differences between the probe calibration results (figure 29b) and the flow surveys are within the flow angle uncertainties previously established.

The variation in upflow angle with tunnel station is shown in figure 30 for Mach 0.6, 0.8 and 0.9. The trends are consistent with those presented in figure 28 and show that there is little variation in upflow angle in the tunnel streamwise (longitudinal) direction.

Sideflow Angles Based on Roll Surveys Test section sideflow angles measured across the horizontal plane containing the tunnel centerline were obtained using local flow angles measured by the parallel taps (P1 and P3) with the rake rolled to the horizontal ($\phi = 90^{o}$). As such, the parallel taps lie in the plane of rake spanwise symmetry and are not affected by rake lift. (The measured sideflow angles have been adjusted for probe and sting misalignments.) The sideflow characteristics at TS 130.6, 133.6 and 136.0 are shown in figure 31. The data show that the tunnel sideflow angle is about +0.1 degree at the center of the tunnel, with the flow diverging away from the center at locations off of the test section centerline. At the outermost probe location (2.3 feet off the centerline) the local sideflow angles are as large as (+/-) 0.90 degree.

Supersonic sideflow angles are also shown in figure 31. In general, the largest supersonic sideflow angles are observed on the left side of the test section (looking downstream) closest to the point where the test section air removal

takeoff ducting is located. The sideflow angles on the outside of the tunnel circuit (right) are small and tend to diverge away from the centerline at the downstream station.

A cross-plot of the subsonic sideflow angles at each tunnel station and at Mach 0.6, 0.8 and 0.9 is presented in figure 32. The data show that the variation in sideflow angle across the horizontal (lateral) centerline is nearly linear, with a gradient of about 0.3 degree per foot. Along the tunnel centerline the sideflow and is about 0.1 degree. In the direction towards the inside of the tunnel circuit (+Y), the sideflow angle increases to an average of about +0.80 degree at a location 2.3 feet from the centerline. Towards the outside of the tunnel circuit (-Y), the sideflow angle increases to average of about -0.70 degree, directed away from the centerline at each station. The variation in sideflow angles with tunnel station is small.

Subsonic Flowfield Contours

Test section upflow and sideflow angle contours are presented for tunnel stations 130.6, 133.6 and 136.0 in figures 33, 34 and 35, respectively. At each tunnel station the local flowfield characteristics are presented for Mach numbers 0.6, 0.8 and 0.9. The data are presented in the wind axes (see figure 9) as if viewed looking downstream through the test section. In general, the flowfield characteristics are similar at all tunnel stations and Mach numbers. The streamwise variation (with tunnel station) of the local flow angles is small. The upflow contours exhibit a line of symmetry (zero upflow angle) extending diagonally across the test section from about 10 o'clock ($\phi = -60^{o}$) to 4 o'clock ($\phi = 120^{o}$) . The sideflow contours are symmetrical about a vertical line located slightly to the right (-Y direction) of the vertical centerline. In each case, the flowfield is characterized by an increase in the local upflow and sideflow angles in a direction perpendicular to the respective lines of symmetry.

The magnitude of the local flow angles away from the center of the test section increases with Mach number. This increase is characterized by the larger flow angles measured at the outside edge of the survey area and a tightening of the flow angle contours at Mach 0.9. As mentioned above, this trend is attributed to the effect of an increase in test section wall divergence at Mach numbers above 0.83.

The flowfield vectors shown for the Mach 0.8 conditions (parts c and d of figures 33 through 35) are indicative of the relative magnitude of the test section crossflow components and indicate that the upflow and sideflow contours are characteristic of an asymmetric swirl about the tunnel centerline. The largest crossflow components exist in the lower left quadrant of the test section.

Supersonic Flowfield Characteristics

The variation in upflow and sideflow angles measured with the center probe (no. 3) at Mach 1.20 is shown in figure 36. The data have been adjusted for

misalignments and are shown for the forward two tunnel stations at which the supersonic flow surveys were made. These data are presented to establish a relative uncertainty in the flow angle measurements. Although the data show repeatable variations in both upflow and sideflow angles as the rake rolls, the overall variation in the upflow and sideflow angles is 0.20 and 0.30 degree, respectively.

The variation in the Mach 1.20 upflow and sideflow angles along the vertical plane containing the tunnel centerline (rake vertical) at $\phi = 0^{o}$ and 180^{o} is presented in figure 37. The trends show good correlation in the upright and inverted rake data at the outermost and center probe locations. The differences in the measured flow angles at tunnel stations 130.6 and 133.6 are small. However, at the locations 1.2 feet from the centerline the upright and inverted measurements differ significantly. This suggests a measurement problem with either probe no. 2 or probe no. 4. A similar set of data is presented in figure 38 for the condition where the rake is rolled to the horizontal ($\phi = 90^{o}$). The no. 4 probe sideflow angle measured with the rake vertical, and the upflow angle measured with the rake horizontal, indicates that the flowfield has a clockwise swirl component (looking downstream). This is contrary to the flowfield established by the other probes and is inconsistent with the previous observed subsonic flowfield characteristics.

To provide a data base from which to develop the supersonic flowfield contours the no. 4 probe was assumed to have been bent or installed incorrectly, thereby introducing an offset in the measured flow angle which would have to be accounted for. Adjustments based on the no. 2 probe data were made to probe no. 4 flow angles to account for this discrepancy. The magnitude of this adjustment is apparent in figures 37 and 38. The flowfield contours presented in figure 39 include this adjustment.

At TS 133.6 the flowfield survey was made at 15 degree increments in rake roll angle. At TS 130.6 the survey was made at 30 degree increments. As shown in figures 37 and 38, the differences in the measured flow angles at tunnel stations 130.6 and 133.6 were small. The local upflow and sideflow angle contours shown in figure 39 are therefore representative of the flowfield characteristics which exist at both tunnel stations. In general, the supersonic contours have symmetry characteristics which are similar to the subsonic contours. Except for that portion of the survey area at about 6 o'clock ($\phi = 180^{o}$), the supersonic flowfield also exhibits a counterclockwise swirl similar to that seen at subsonic speeds. The supersonic contours also include two localized regions of high flow angles that were not observed at the subsonic conditions. The existence of apparent pockets of complex flow is not readily explainable other than to acknowledge that the magnitude of the differences in flow angles is less than the measurement uncertainty discussed above. The overall variation in measured upflow angles over the entire test section survey area is about 0.8 degrees (+0.4 to -0.4 degree). The maximum sideflow angle measured is +0.6 degrees, leading to an overall variation of about 1 degree across the test section survey area (+0.6 to -0.4 degree).

Tunnel Centerline Axes Mach Number Distributions

As indicated in the probe calibration section a local Mach number is determined for each probe at each survey location. Test section Mach number distributions are presented below in terms of a local Mach number increment defined as the difference between the freestream Mach number (M_∞) and the local probe Mach number (M_l).

The variation in the local Mach number increment along the vertical and horizontal (lateral) centerlines at TS 130.6, 133.6 and 136.0 are shown in figure 40 and 41, respectively. Along the vertical centerline the local Mach number increments are presented for the rake upright ($\phi = 0^o$) and inverted ($\phi = 180^o$). Cross-plots of the local Mach number increments at freestream Mach numbers of 0.6, 0.8 and 0.9 and the three tunnel stations surveyed are shown in figures 42 and 43 for the vertical and horizontal centerlines respectively. Although the incremental Mach numbers are predominately negative, varying from a nominal -0.002 at low subsonic Mach numbers to about -0.005 at the near sonic conditions, the variation across the survey area are typically small. In general, these data indicate a uniform subsonic Mach number distribution over the portion of the test section survey. At supersonic speeds the general trend is for positive Mach number increments.

CONCLUDING REMARKS

A flowfield angularity survey has been made of the test section of the NASA Langley 16-Foot Transonic Tunnel. At subsonic speeds the overall flow angle trends indicate a flowfield that diverges away from the tunnel centerline, with a counterclockwise swirl (looking downstream) about the center of the test section. The magnitude of the local flow divergence increases with an increase in test section wall divergence for Mach numbers greater than 0.83. The longitudinal variation in flow angles from tunnel stations 130.6 to 136.0 is small.

At subsonic speeds the test section upflow angles vary from about -0.3 degree below the tunnel centerline to about +0.9 degree above the centerline, with a nominal upflow angle along the centerline of about +0.1 degree. Sideflow angles vary from about -0.7 degree at the outside of the test section (away from the tunnel circuit center) to about +0.8 degree at the inside of the tunnel circuit, with a sideflow angle of about +0.1 degree at the tunnel centerline. For a model located on the test section centerline, the nominal upflow and sideflow angle at subsonic speeds is about 0.10 degree.

At supersonic speeds the test section flowfield exhibits a counterclockwise swirl, with regions of localized high flow angles contributing to a more complex flowfield than that observed at subsonic conditions. The overall variation in the measured upflow and sideflow angles across the entire survey area was about

1.0 degree. For a model located on the test section centerline, the nominal upflow and sideflow angles at Mach 1.20 is about 0.15 degree.

The local incremental test section Mach number distributions show a uniform Mach number distribution over the portion of the test section surveyed.

The data discrepancies observed during the data analysis indicate that a more detailed installation check must be made to quantify the actual sting and rake misalignments, and to establish, with an acceptable degree of accuracy, the position and alignment of the survey probes relative to the test section centerline. A repeatable probe installation procedure is also required and care must be taken to protect probes from being bent.

NASA Langley Research Center
Hampton, VA 23681-0001
December, 1994

REFERENCES

1. Corson, Blake W., Jr.; Runckel, Jack F.; and Igoe, William B.: Calibration of the Langley 16-Foot Transonic Tunnel With Test Section Air Removal. NASA TR R-423, 1974.

2. Staff of the Propulsion Aerodynamics Branch: A User's Guide to the Langley 16-Foot Transonic Tunnel Complex, Revision 1. NASA TM-102750, 1990.

3. Smith, L.; and Adcock, J. : Effect of Reynolds Number and Mach Number on Flow Angularity Probe Sensitivity. NASA TM 87750, September 1986

4. Mercer, C. E.; Berrier, Bobby L.,; Capone, Francis J.; Grayston, Alan M.; and Sherman, C. D.: Computations for the 16-Foot Transonic Tunnel - NASA Langley Research Center, Revision 1. NASA TM-86319, 1987.

Table I. Flowfield Survey Probe Calibration Summary - Parallel Orifices

MACH NO.	PROBE NO.	PROBE UPRIGHT * RUN	SLOPE m	INTERCEPT b	Data Rating	PROBE INVERTED * RUN	SLOPE m	INTERCEPT b	Data Rating	ALIGNMENT FACTORS HORIZ'TL OFFSET	VERTICAL OFFSET	TUNNEL UPFLOW deg	Percent Difference in Slope	PROBE CALIBRATION ** Slope m	Intercept b
0.50	1	3	-0.05426	-0.0428	E	5	0.05500	0.0250	E	-0.621	-0.009	0.621	1.35	-0.05426	-0.009
	2		-0.04814	-0.0159	G		0.04812	0.0191	N	-0.364	0.002	0.364	-0.04	-0.04814	0.002
	3		-0.05170	0.0416	E		0.05289	0.0404	E	0.011	0.041	-0.011	2.28	-0.05170	0.041
	4		-0.05410	0.0153	E		0.05453	-0.0056	E	0.192	0.005	-0.192	0.79	-0.05410	0.005
	5		-0.05073	0.0036	E		0.04996	0.0465	E						
	Adjusted for bent no. 5 probe:														
	5'		-0.05073	0.0720		5	0.04996	0.0465		0.253	0.059	-0.253	-1.53	-0.05073	0.059
0.60	1	2	-0.05414	-0.0463	E	5	0.05508	0.0235	E	-0.639	-0.012	0.639	1.72	-0.05414	-0.012
	2		-0.04608	-0.0319	G		0.04710	0.0184	N	-0.540	-0.007	0.540	2.19	-0.04608	-0.007
	3		-0.05236	0.0386	E		0.05218	0.0431	E	-0.043	0.041	0.043	-0.34	-0.05236	0.041
	4		-0.05515	0.0151	E		0.05414	-0.0054	E	0.188	0.005	-0.188	-1.85	-0.05515	0.005
	5		-0.04980	-0.0079	G		0.04979	0.0503	G						
	Adjusted for bent no. 5 probe:														
	5'		-0.04980	0.0593		5	0.04979	0.0503		0.090	0.055	-0.090	-0.02	-0.04980	0.055
	1	7	-0.05428	-0.0335	E	Use data from Run 5				-0.521	-0.005	0.521	1.46		
	2		-0.04694	-0.0191	G					-0.399	0.000	0.399	0.34		
	3		-0.05282	0.0363	E					-0.065	0.040	0.065	-1.22		
	4		-0.05479	0.0156	E					0.193	0.005	-0.193	-1.19		
	5		-0.04934	0.0622	E					0.120	0.056	-0.120	0.91		
	Apparent intercept shift (bent) in Probe 5, deg = 1.42														
0.70	1	3	-0.05516	-0.0436	E	5	0.05554	0.0242	E	-0.612	-0.010	0.612	0.69	-0.05516	-0.010
	2		-0.04622	-0.0155	N		0.04580	0.0137	N	-0.317	-0.001	0.317	-0.91	-0.04622	-0.001
	3		-0.05248	0.0445	E		0.05257	0.0473	E	-0.027	0.046	0.027	0.17	-0.05248	0.046
	4		-0.05487	0.0132	E		0.05436	-0.0080	E	0.194	0.003	-0.194	-0.93	-0.05487	0.003
	5		-0.04970	0.0019	E		0.04981	0.0489	E						
	Adjusted for bent no. 5 probe:														
	5'		-0.04970	0.0699		5	0.04981	0.0489		0.201	0.059	-0.201	0.22	-0.04970	0.059

Table I. Continued.

MACH NO.	PROBE NO.	RUN	PROBE UPRIGHT * SLOPE m	INTERCEPT b	Data Rating	RUN	PROBE INVERTED * SLOPE m	INTERCEPT b	Data Rating	ALIGNMENT FACTORS HORIZ'TL OFFSET	VERTICAL OFFSET	TUNNEL UPFLOW deg	Percent Difference in Slope	PROBE CALIBRATION ** Slope m	Intercept b
0.80	1	2	-0.05661	-0.0452	E	5	0.05630	0.0257	E	-0.628	-0.010	0.628	-0.55	-0.05661	-0.010
	2		-0.04462	-0.0303	S		0.04491	0.0090	S	-0.439	-0.011	0.439	0.65	-0.04462	-0.011
	3		-0.05331	0.0435	E		0.05309	0.0493	E	-0.055	0.046	0.055	-0.41	-0.05331	0.046
	4		-0.05622	0.0148	E		0.05612	-0.0062	E	0.187	0.004	-0.187	-0.18	-0.05622	0.004
	5		-0.04916	-0.0061	G		0.05097	0.0408	G						
	Adjusted for bent no. 5 probe:														
	5'		-0.04916	0.0602		5	0.05097	0.0408		0.194	0.051	-0.194	3.62	-0.04916	0.051
	Apparent intercept shift (bent) in Probe 5, deg = 1.42														
	1	7	-0.05671	-0.0312	E	Use data from Run 5				-0.503	-0.003	0.503	-0.73		
	2		-0.04386	-0.0209	S					-0.337	-0.006	0.337	2.37		
	3		-0.05363	0.0423	E					-0.066	0.046	0.066	-1.01		
	4		-0.05663	0.0166	E					0.202	0.005	-0.202	-0.90		
	5		-0.05056	0.0656	G					0.244	0.053	-0.244	0.81		
	1	27 & 32	-0.05749	-0.0436	E	29, 30 & 31	0.05698	0.0237	E	-0.588	-0.010	0.588	-0.89		
	2		-0.04255	0.0058	G		0.04376	0.0091	G	-0.038	0.007	0.038	2.80		
	3		-0.05223	0.0860	E		0.05177	0.0931	E	-0.068	0.090	0.068	-0.88		
	4		-0.05621	0.0061	E		0.05493	-0.0070	I	0.118	-0.001	-0.118	-2.30		
	5		-0.05592	0.0630	G		0.05470	0.0435	G	0.176	0.053	-0.176	-2.21		

Table I. Continued.

MACH NO.	PROBE NO.	RUN	PROBE UPRIGHT * SLOPE m	INTERCEPT b	Data Rating	RUN	PROBE INVERTED * SLOPE m	INTERCEPT b	Data Rating	ALIGNMENT FACTORS HORIZ'TL OFFSET	VERTICAL OFFSET	TUNNEL UPFLOW deg	Percent Difference in Slope	PROBE CALIBRATION ** Slope m	Intercept b
0.90	1	2	-0.05729	-0.0576	E	5	0.05761	0.0347	E	-0.803	-0.012	0.803	0.56	-0.05729	-0.012
	2		-0.04356	-0.0373	N		0.04366	0.0089	G	-0.530	-0.014	0.530	0.23	-0.04356	-0.014
	3		-0.05459	0.0416	E		0.05427	0.0521	E	-0.096	0.047	0.096	-0.59	-0.05459	0.047
	4		-0.05647	0.0150	E		0.05676	-0.0096	E	0.217	0.003	-0.217	0.51	-0.05647	0.003
	5		-0.05081	-0.0006	G		0.05155	0.0340	E						
	Adjusted for bent no. 5 probe:														
	5'		-0.05081	0.0679		5	0.05155	0.0340		0.332	0.051	-0.332	1.45	-0.05081	0.051
	Apparent intercept shift (bent) in Probe 5, deg = 1.42														
	1	3	-0.05726	-0.0549	E	Use data from Run 5				-0.780	-0.010	0.780	0.61		
	2		-0.04330	-0.0316	N					-0.466	-0.011	0.466	0.83		
	3		-0.05447	0.0449	E					-0.066	0.049	0.066	-0.37		
	4		-0.05677	0.0134	E					0.203	0.002	-0.203	-0.02		
	5		-0.05130	0.0092	E										
	Adjusted for bent no. 5 probe:														
	5'		-0.05130	0.0784		5	0.05155	0.0340		0.432	0.056	-0.432	0.49		
	Apparent intercept shift (bent) in Probe 5, deg = 1.23														
	1	7	-0.05734	-0.0461	E	Use data from Run 5				-0.703	-0.006	0.703	0.47		
	2		-0.04363	-0.0303	G					-0.449	-0.011	0.449	0.07		
	3		-0.05445	0.0422	E					-0.091	0.047	0.091	-0.33		
	4		-0.05780	0.0175	E					0.237	0.004	-0.237	-1.82		
	5		-0.05237	0.0736	E					0.381	0.054	-0.381	-1.58		
0.95	1	3	-0.05740	-0.0645	E	5	0.05826	0.0432	E	-0.931	-0.011	0.931	1.49	-0.05740	-0.011
	2		-0.04601	-0.0383	N		0.04442	0.0124	N	-0.561	-0.013	0.561	-3.52	-0.04601	-0.013
	3		-0.05540	0.0415	E		0.05567	0.0567	E	-0.137	0.049	0.137	0.49	-0.05540	0.049
	4		-0.05732	0.0169	E		0.05729	-0.0122	E	0.254	0.002	-0.254	-0.05	-0.05732	0.002
	5		-0.05110	0.0117	E		0.05089	0.0290	G						
	Adjusted for bent no. 5 probe:														
	5'		-0.05110	0.0806		5	0.05089	0.0290		0.506	0.055	-0.506	-0.41	-0.05110	0.055
	Apparent intercept shift (bent) in Probe 5, deg = 1.33														
	1	7	-0.05773	-0.0560	E	Use data from Run 5				-0.855	-0.007	0.855	0.91		
	2		-0.04324	-0.0358	G					-0.550	-0.012	0.550	2.69		
	3		-0.05536	0.0433	E					-0.121	0.050	0.121	0.56		
	4		-0.05764	0.0192	E					0.273	0.003	-0.273	-0.61		
	5		-0.05272	0.0821	E					0.512	0.055	-0.512	-3.53		

Table I. Concluded.

MACH NO.	PROBE NO.	PROBE UPRIGHT * RUN	SLOPE m	INTERCEPT b	Data Rating	PROBE INVERTED * RUN	SLOPE m	INTERCEPT b	Data Rating	ALIGNMENT FACTORS HORIZ'TL OFFSET	VERTICAL OFFSET	TUNNEL UPFLOW deg	Percent Difference in Slope	PROBE CALIBRATION ** Slope m	Intercept b
1.18	1	27	-0.05546	-0.0181	N	31	0.05770	0.0007	G	-0.166	-0.009	0.166	3.96	-0.05546	-0.009
	2		-0.03516	0.0229	S		0.04399	-0.0090	G	0.403	0.009	-0.403	22.31	-0.03516	0.009
	3		-0.05003	0.0867	G		0.05197	0.1084	E	-0.213	0.097	0.213	3.80	-0.05003	0.097
	4	32	-0.05510	-0.0213	E	30	0.05426	0.0108	E	-0.294	-0.005	0.294	-1.54	-0.05510	-0.005
	5	27	-0.05521	0.0345	E	31	0.05655	0.0802	E	-0.409	0.057	0.409	2.40	-0.05521	0.057
1.20	1	27	-0.05717	-0.0217	E	31	0.05727	0.0005	E	-0.194	-0.011	0.194	0.17	-0.05717	-0.011
	2		-0.03004	0.0154	S		0.04267	-0.0119	S	0.375	0.004	-0.375	34.74	-0.03004	0.004
	3		-0.05050	0.0916	E		0.05154	0.1072	E	-0.153	0.099	0.153	2.04	-0.05050	0.099
	4	32	-0.05528	-0.0212	G	29, 30	0.05473	0.0086	G	-0.271	-0.006	0.271	-1.00	-0.05528	-0.006
	5	27	-0.05581	0.0392	E	31	0.05759	0.0763	E	-0.327	0.057	0.327	3.14	-0.05581	0.057
1.23	1	27	-0.05628	-0.0186	E	31	0.05640	-0.0031	E	-0.138	-0.011	0.138	0.21	-0.05628	-0.011
	2		-0.04668	-0.0190	N		0.04441	-0.0109	G	-0.089	-0.015	0.089	-4.98	-0.04668	-0.015
	3		-0.05251	0.0901	E		0.05116	0.1073	E	-0.166	0.099	0.166	-2.60	-0.05251	0.099
	4	32	-0.05517	-0.0221	E	29	0.05329	0.0053	E	-0.253	-0.008	0.253	-3.47	-0.05517	-0.008
	5	27	-0.05495	0.0361	G	31	0.05762	0.0786	E	-0.378	0.057	0.378	4.74	-0.05495	0.057

* Calibration data linear curve fit, Cp = m(x)+b, where x = pitch angle.

** Probe calibration coefficients used to reduce flowfield data (selected form upright and inverted calibration data).

Data Ratings:

E - Excellent - All data conforms to a linear calibration curve fit.

G - Good - Only a couple of data points fall off the linear curve fit.

S - Scattered - Data is more scattered than with "G" rating, but a linear curve fit can be made.

N - Nonlinear - Data at higher pitch angles (+/-) are nonlinear (deviate from curve fit formed by majority of points).

I - Indeterminate - Definite differences between non-consecutive data points . Data has same slope but has a shift in curve position with pitch angle.

Table II. Flowfield Survey Probe Calibration Summary - Perpendicular Orifices

MACH NO.	PROBE NO.	PROBE UPRIGHT * RUN	SLOPE m	INTERCEPT b	Data Rating	PROBE INVERTED * RUN	SLOPE m	INTERCEPT b	Data Rating	ALIGNMENT FACTORS HORIZ'TL OFFSET	VERTICAL OFFSET	TUNNEL UPFLOW deg	Percent Difference in Slope	PROBE CALIBRATION ** Slope m	Intercept b		
0.50	1	6	-0.05275	-0.0558	E	4	0.05318	0.0037	E	-0.562	-0.026	0.562	0.81	0.0530	0.0168	0.0698	-0.024
	2		-0.04792	-0.0644	G		0.04803	-0.0206	G	-0.456	-0.043	0.456	0.23	0.0480	0.0220	0.0700	-0.042
	3		-0.05223	-0.0064	E		0.05310	-0.0046	E	-0.017	-0.006	0.017	1.65	0.0522	0.0226	0.0748	-0.005
	4		-0.05355	-0.0412	E		0.05398	-0.0577	G	0.153	-0.049	-0.153	0.80	0.0538	0.0220	0.0758	-0.049
	5		-0.05712	-0.0544	E		0.05702	-0.0542	E	-0.002	-0.054	0.002	-0.18	0.0570	0.0168	0.0738	-0.055
0.60	1	6	-0.05415	-0.0538	E	4	0.05334	0.0077	E	-0.572	-0.023	0.572	-1.51	0.0537	0.0168	0.0705	-0.025
	2		-0.04900	-0.0530	N		0.04592	-0.0186	N	-0.362	-0.035	0.362	-6.49	0.0473	0.0220	0.0693	-0.036
	3		-0.05206	-0.0051	E		0.05123	-0.0011	E	-0.039	-0.003	0.039	-1.61	0.0522	0.0226	0.0748	-0.004
	4		-0.05412	-0.0391	E		0.05183	-0.0581	N	0.179	-0.049	-0.179	-4.32	0.0541	0.0220	0.0761	-0.050
	5		-0.05570	-0.0556	E		0.05585	-0.0567	G	0.010	-0.056	-0.010	0.27	0.0558	0.0168	0.0726	-0.055
0.70	1	6	-0.05461	-0.0521	E	4	0.05350	0.0011	E	-0.492	-0.025	0.492	-2.05	0.0540	0.0166	0.0706	-0.025
	2		-0.04876	-0.0441	N		0.04544	-0.0142	N	-0.317	-0.029	0.317	-7.05	0.0466	0.0211	0.0677	-0.029
	3		-0.05230	-0.0040	E		0.05189	-0.0044	E	0.004	-0.004	-0.004	-0.79	0.0522	0.0221	0.0743	-0.004
	4		-0.05490	-0.0414	E		0.05404	-0.0615	G	0.185	-0.052	-0.185	-1.58	0.0544	0.0211	0.0755	-0.052
	5		-0.05497	-0.0519	E		0.05464	-0.0582	E	0.057	-0.055	-0.057	-0.60	0.0498	0.0166	0.0664	-0.055
0.80	1	6	-0.05532	-0.0539	E	4	0.05477	0.0027	E	-0.514	-0.025	0.514	-1.00	0.0554	0.0135	0.0689	-0.026
	2		-0.04052	-0.0437	N		0.04242	-0.0137	S	-0.362	-0.029	0.362	4.58	0.0459	0.0170	0.0629	-0.029
	3		-0.05333	-0.0047	E		0.05270	-0.0022	E	-0.024	-0.003	0.024	-1.19	0.0530	0.0183	0.0713	-0.003
	4		-0.05489	-0.0432	E		0.05554	-0.0634	E	0.183	-0.053	-0.183	1.18	0.0553	0.0170	0.0723	-0.053
	5		-0.05496	-0.0500	E		0.05505	-0.0640	E	0.127	-0.057	-0.127	0.16	0.0553	0.0135	0.0688	-0.055
	1	27, 29 & 30	-0.05541	-0.0556	I	31 & 32	0.05582	0.0093	I	-0.583	-0.023	0.583	0.74				
	2		-0.04888	-0.0460	I		0.05232	-0.0593	I	0.131	-0.052	-0.131	6.80				
	3		-0.05393	-0.0066	G		0.05137	-0.0017	S	-0.047	-0.004	0.047	-4.86				
	4		-0.05857	-0.0894	I		0.05584	-0.0619	E	-0.240	-0.075	0.240	-4.77				
	5		-0.05508	0.0193	I		0.05537	0.0039	G	0.139	0.012	-0.139	0.53				
0.90	1	6	-0.05638	-0.0663	E	4	0.05621	0.0135	E	-0.709	-0.026	0.709	-0.30	0.0563	0.0067	0.0630	-0.026
	2		-0.04675	-0.0499	N		0.04158	-0.0183	N	-0.358	-0.033	0.358	-11.71	0.0453	0.0084	0.0537	-0.032
	3		-0.05332	-0.0066	E		0.05377	0.0021	E	-0.081	-0.002	0.081	0.84	0.0536	0.0093	0.0629	-0.002
	4		-0.05541	-0.0436	E		0.05513	-0.0692	N	0.232	-0.056	-0.232	-0.51	0.0553	0.0084	0.0637	-0.055
	5		-0.05573	-0.0391	E		0.05646	-0.0721	E	0.294	-0.055	-0.294	1.30	0.0560	0.0067	0.0627	-0.055

Table II. Concluded.

MACH NO.	PROBE NO.	PROBE UPRIGHT * RUN	SLOPE m	INTERCEPT b	Data Rating	PROBE INVERTED * RUN	SLOPE m	INTERCEPT b	Data Rating	ALIGNMENT FACTORS HORIZ'TL OFFSET	VERTICAL OFFSET	TUNNEL UPFLOW deg	Percent Difference in Slope	PROBE CALIBRATION ** Slope m	Intercept b		
0.95	1	6	-0.05701	-0.0755	E	4	0.05675	0.0221	E	-0.858	-0.027	0.858	-0.46	0.0569	0.0034	0.0603	-0.026
	2		-0.04830	-0.0548	N		0.04391	-0.0116	N	-0.468	-0.032	0.468	-9.52	0.0449	0.0042	0.0491	-0.033
	3		-0.05485	-0.0087	E		0.05427	0.0055	E	-0.130	-0.002	0.130	-1.06	0.0546	0.0047	0.0593	-0.002
	4		-0.05622	-0.0413	E		0.05604	-0.0695	E	0.251	-0.055	-0.251	-0.32	0.0560	0.0042	0.0602	-0.055
	5		-0.05641	-0.0332	E		0.05646	-0.0770	E	0.388	-0.055	-0.388	0.09	0.0565	0.0034	0.0599	-0.055
1.18	1	30	-0.05638	-0.0395	E	32	0.05487	-0.0180	G	-0.193	-0.029	0.193	-2.71	0.0549	0.0000	0.0549	-0.029
	2		-0.04023	-0.0519	G		0.03926	-0.0342	G	-0.223	-0.043	0.223	-2.44	0.0393	0.0000	0.0393	-0.043
	3		-0.05413	-0.0172	G		0.05332	0.0124	E	-0.275	-0.002	0.275	-1.51	0.0533	0.0000	0.0533	-0.002
	4	27	-0.05187	-0.0868	E	31	0.05390	-0.0432	E	-0.412	-0.065	0.412	3.84	0.0539	0.0000	0.0539	-0.065
	5	30	-0.05385	-0.0041	E	32	0.05457	0.0380	E	-0.388	0.017	0.388	1.33	0.0546	0.0000	0.0546	0.017
1.20	1	29 & 30	-0.05629	-0.0382	E	32	0.05677	-0.0171	S	-0.187	-0.028	0.187	0.85	0.0568	0.0000	0.0568	-0.028
	2		-0.03335	-0.0475	S		0.03765	-0.0380	S	-0.134	-0.043	0.134	12.11	0.0377	0.0000	0.0377	-0.043
	3		-0.05336	-0.0146	G		0.05345	0.0092	S	-0.223	-0.003	0.223	0.17	0.0535	0.0000	0.0535	-0.003
	4	27	-0.05395	-0.1228	G	31	0.05388	-0.0433	E	-0.737	-0.083	0.737	-0.13	0.0539	0.0000	0.0539	-0.083
	5	29 & 30	-0.05401	-0.0012	E	32	0.05558	0.0356	E	-0.336	0.017	0.336	2.87	0.0556	0.0000	0.0556	0.017
1.23	1	29	-0.05591	-0.0315	E	32	0.05335	-0.0230	S	-0.078	-0.027	0.078	-4.69	0.0534	0.0000	0.0534	-0.027
	2		-0.03375	-0.0414	N		0.03988	-0.0399	S	-0.020	-0.041	0.020	16.65	0.0399	0.0000	0.0399	-0.041
	3		-0.05360	-0.0127	E		0.05293	0.0077	G	-0.191	-0.002	0.191	-1.26	0.0529	0.0000	0.0529	-0.002
	4	27	-0.04856	-0.0827	S	31	0.05306	-0.0430	G	-0.391	-0.064	0.391	8.86	0.0531	0.0000	0.0531	-0.064
	5	29	-0.05455	-0.0021	G	32	0.05519	0.0372	E	-0.358	0.017	0.358	1.17	0.0552	0.0000	0.0552	0.017

* Calibration data linear curve fit, Cp = m(x)+b, where x = pitch angle.

** Probe calibration coefficients used to reduce flowfield data (selected form upright and inverted calibration data).

Data Ratings:

E - Excellent - All data conforms to a linear calibration curve fit.

G - Good - Only a couple of data points fall off the linear curve fit.

S - Scattered - Data is more scattered than with "G" rating, but a linear curve fit can be made.

N - Nonlinear - Data at higher pitch angles (+/-) are nonlinear (deviate from curve fit formed by majority of points).

I - Indeterminate - Definite differences between non-consecutive data points . Data has same slope but has a shift in curve position with pitch angle.

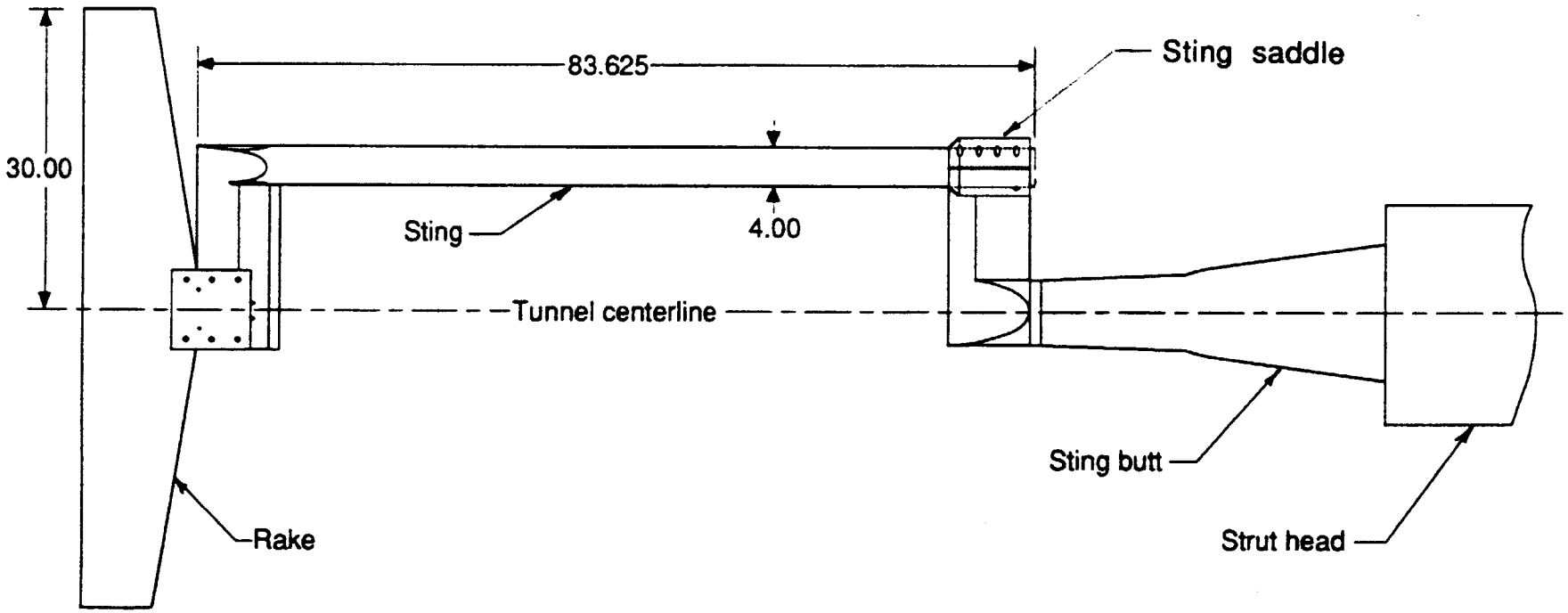

Figure 1. - Test section flowfield survey rake and translating support sting assembly. (Dimensions in inches.)

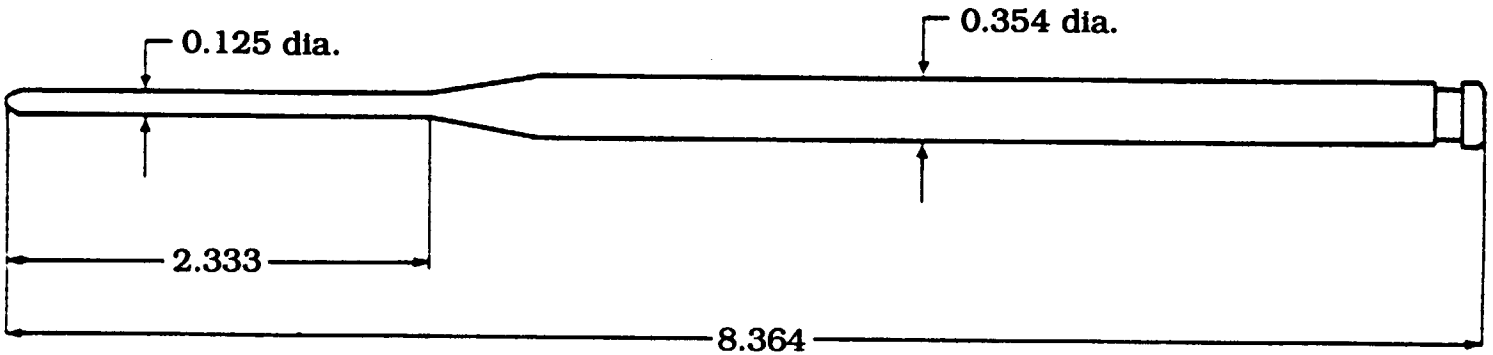

P1 and P3 are vertical plane taps

P2 and P4 are horizontal plane taps

Enlarged view of probe tip

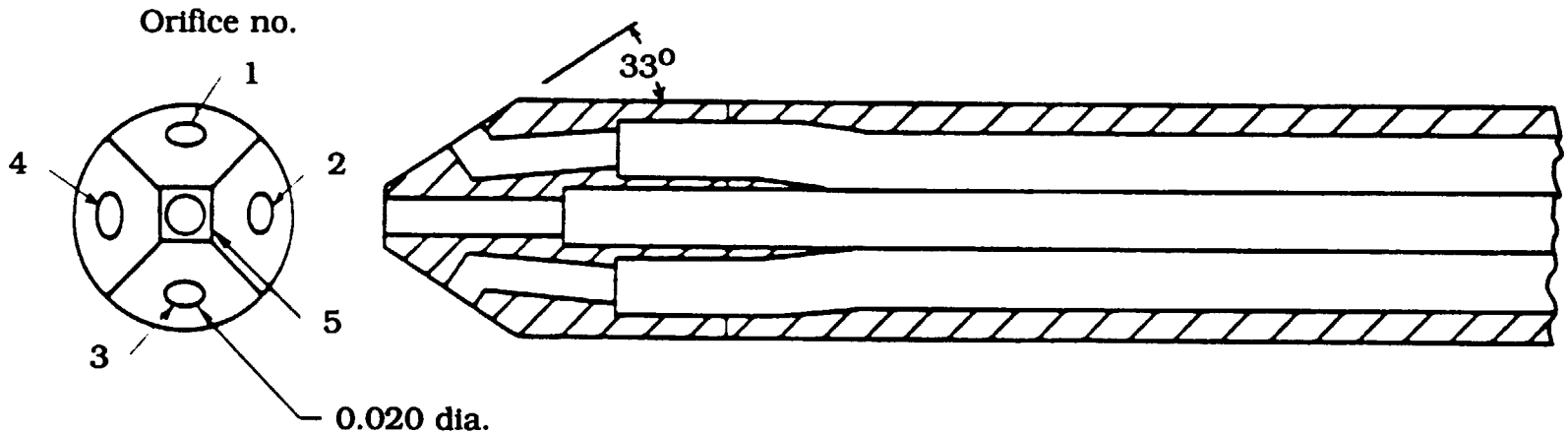

Figure 2. - Five-hole pyramid-head flow angularity probe. (Dimensions in inches.)

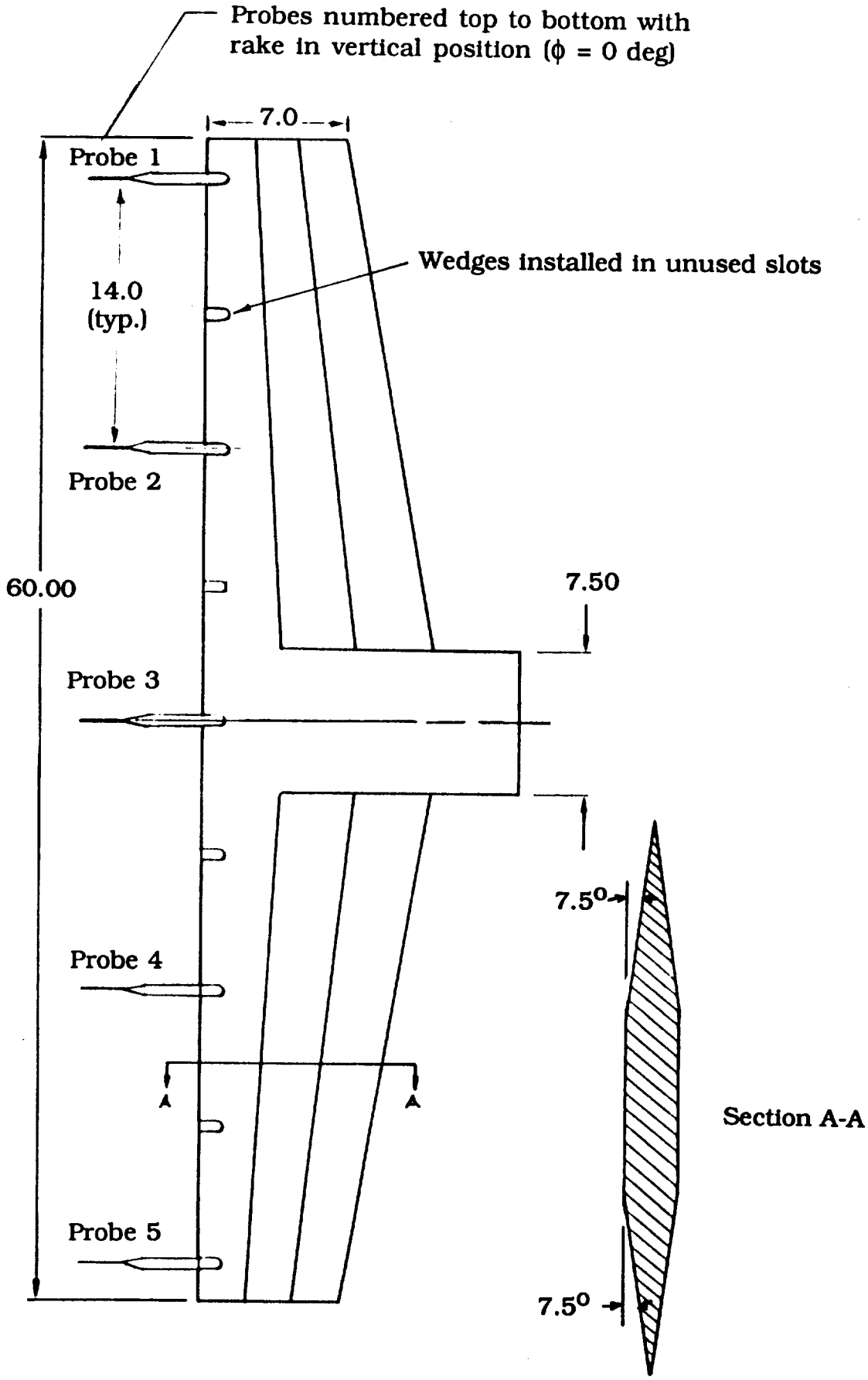

Figure 3. - Flowfield survey rake details. (Dimensions in inches.)

Figure 4. - Photograph of the flowfield survey rake and support sting installed in the 16-Foot Transonic Tunnel.

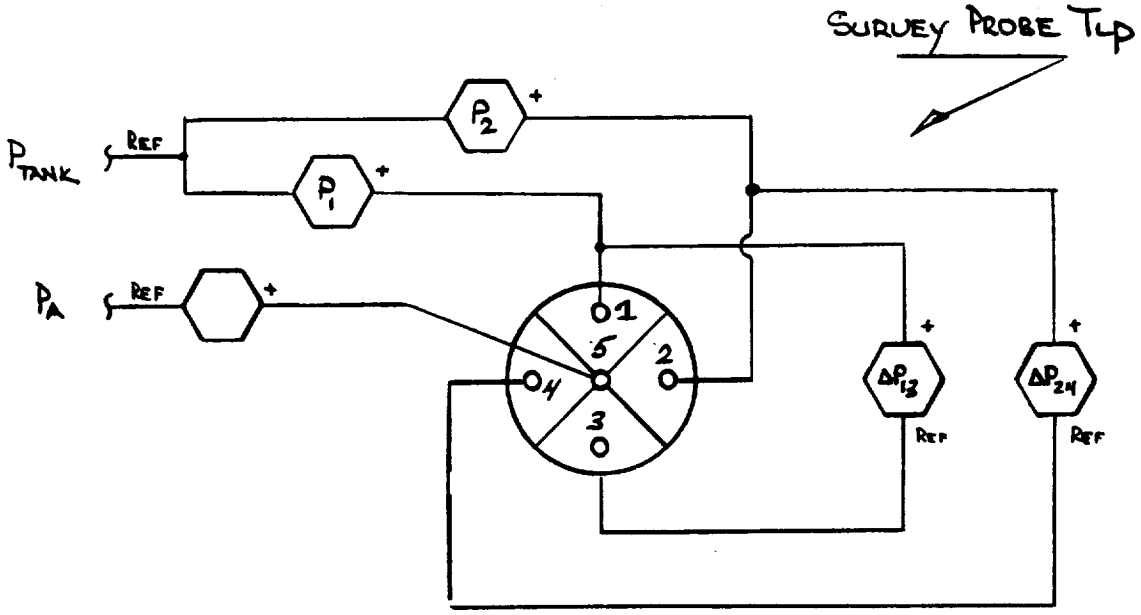

$\Delta P_{13} = P_1 - P_3 \quad \therefore P_3 = P_1 - \Delta P_{13}$

$\Delta P_{24} = P_2 - P_4 \quad \therefore P_4 = P_2 - \Delta P_{24}$

} P_3 & P_4 ARE COMPUTED.

TRANSDUCER SIZES

TRANSDUCER	SUBSONIC SURVEY	SUPERSONIC SURVEY	REFERENCE
P_1 & P_2	2.5 psid	5.0 psid	P_{TANK}
ΔP_{13} & ΔP_{24}	1.0 psid	1.0 psid	N/A
P_5	0.5 psid	0.5 psid.	PA

P_{TANK} = PLENUM STATIC PRESSURE

PA = ATMOSPHERIC PRESSURE

Figure 5. - Flowfield survey probe instrumentation setup.

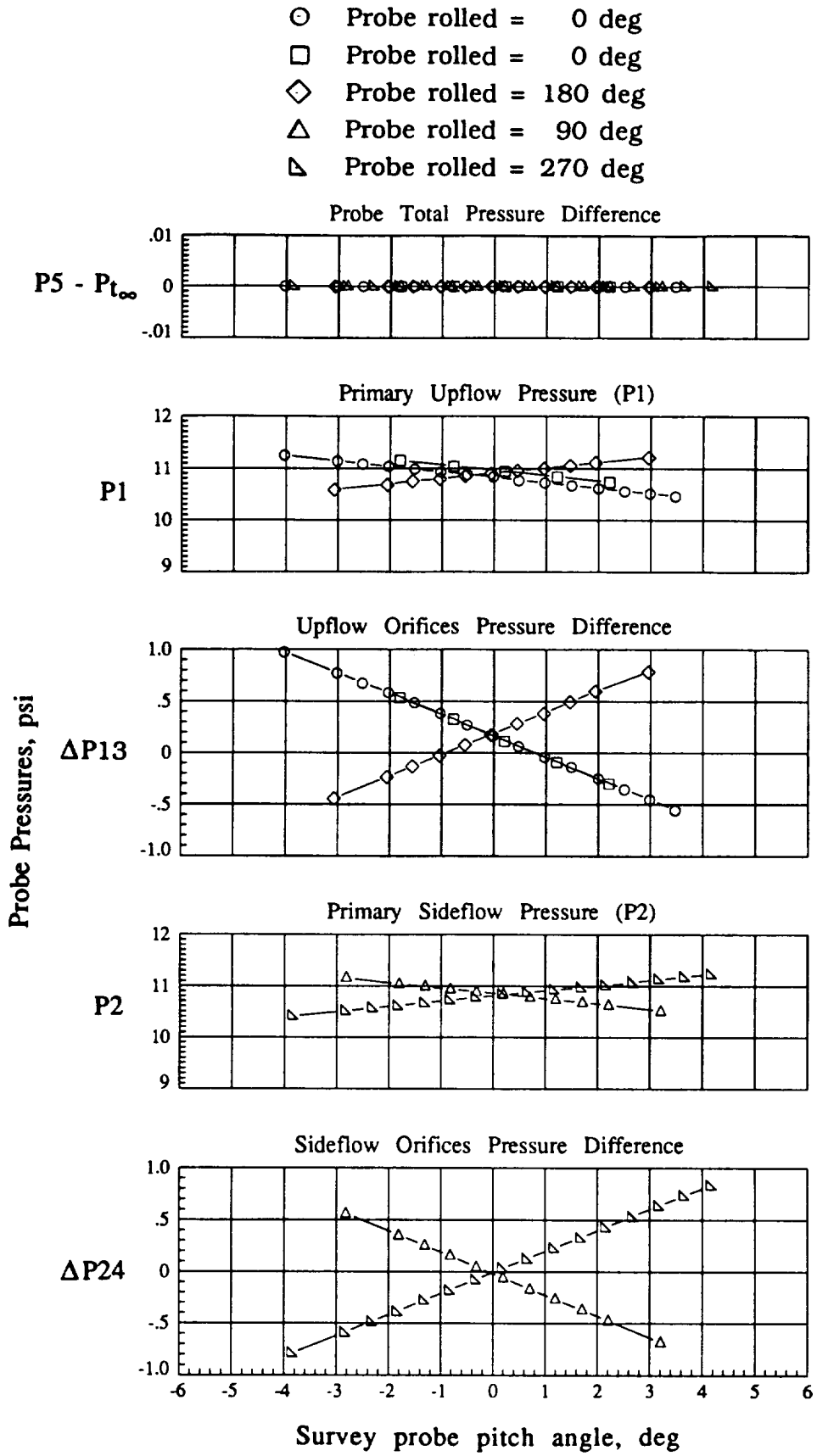

Figure 6. - Typical survey probe pressure measurement characteristics (Probe 3, centerline probe) at Mach 0.8.

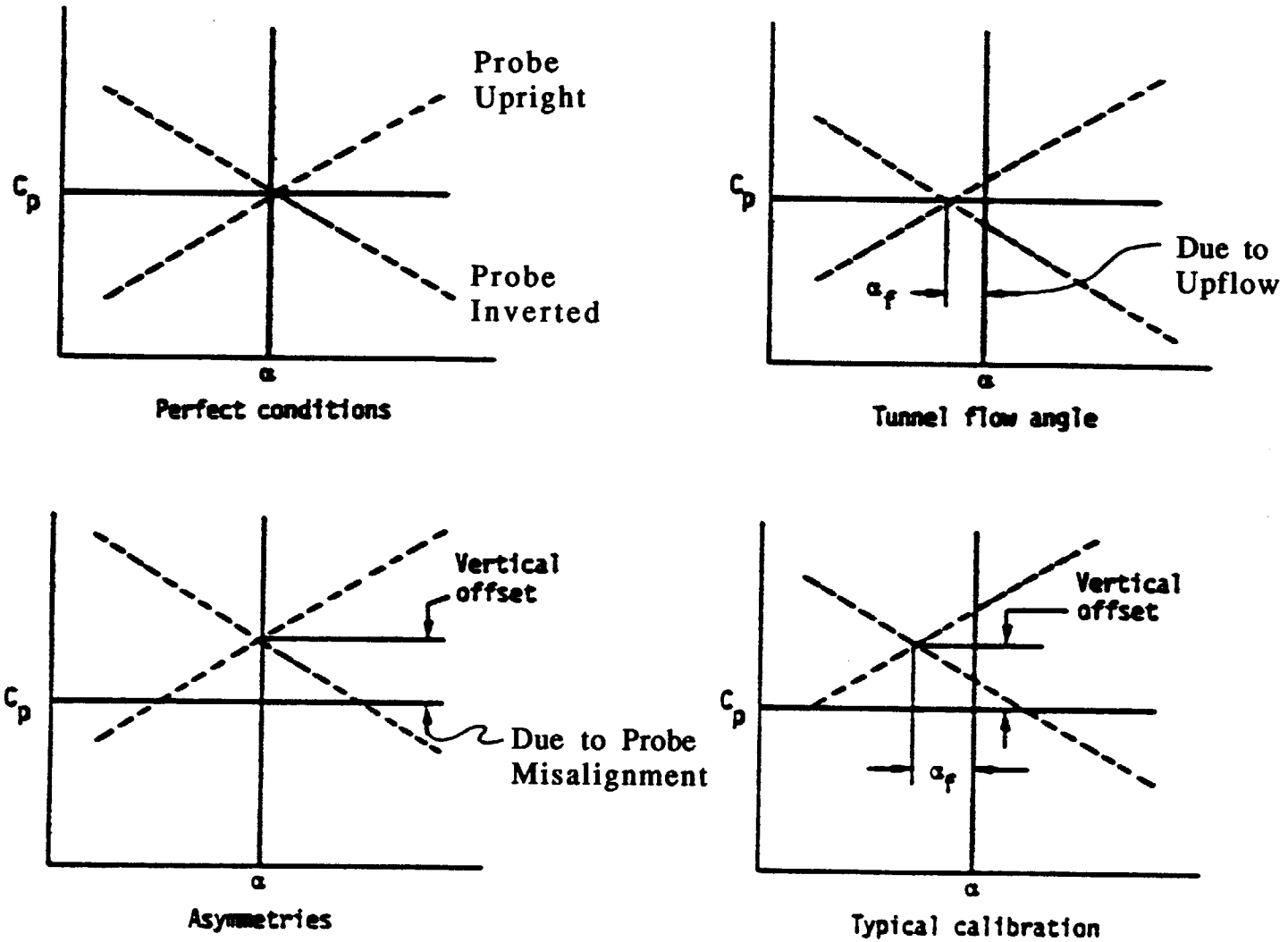

Figure 7. - Typical flowfield survey probe calibration characteristics.

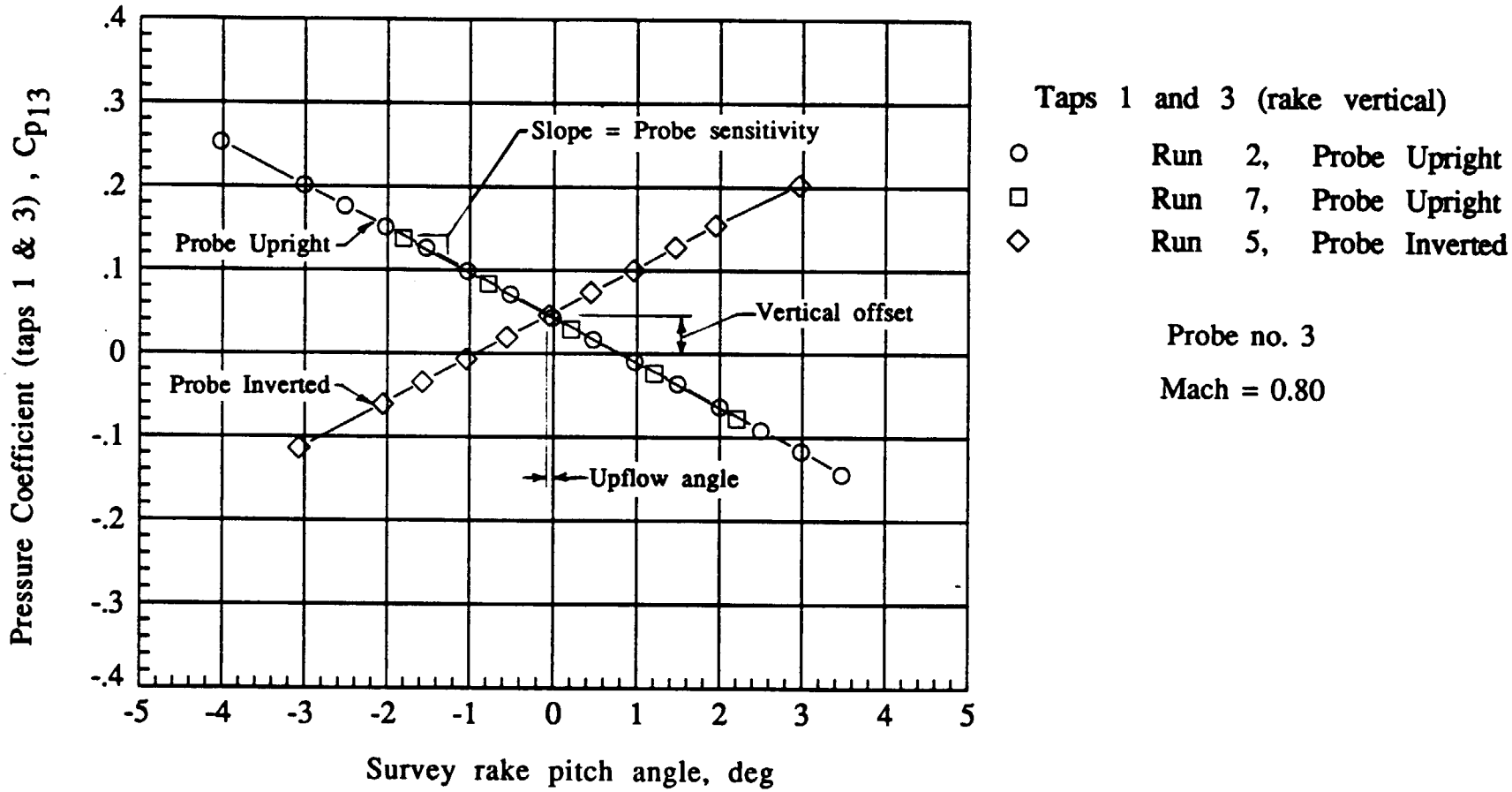

Figure 8. - Typical flowfield survey probe calibration characteristics.

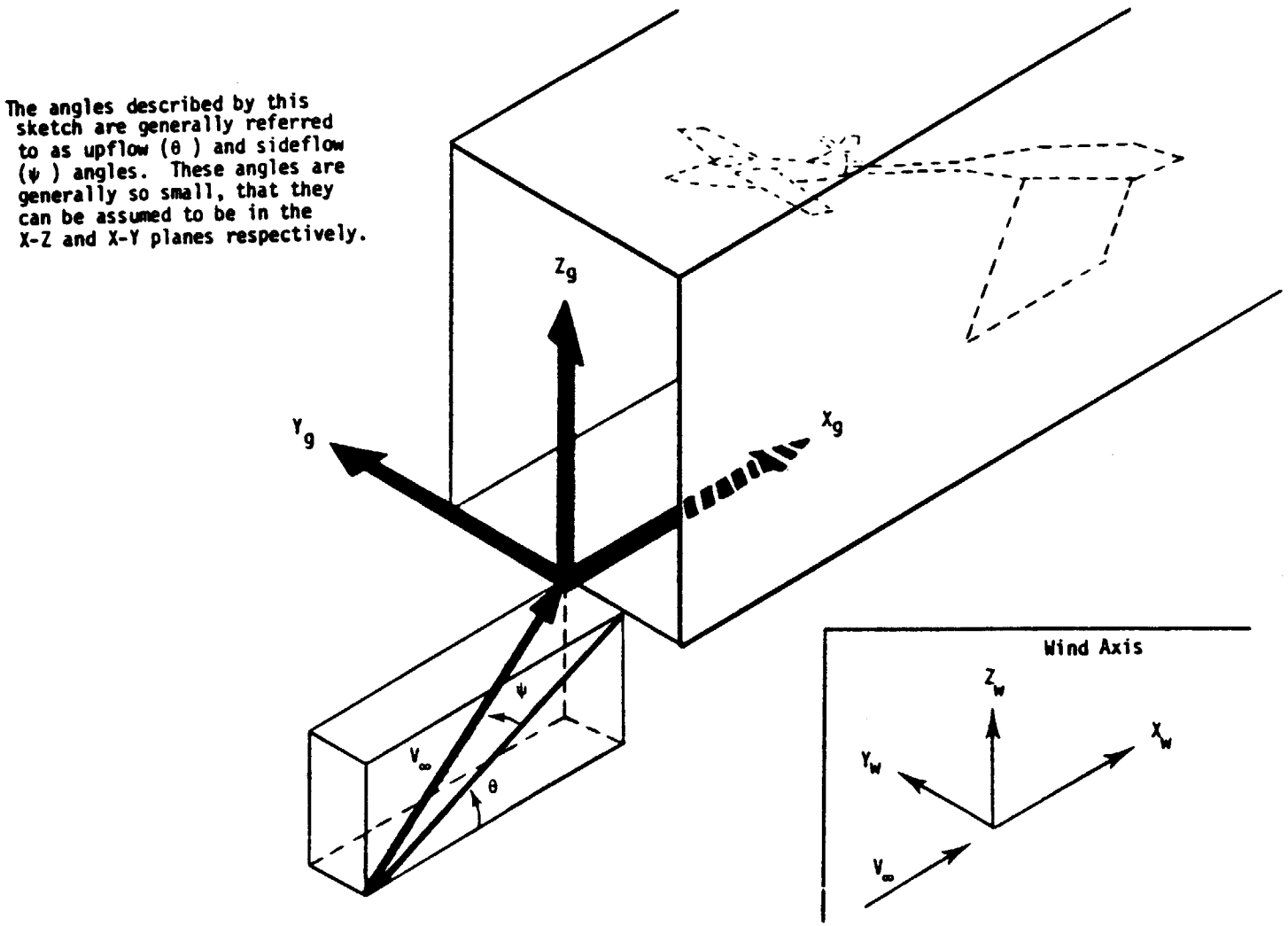

Figure 9. - Definition of wind axes and upflow and sideflow angle convention.

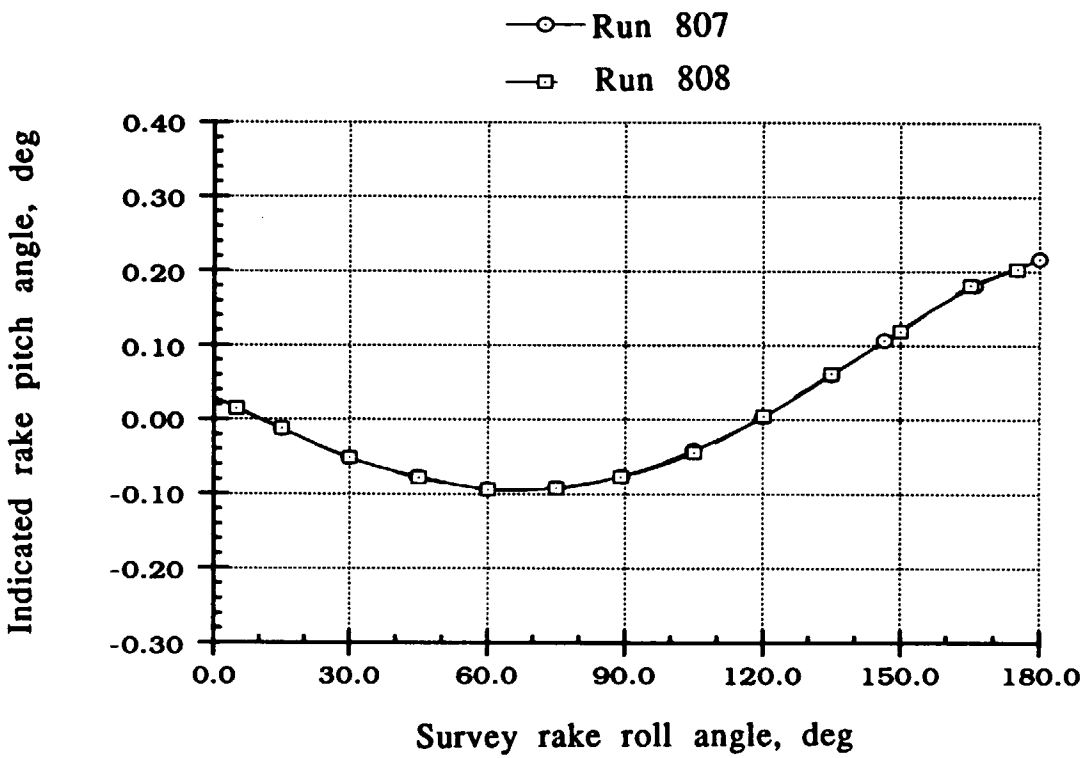

Figure 10. - Survey rake pitch angle variation with rake roll angle.

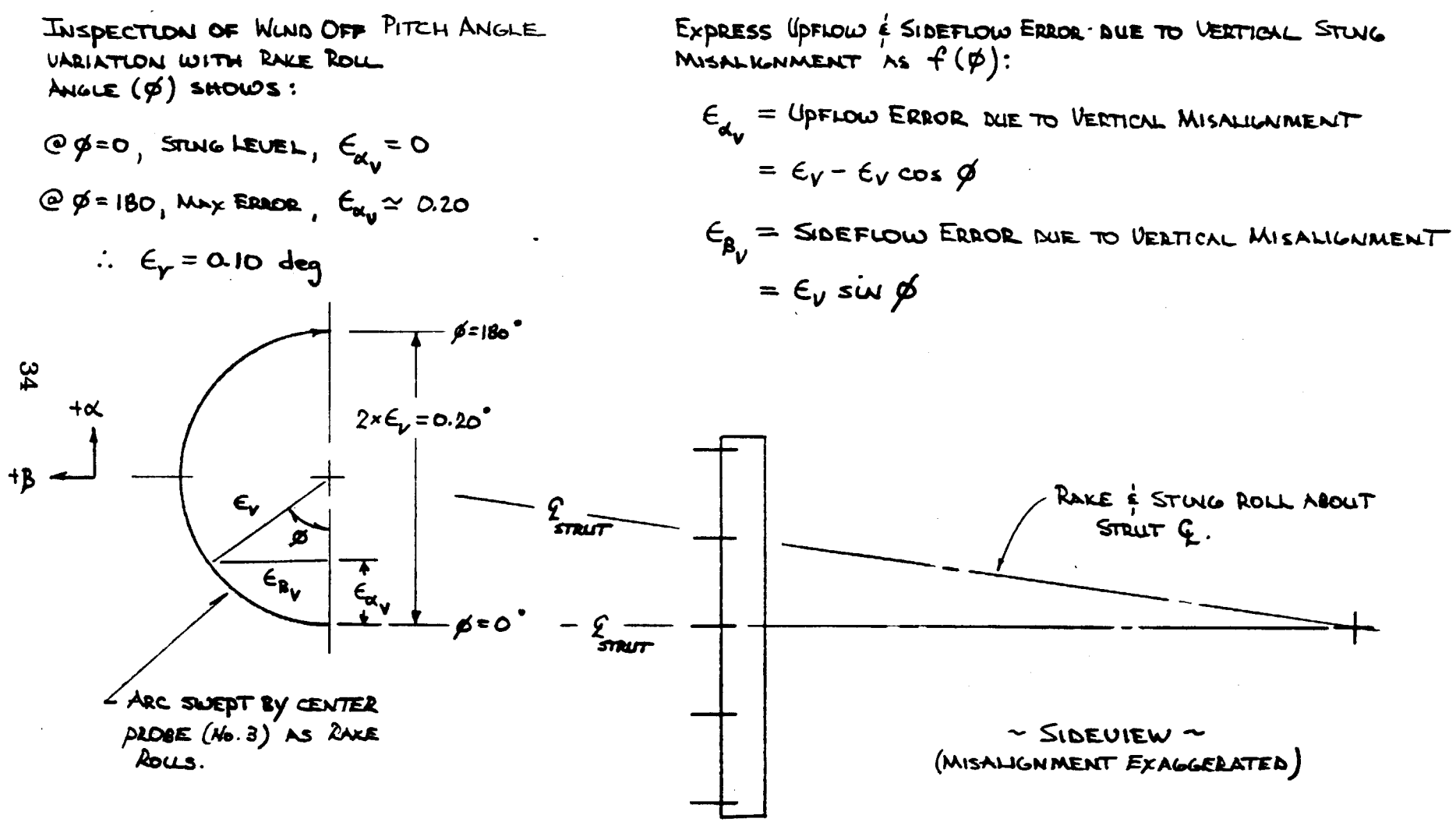

Figure 11. - Adjustments accounting for sting vertical misalignment.

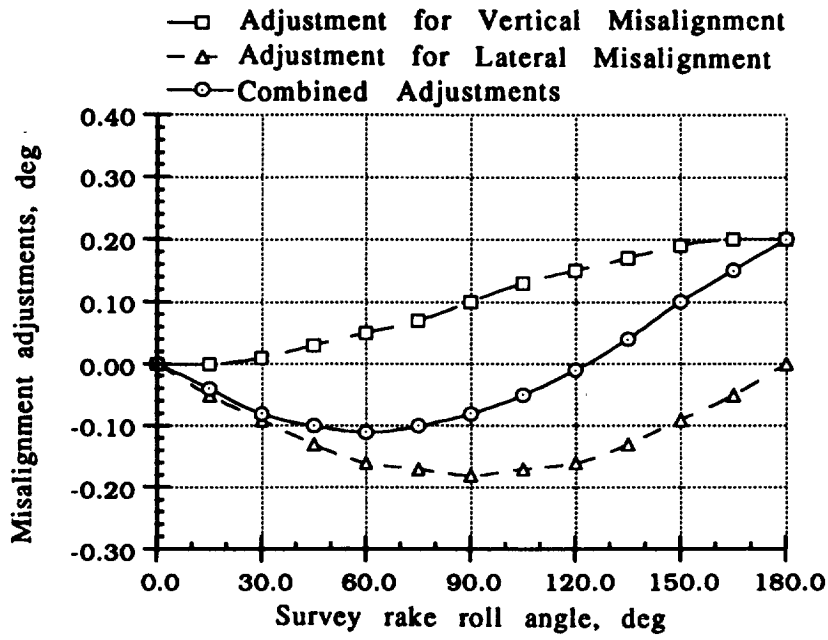

a. Relative magnitude and effect of vertical and lateral misalignment adjustments when applied to upflow component.

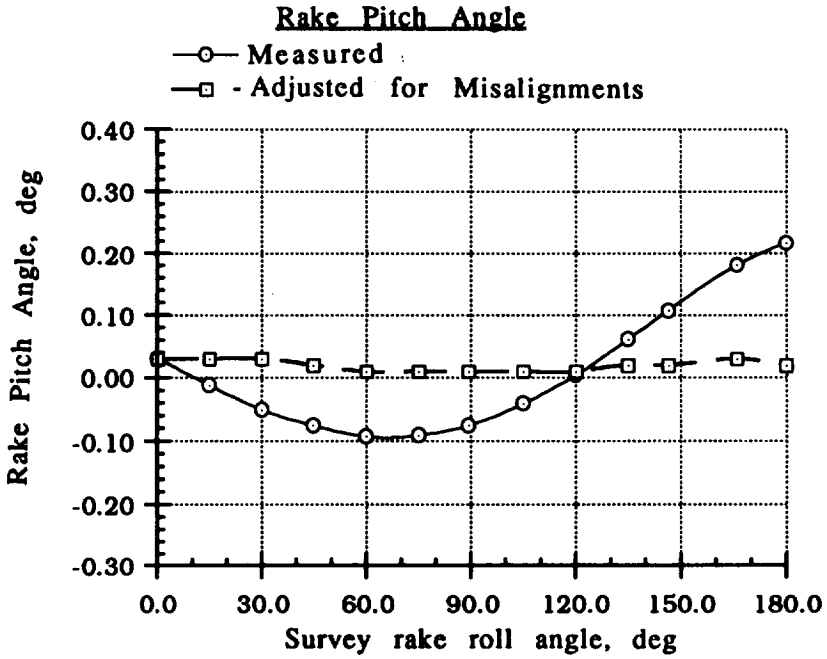

b. Effect of misalignment adjustments on measured rake pitch angle.

Figure 12. - Effect of vertical and lateral misalignment adjustments in vertical (upflow) direction.

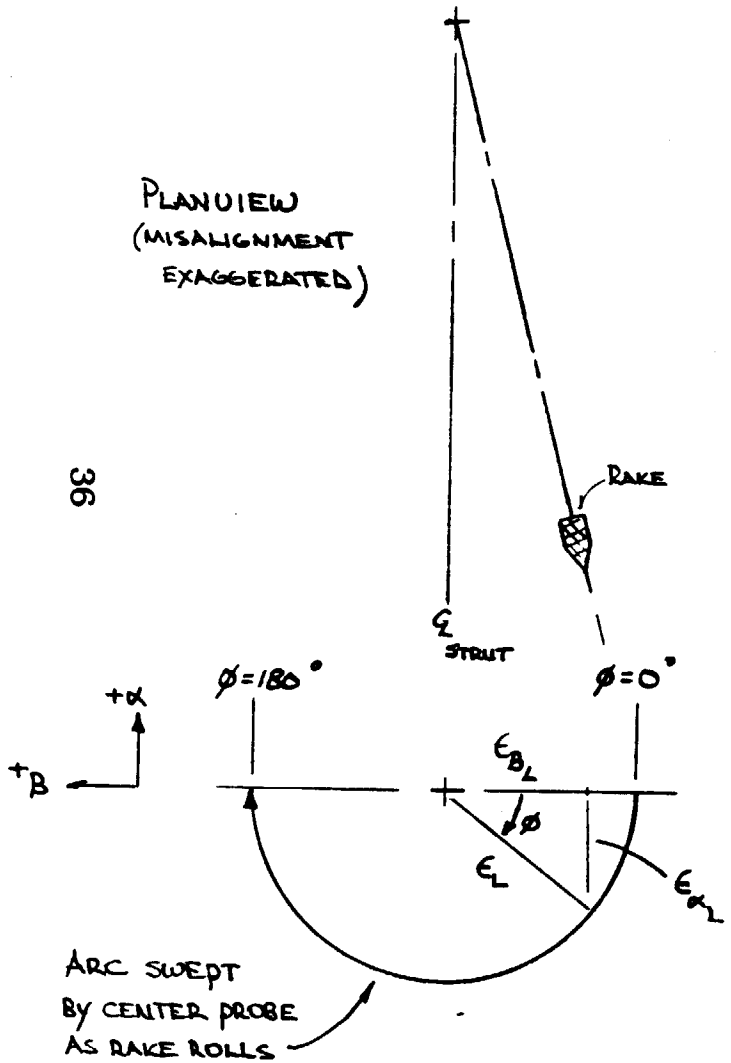

LATERAL ERROR ESTIMATED FROM WIND OFF AoA DISCREPANCY WHEN RAKE IS ROLLED TO 90° (ϕ=90°) AND AFTER APPLYING CORRECTIONS FOR VERTICAL MISALIGNMENT.

a.) MEASURED AoA = −0.08 deg

b.) VERTICAL MISALIGNMENT CORRECTION = 0.10

c.) RESIDUAL ERROR (a−b.) = −0.18 deg

$\therefore \epsilon_L = -0.18$ deg

EXPRESS UPFLOW AND SIDEFLOW ERROR DUE TO LATERAL MISALIGNMENT AS $f(\phi)$:

ϵ_{α_L} = UPFLOW ERROR DUE TO LATERAL MISALIGNMENT

$= \epsilon_L \sin\phi$

ϵ_{β_L} = SIDEFLOW ERROR DUE TO LATERAL MISALIGNMENT

$= \epsilon_L \cos\phi$

Figure 13. - Adjustments accounting for sting lateral misalignment.

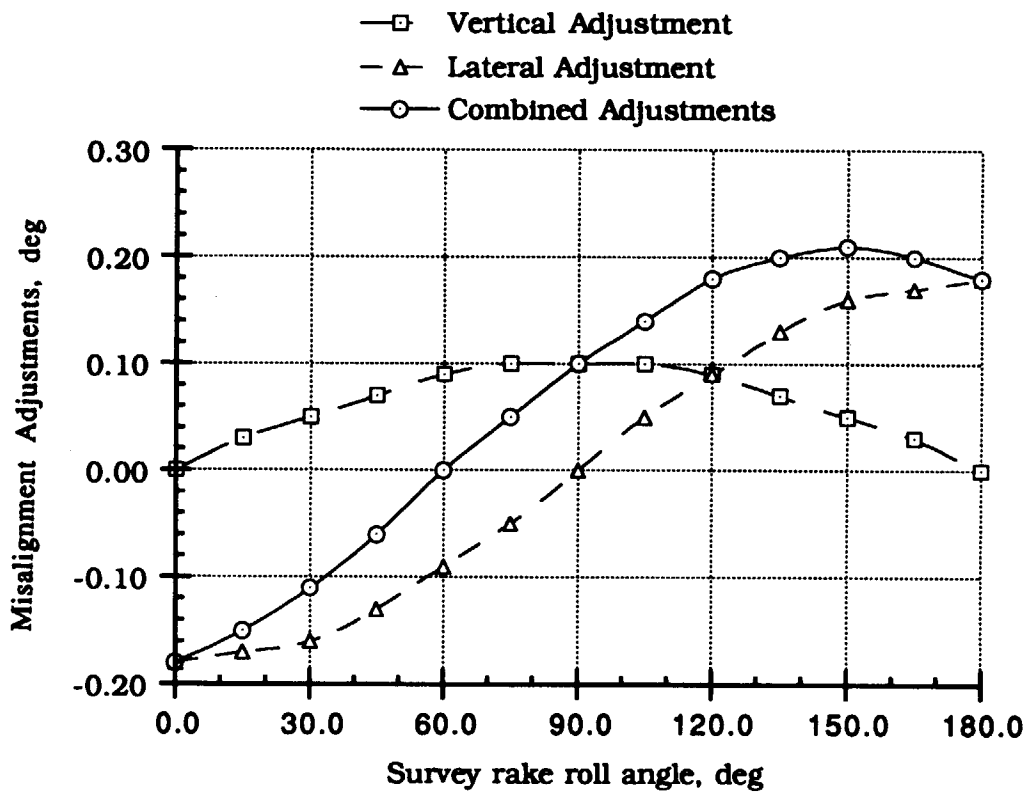

Figure 14. - Effect of vertical and lateral misalignment adjustments in lateral (sideflow) direction.

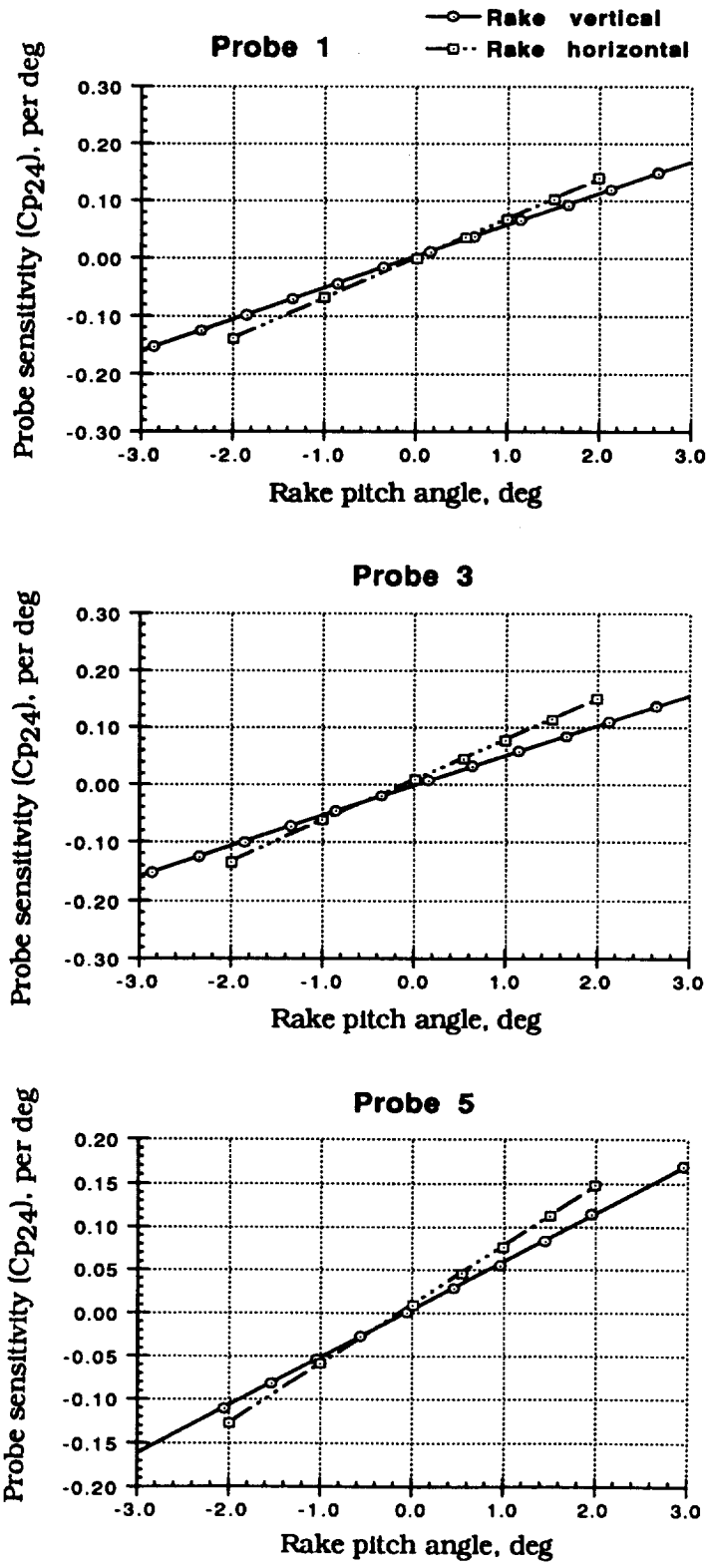

Figure 15. - Effect of rake lift on flowfield survey probe calibration sensitivity, TS 133.6, Mach 0.80.

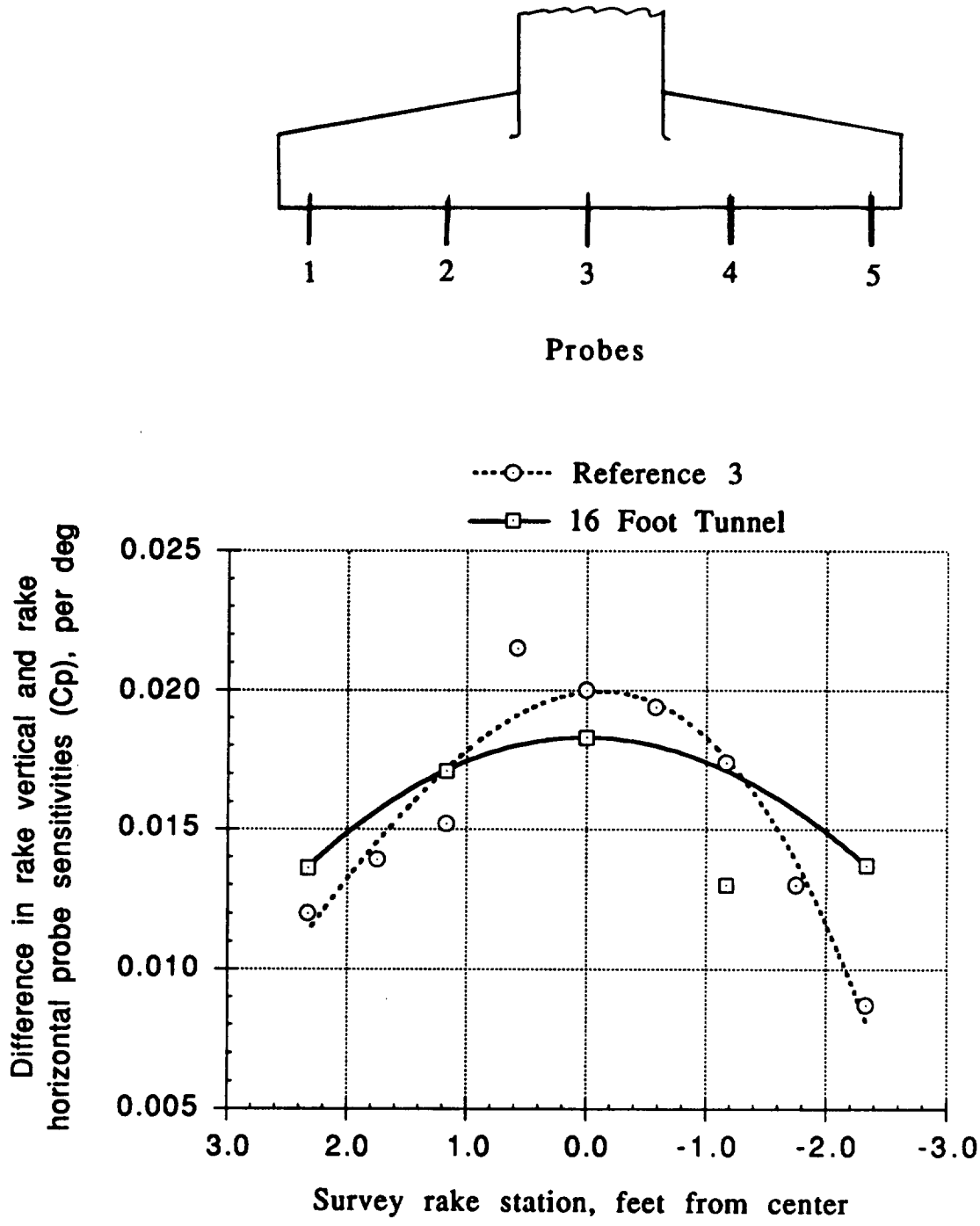

Figure 16. - Spanwise variation in probe sensitivity due to rake lift effects, Mach 0.80.

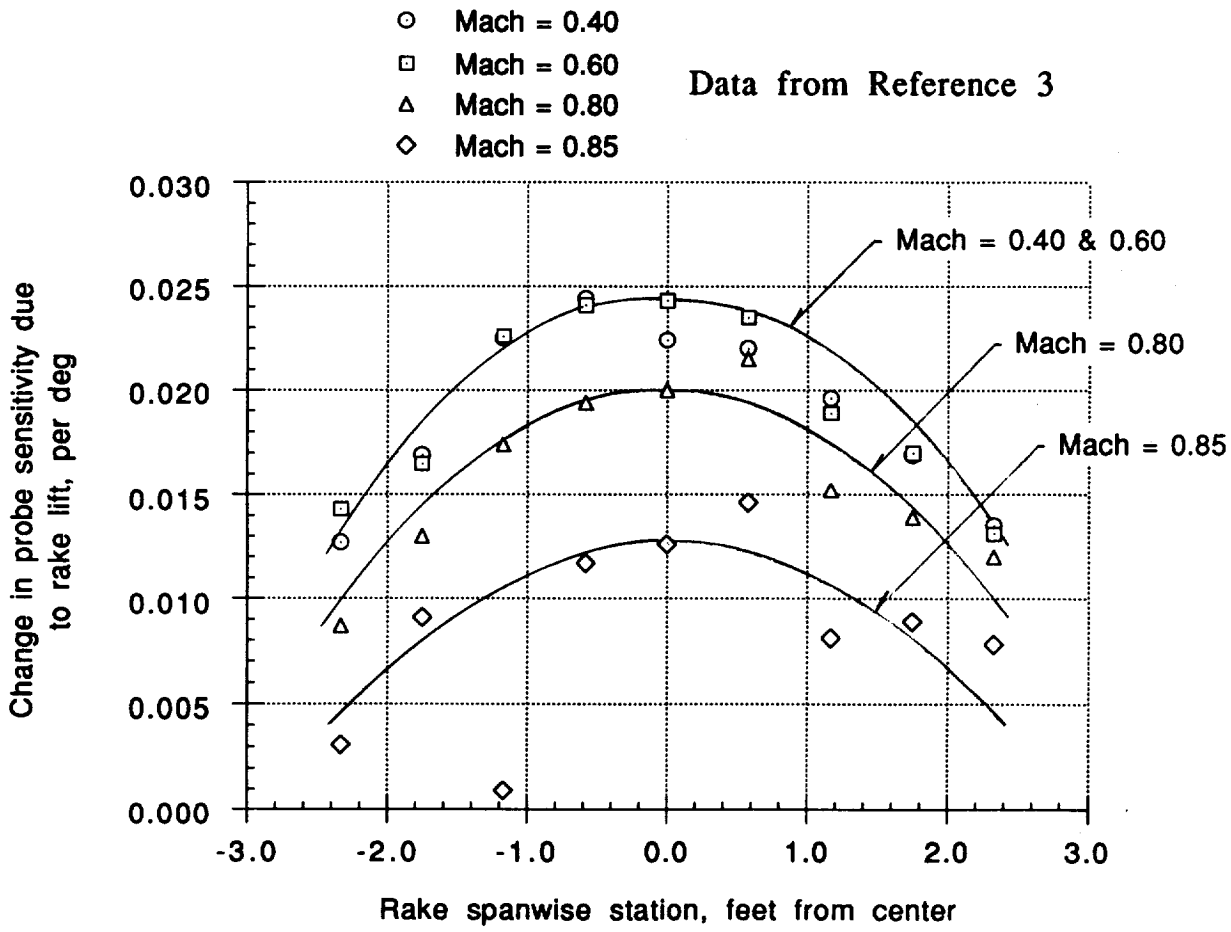

Figure 17. - Effect of Mach number on the measured spanwise variation in probe sensitivity due to rake lift effects.

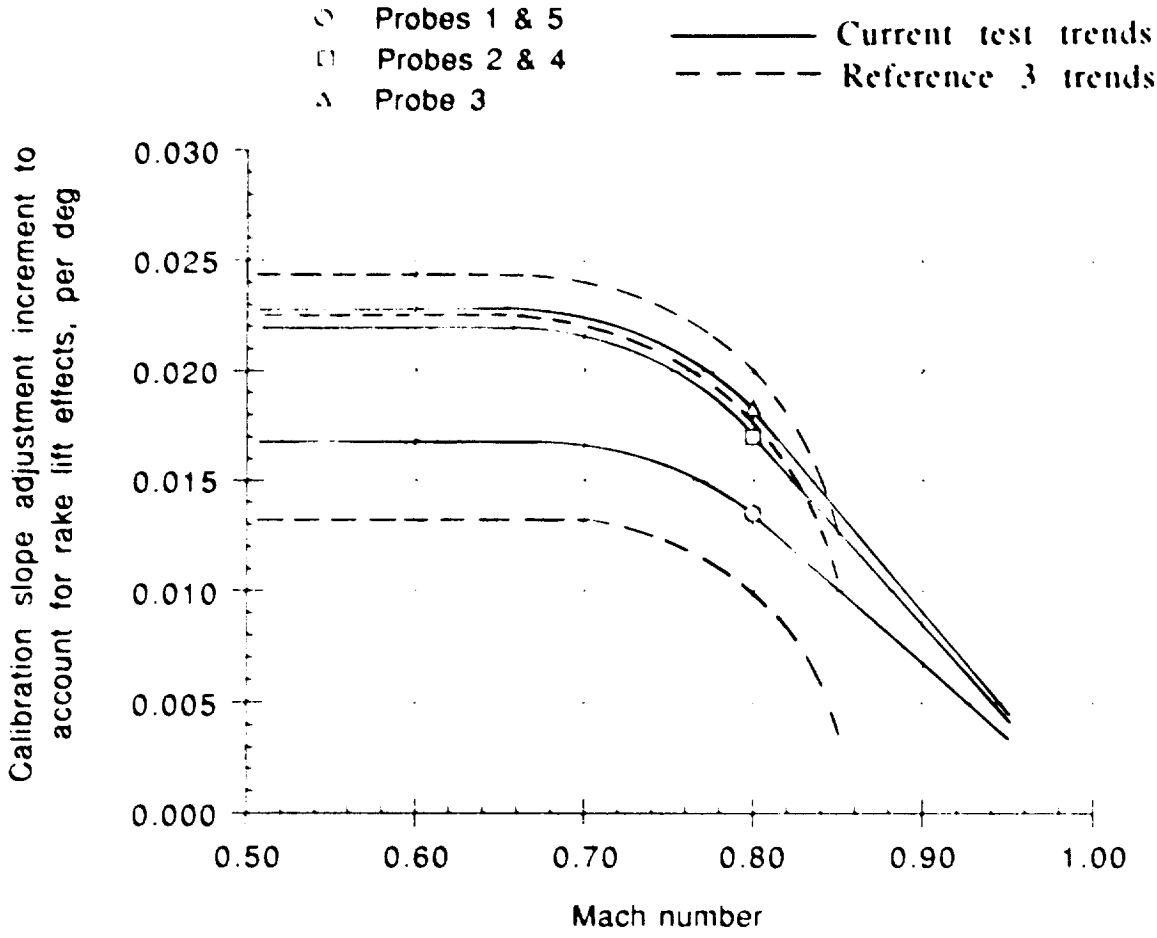

Figure 18. - Adjustments made to survey probe sensitivities, as a function of Mach number and spanwise position, to account for rake lift effects.

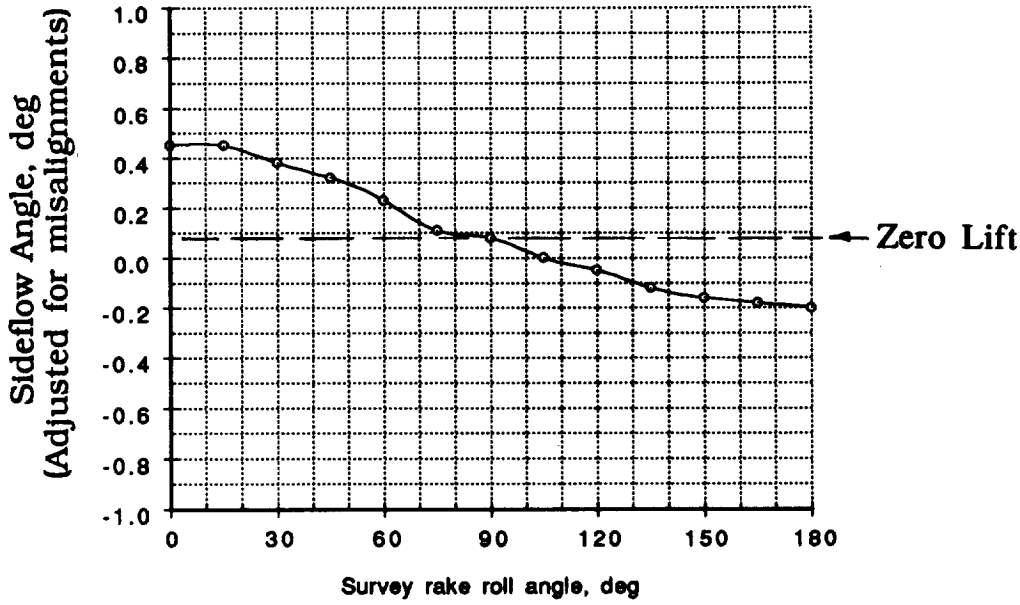

Sideflow Angle

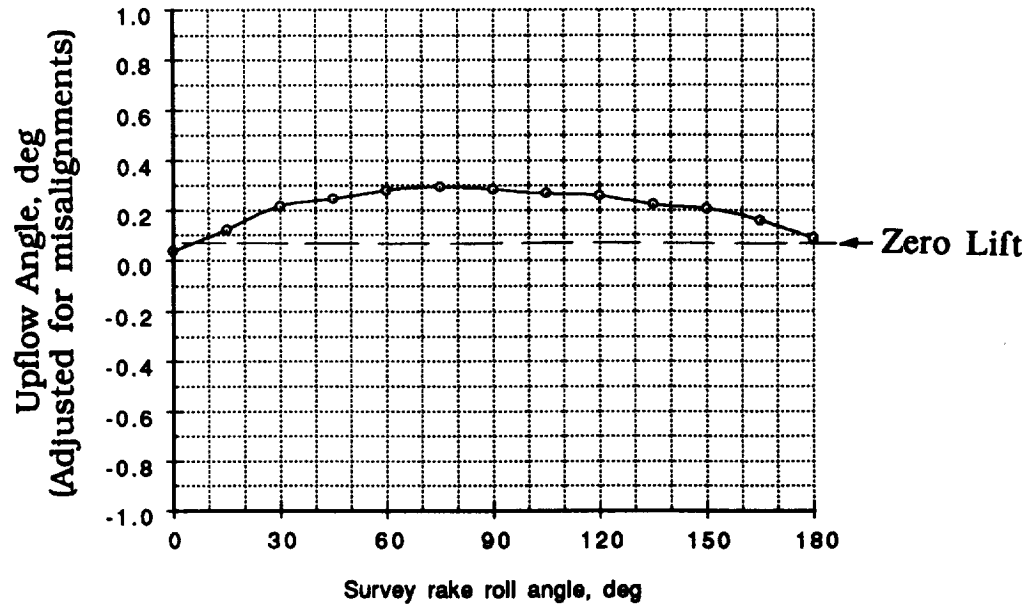

Upflow Angle

Figure 19. - Variation in test section centerline (probe 3) upflow and sideflow angles with rake roll angle after adjusting for misalignment. Tunnel station 133.6, Mach 0.80.

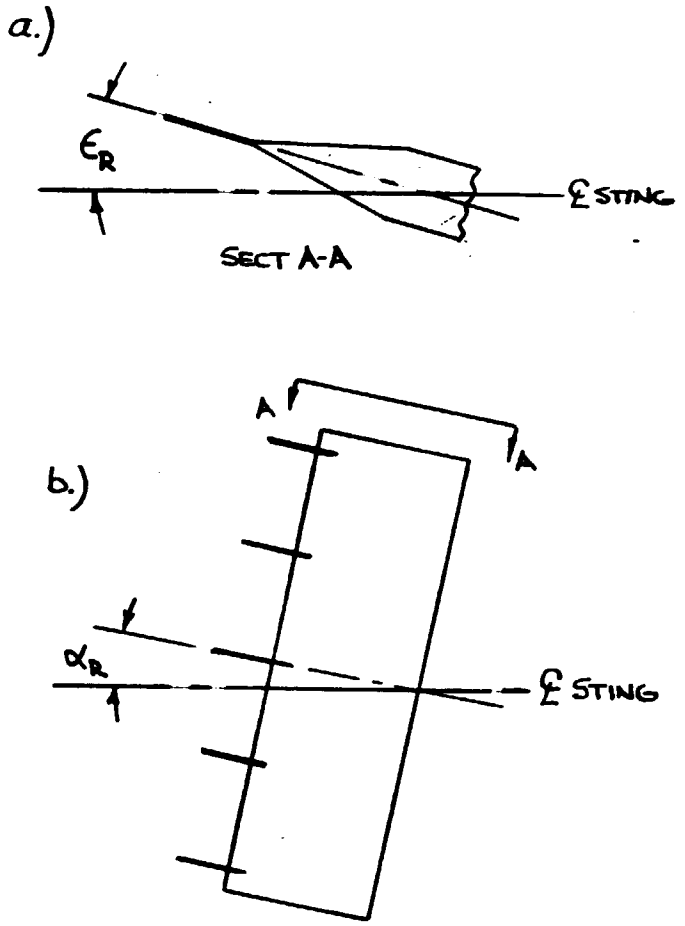

- A VERTICAL RAKE MISALIGNMENT, AS SHOWN IN b. (α_R) IS ACCOUNTED FOR WITH PROBE CALIBRATION (PROBE MISALIGNMENT.)
- A LATERAL RAKE MISALIGNMENT AS SHOWN IN a. PRODUCES A CHANGE IN THE PROBE ORIENTATION AS THE RAKE ROLLS.
- THE EFFECT OF THIS RAKE MISALIGNMENT ON UPFLOW AND SIDEFLOW COMPONENTS ARE:

ROLL ANGLE (ϕ)	UPFLOW	SIDEFLOW
0 deg	0	ϵ_R
90	ϵ_R	0
180	0	$-\epsilon_R$

- EQUATIONS TO ACCOUNT FOR MISALIGNMENT:

UPFLOW: $\epsilon_{R_U} = \epsilon_R \sin\phi$

SIDEFLOW: $\epsilon_{R_S} = \epsilon_R \cos\phi$

Figure 20. - Adjustments accounting for survey probe lateral misalignment.

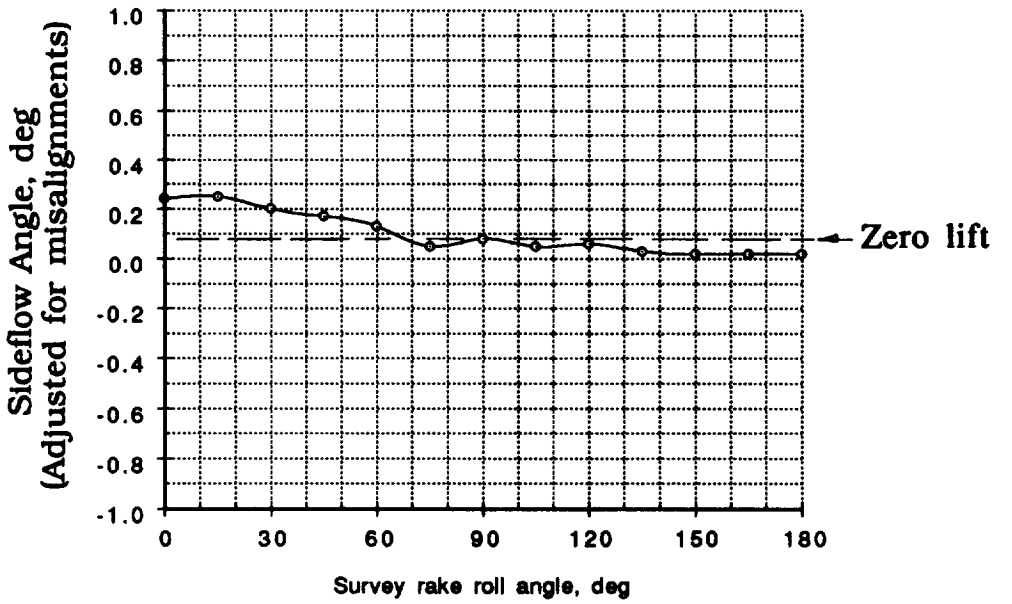

Sideflow Angle

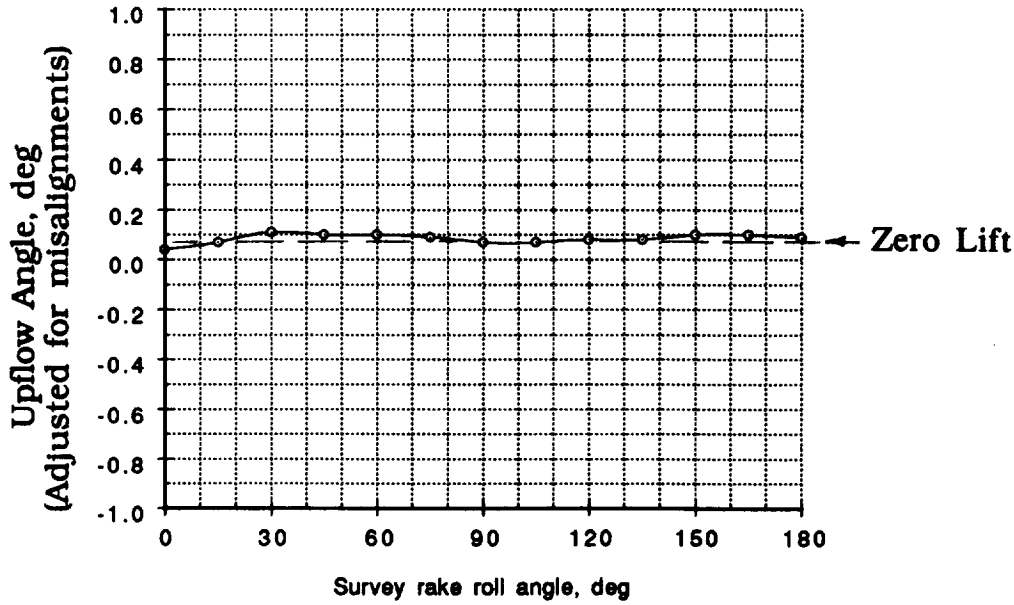

Upflow Angle

Figure 21. - Variation in test section centerline (probe 3) upflow and sideflow angles with rake roll angle after adjusting for sting and rake misalignments. Tunnel station 133.6, Mach 0.80.

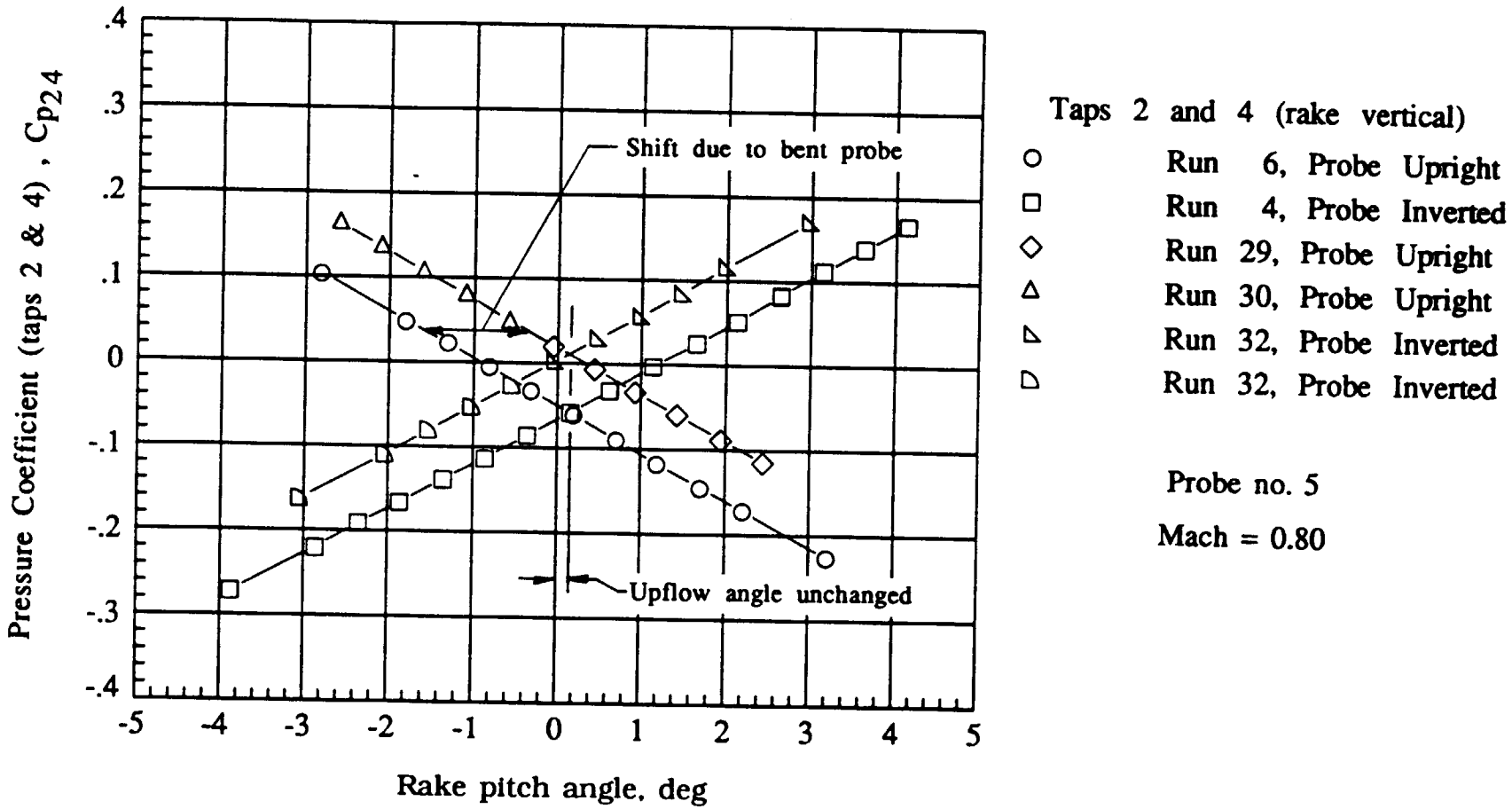

Figure 22. - Effects of a bent probe on the survey probe calibration characteristics.

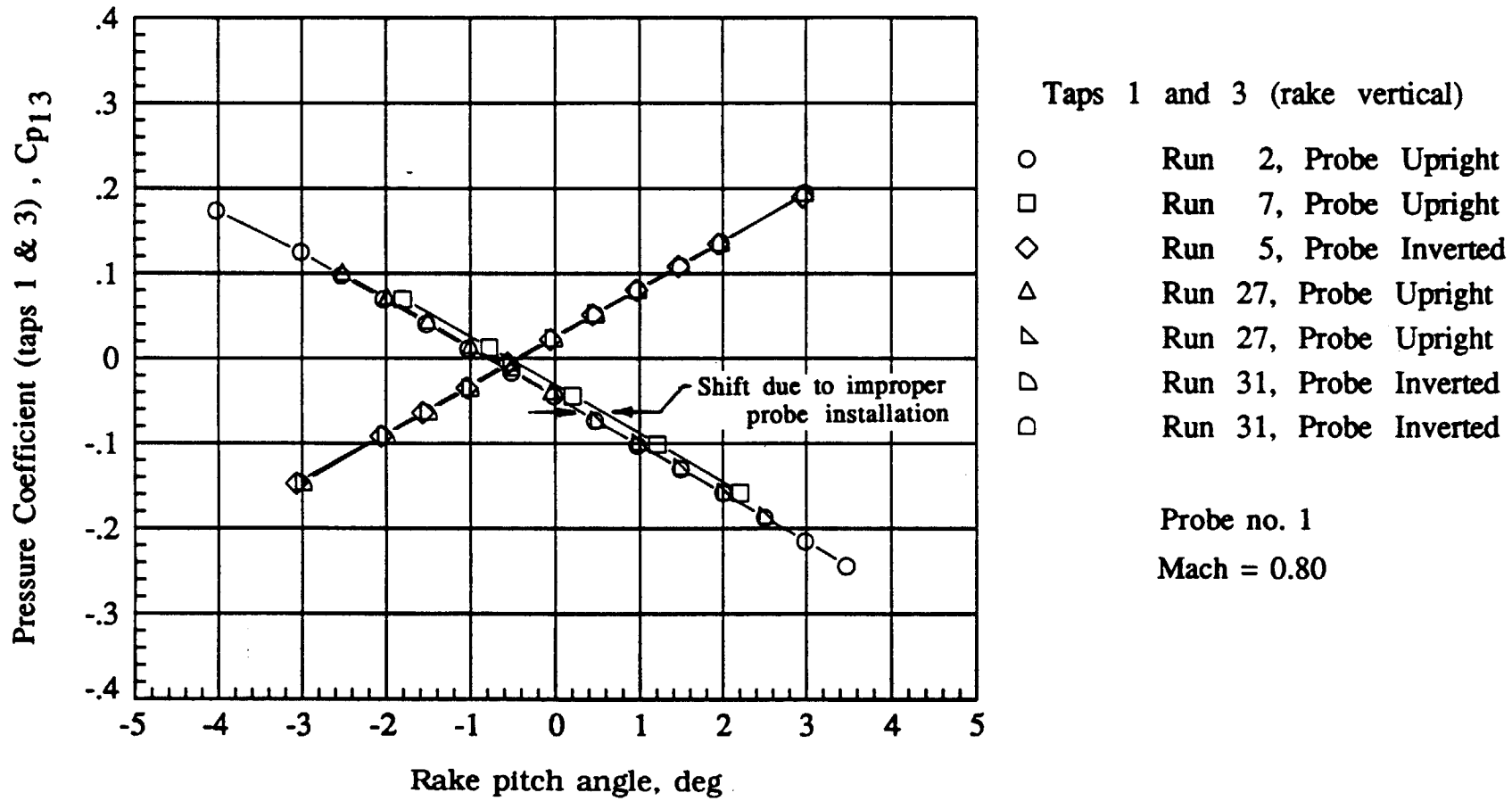

Figure 23. - Effects of an improper probe installation on the survey probe calibration characteristics.

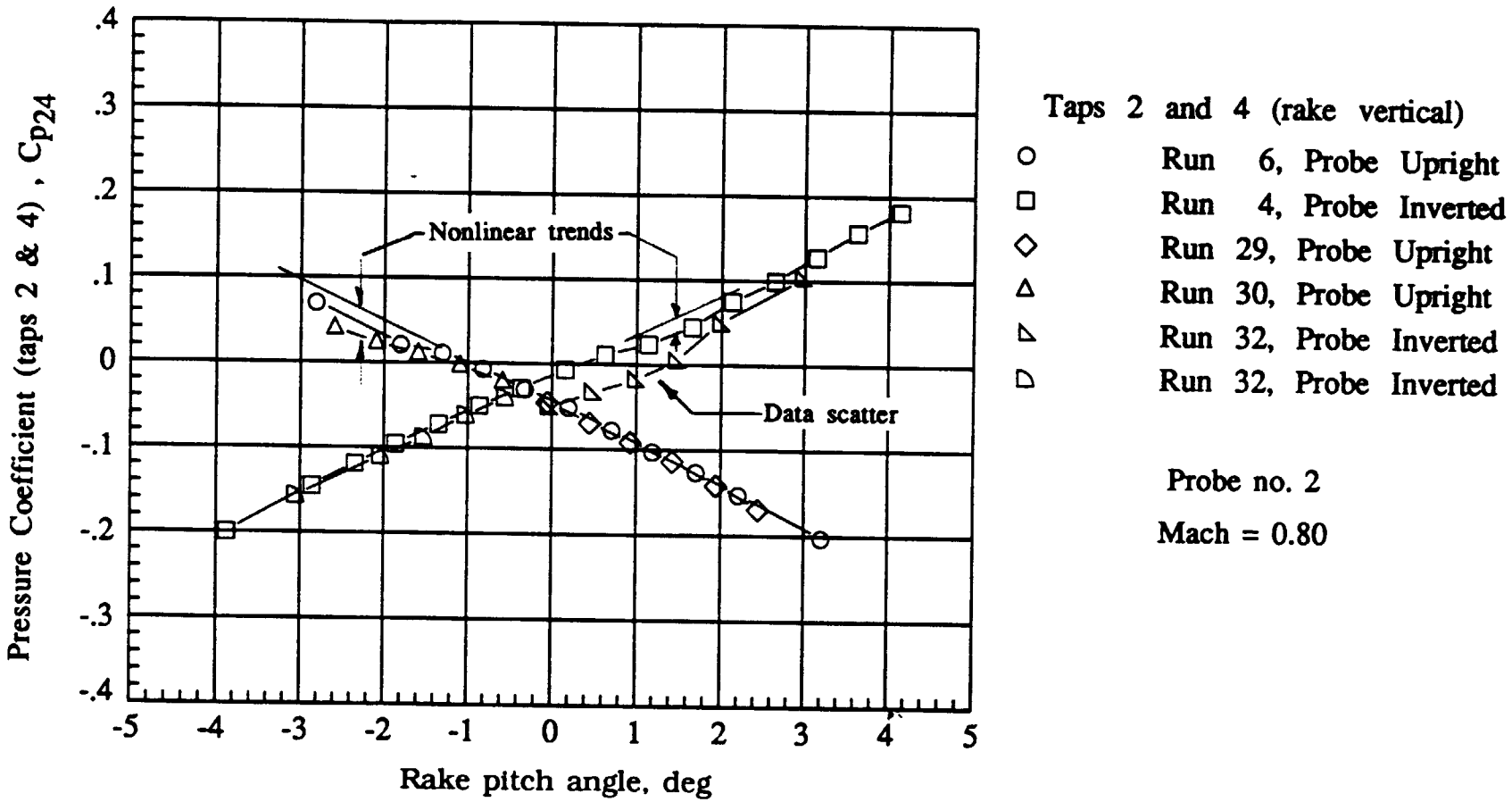

Figure 24. - Effects of unsettled pressures on the survey probe calibration characteristics.

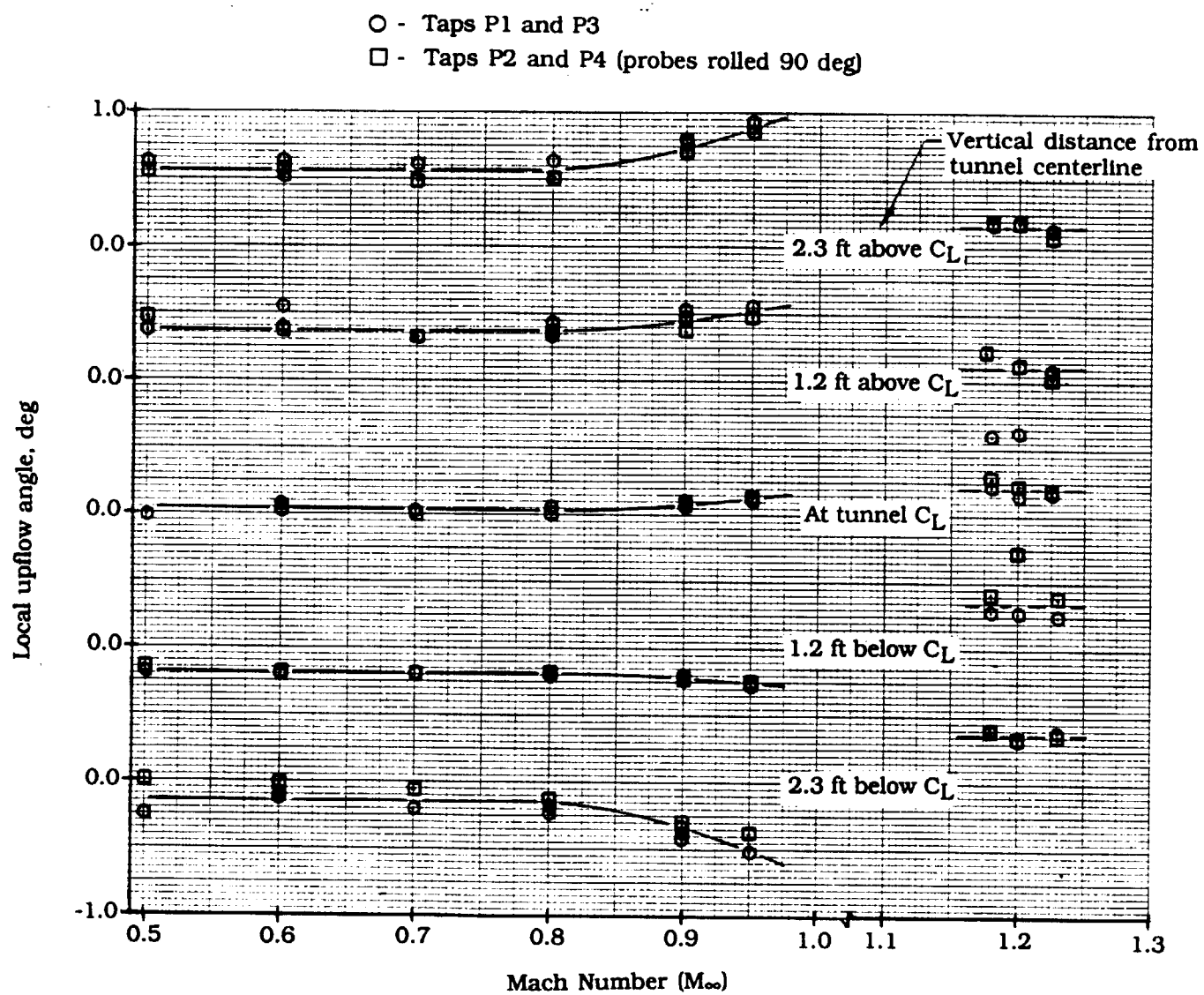

Figure 25. - Tunnel upflow angles at TS 133.6 across vertical plane through tunnel centerline. Upflow angles are based on probe calibration results.

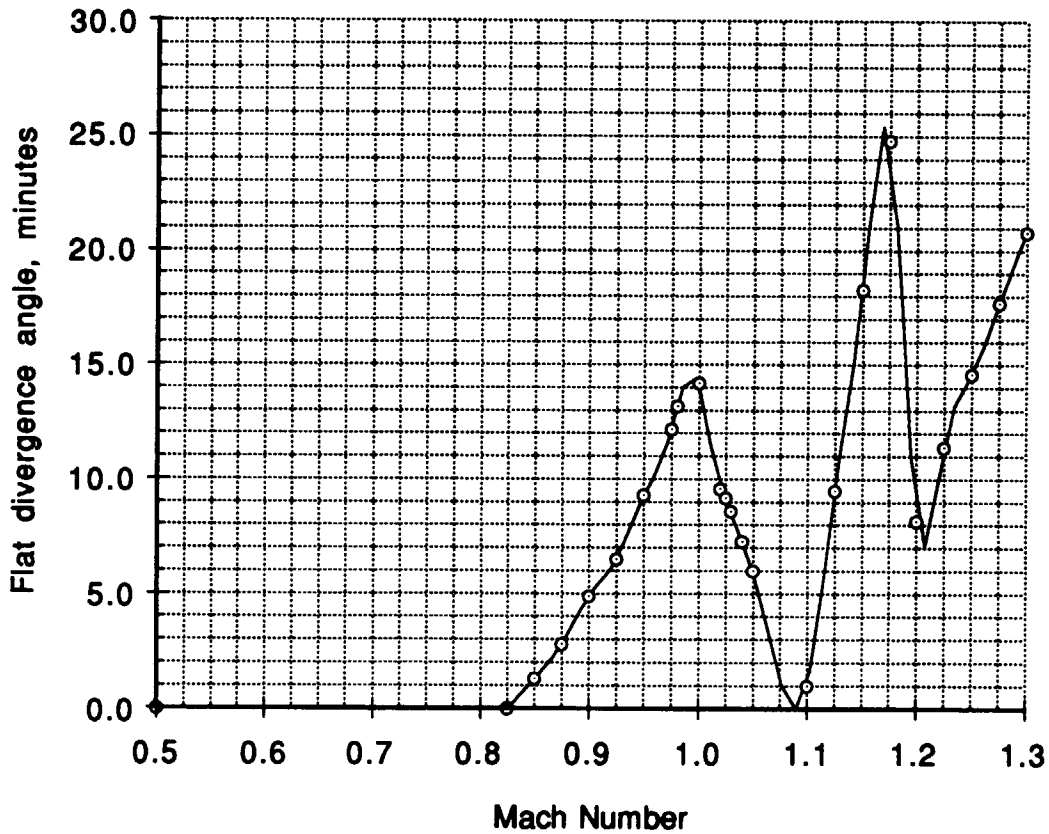

Figure 26. - Test section flat divergence schedule for zero centerline Mach gradient (dM/dX = 0).

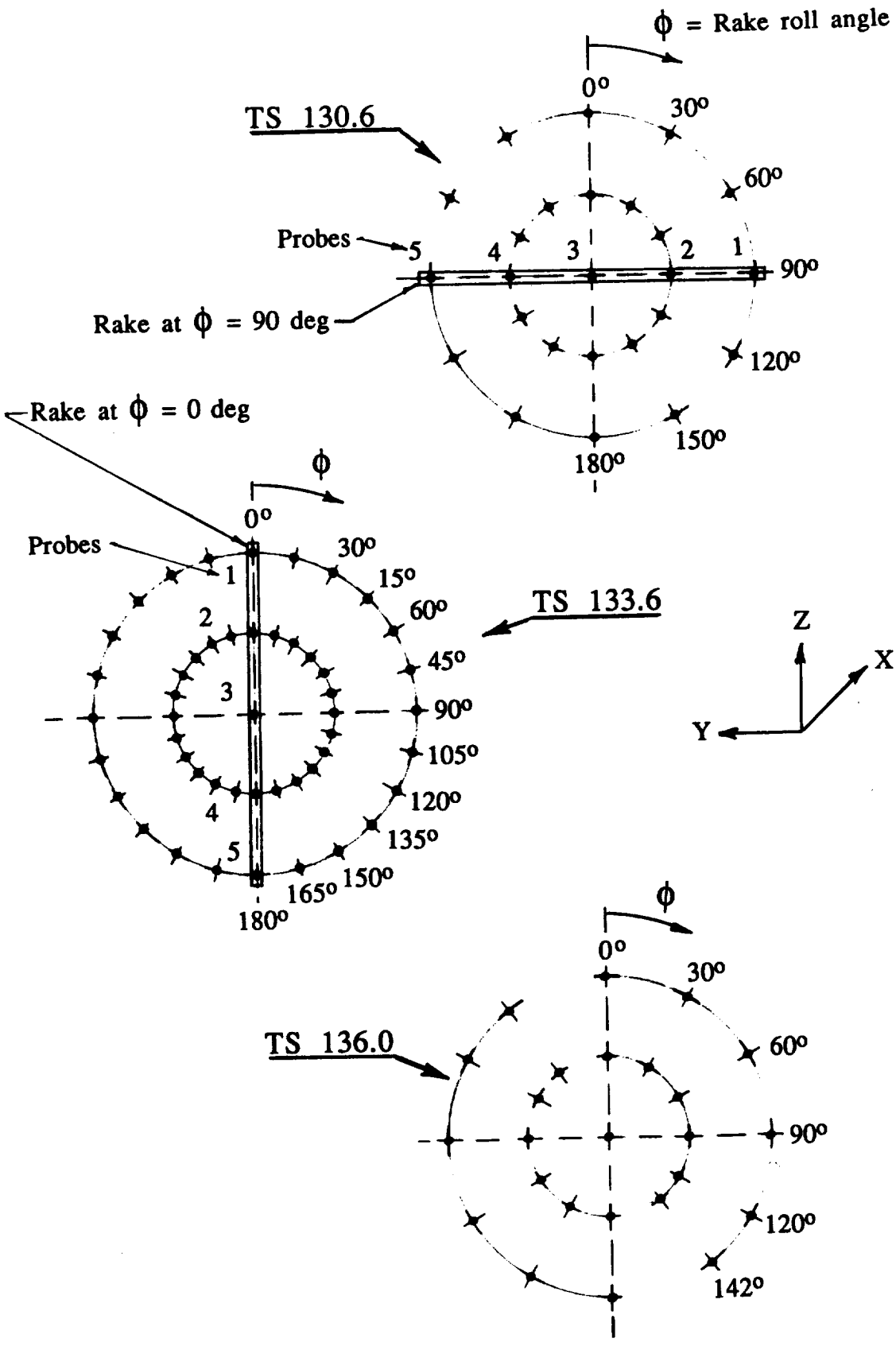

Figure 27. - Test section flowfield survey locations and roll angle increments (looking downstream).

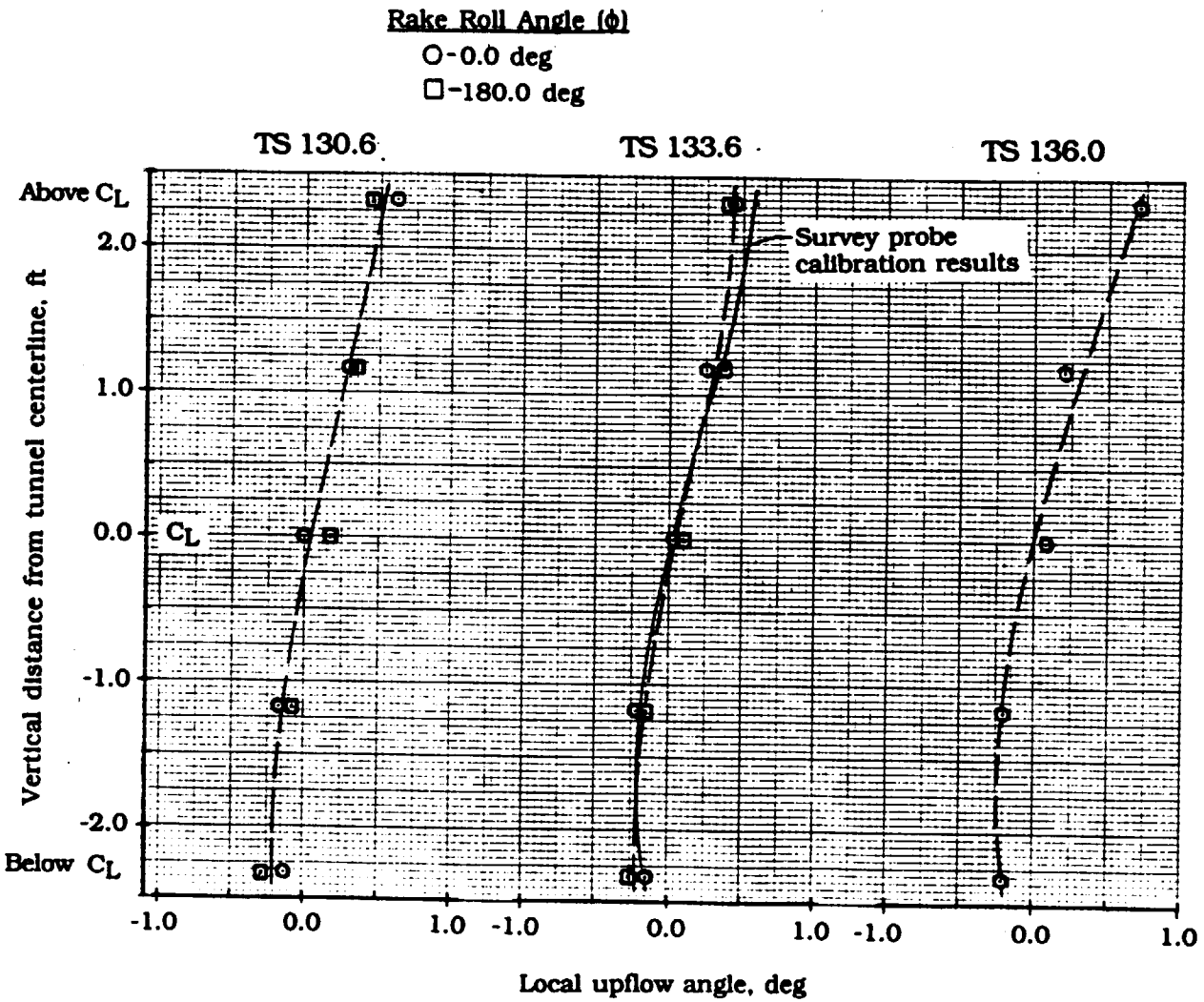

Figure 28. - Variation in tunnel upflow angles across vertical plane through the tunnel centerline at tunnel stations 130.6, 133.6 and 136.0 (M = 0.80).

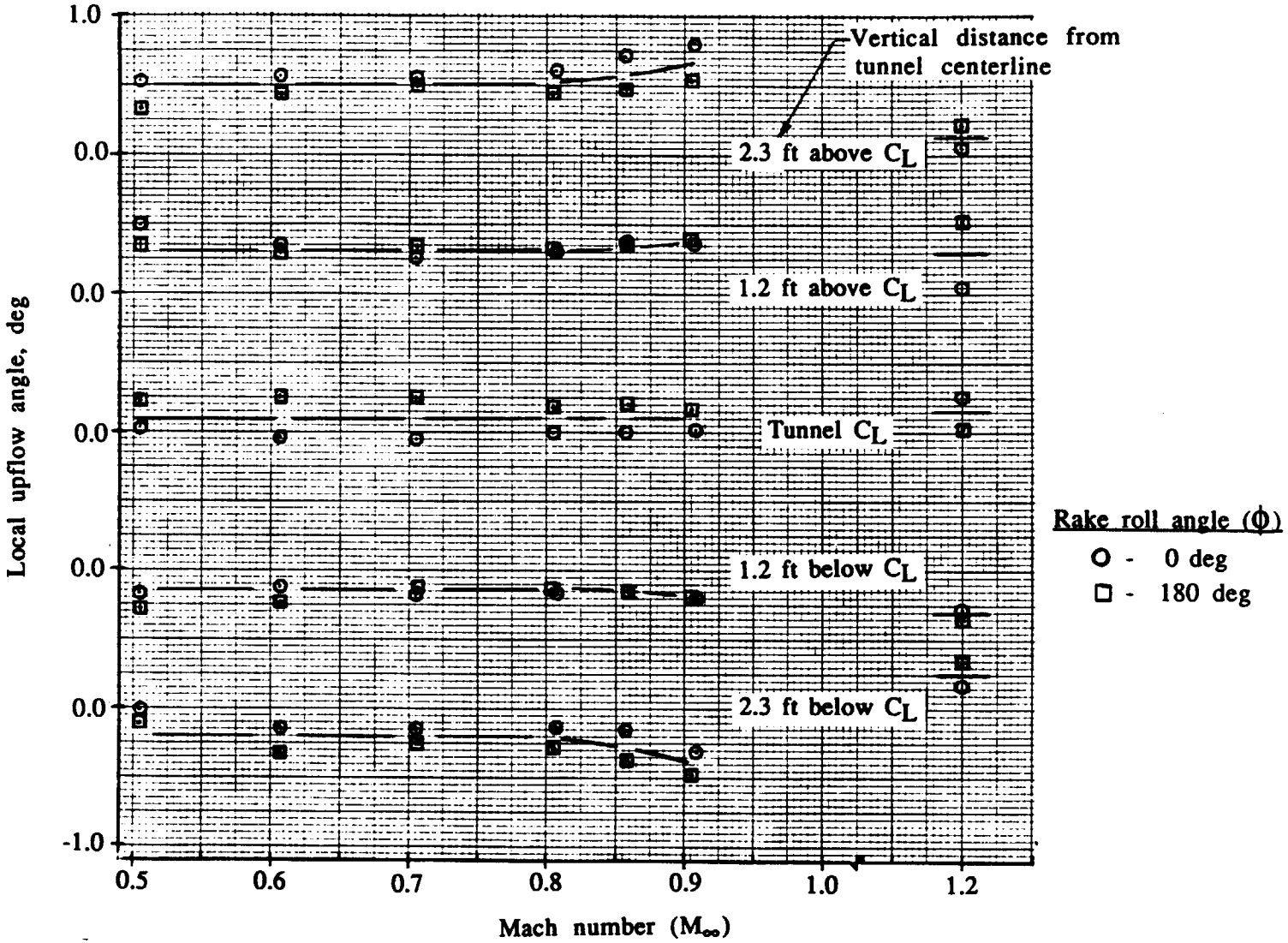

a.) Tunnel station 130.6.

Figure 29. - Test section upflow angles across vertical plane containing tunnel centerline at tunnel stations 130.6, 133.6 and 136.0. Upflow angles obtained during flowfield surveys.

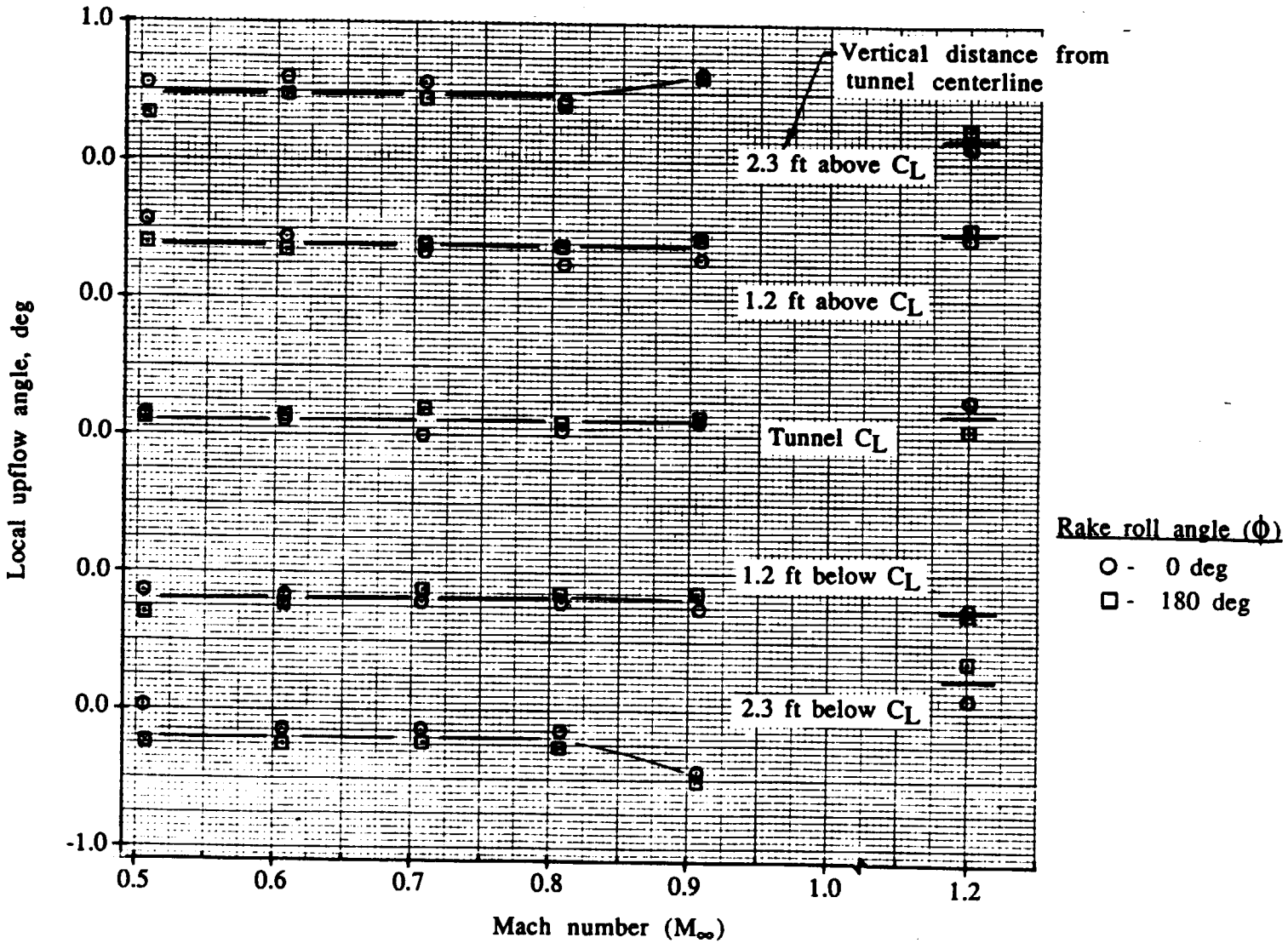

b.) Tunnel station 133.6.

Figure 29. - Continued.

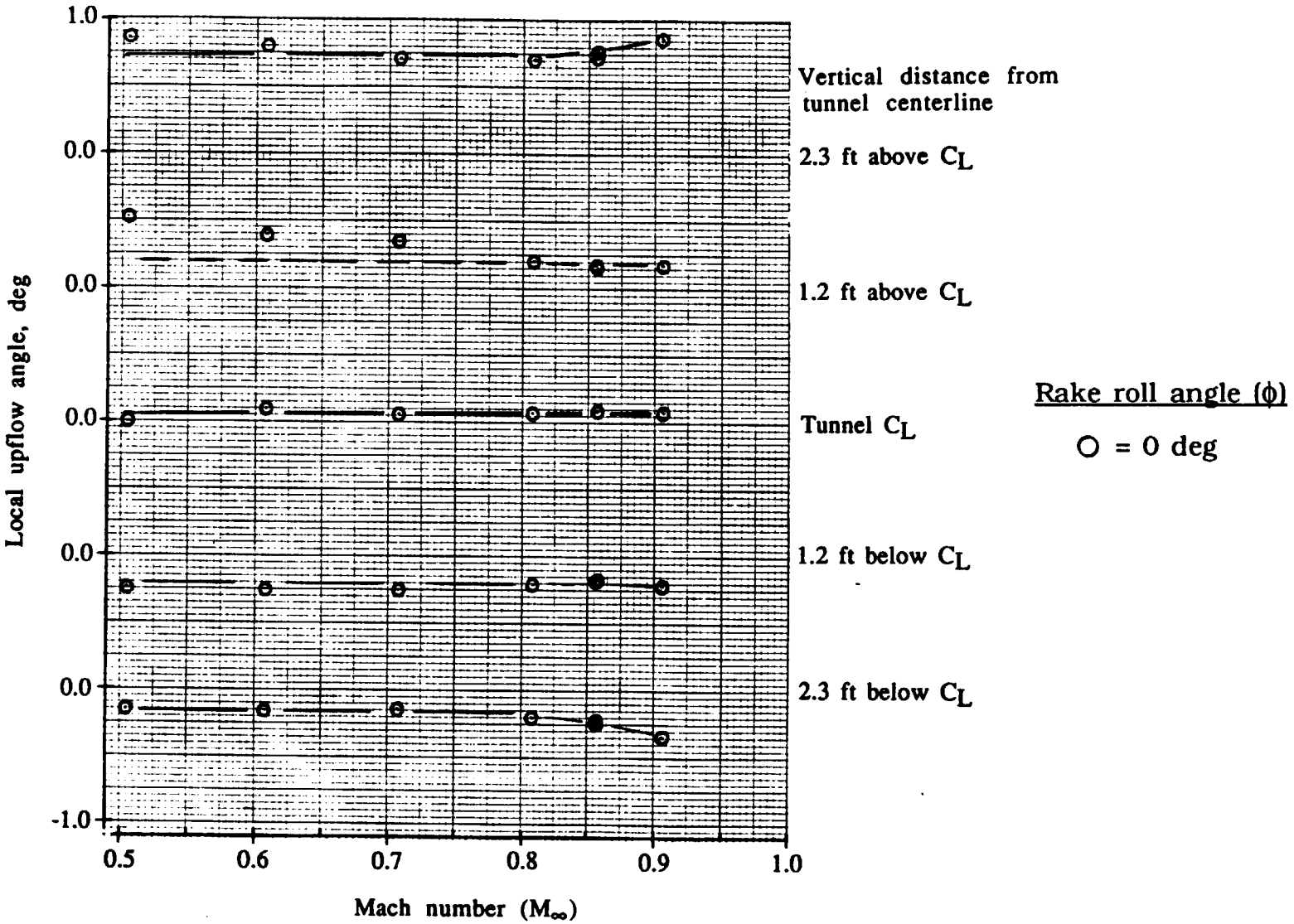

c.) Tunnel station 136.0.

Figure 29. - Concluded.

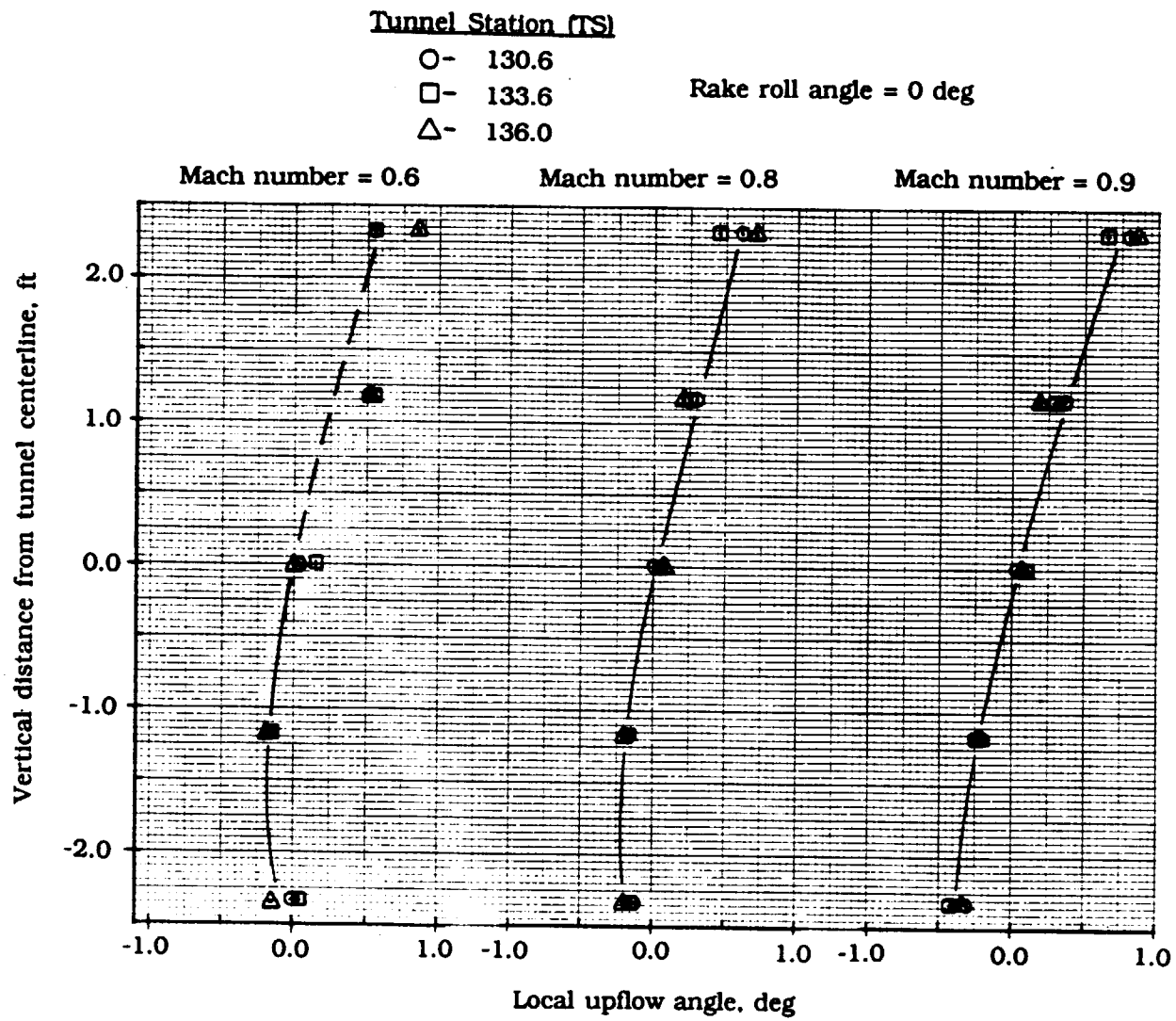

Figure 30. - Cross-plot of test section upflow characteristics at tunnel stations 130.6, 133.6 and 136.0.

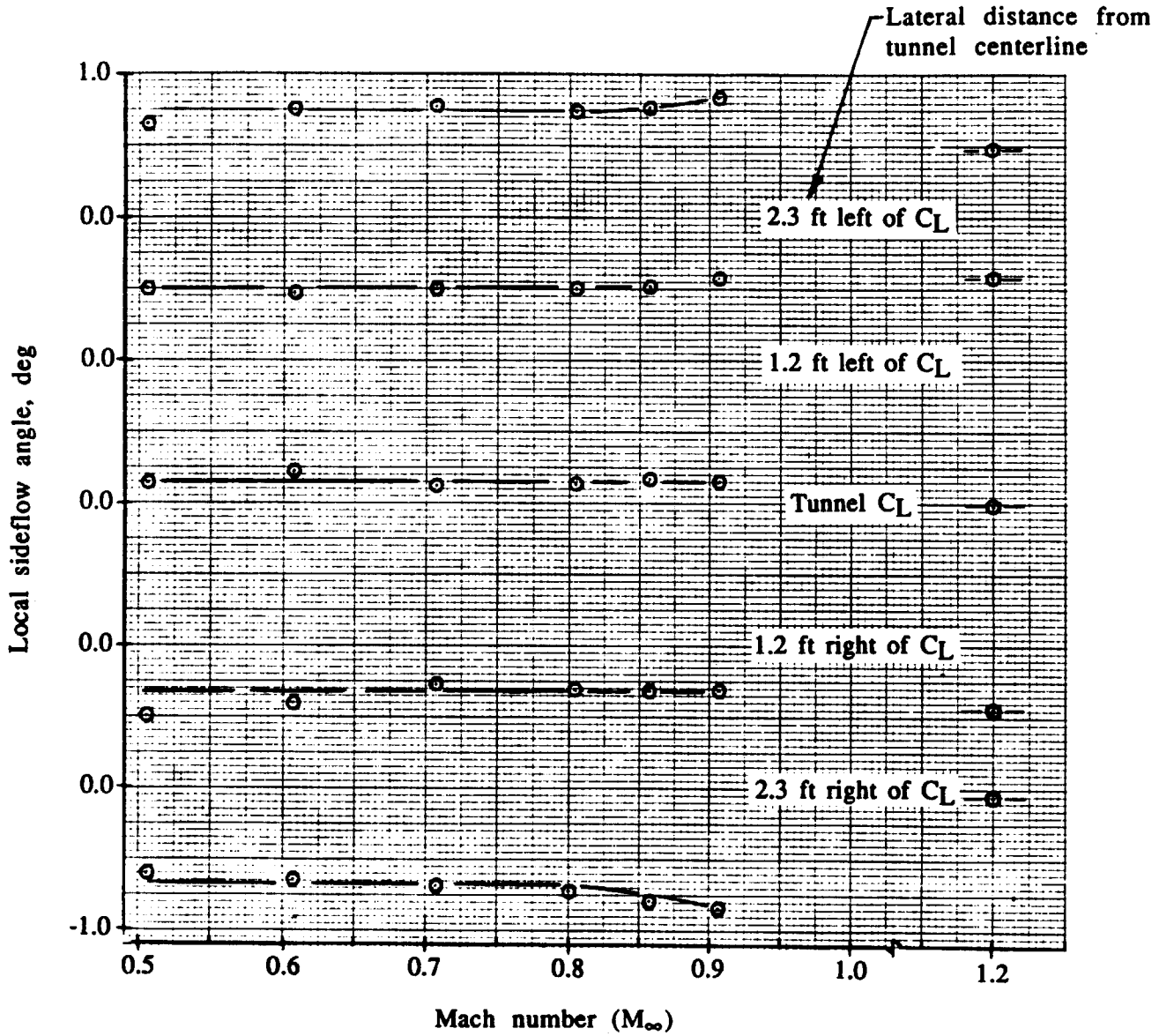

a.) Tunnel station 130.6.

Figure 31. - Test section sideflow angle across horizontal plane containing tunnel centerline at tunnel stations 130.6, 133.6 and 136.0. Data taken during flowfield survey with rake rolled (ϕ) to 90 deg.

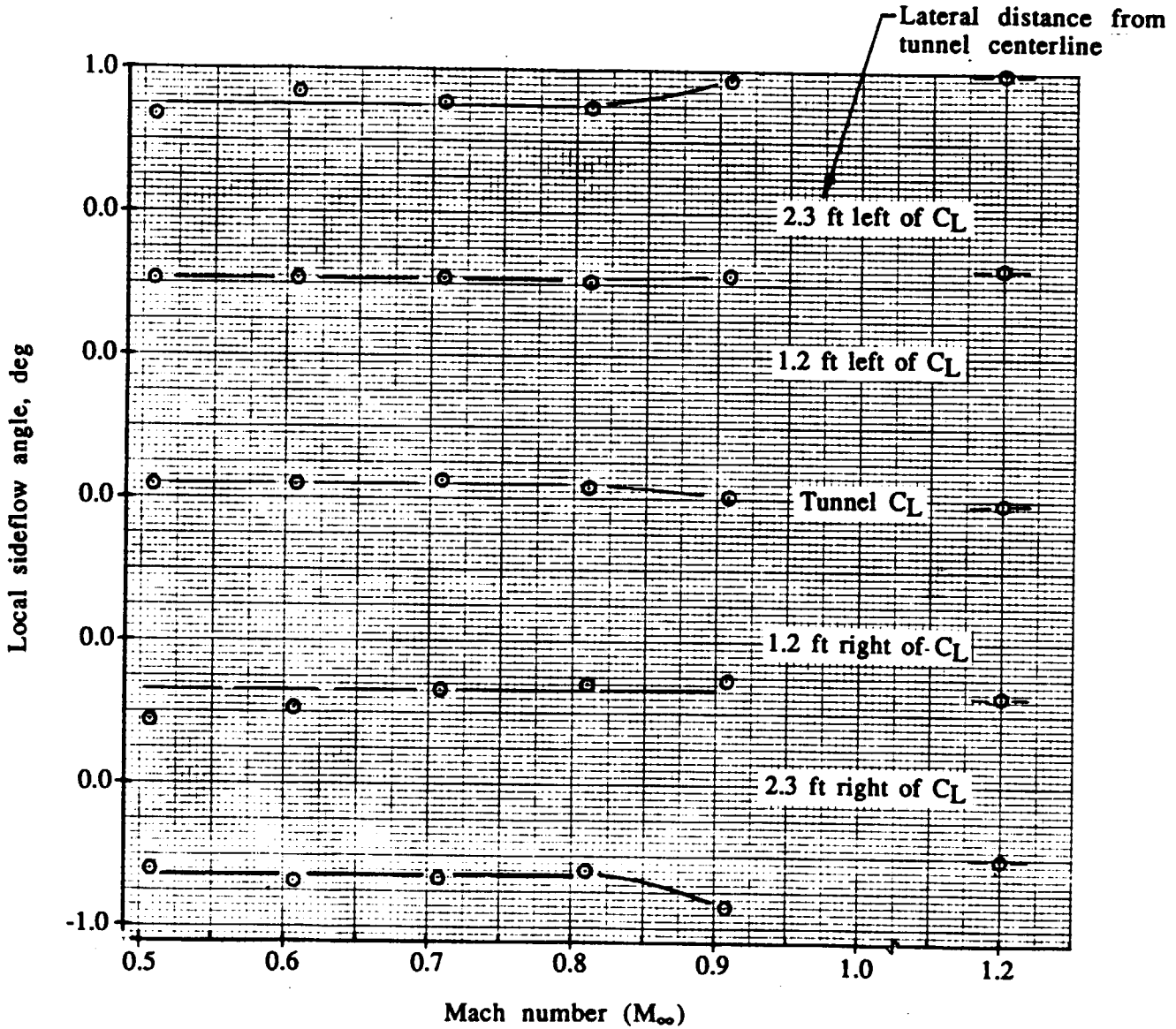

b.) Tunnel station 133.6.

Figure 31. - Continued.

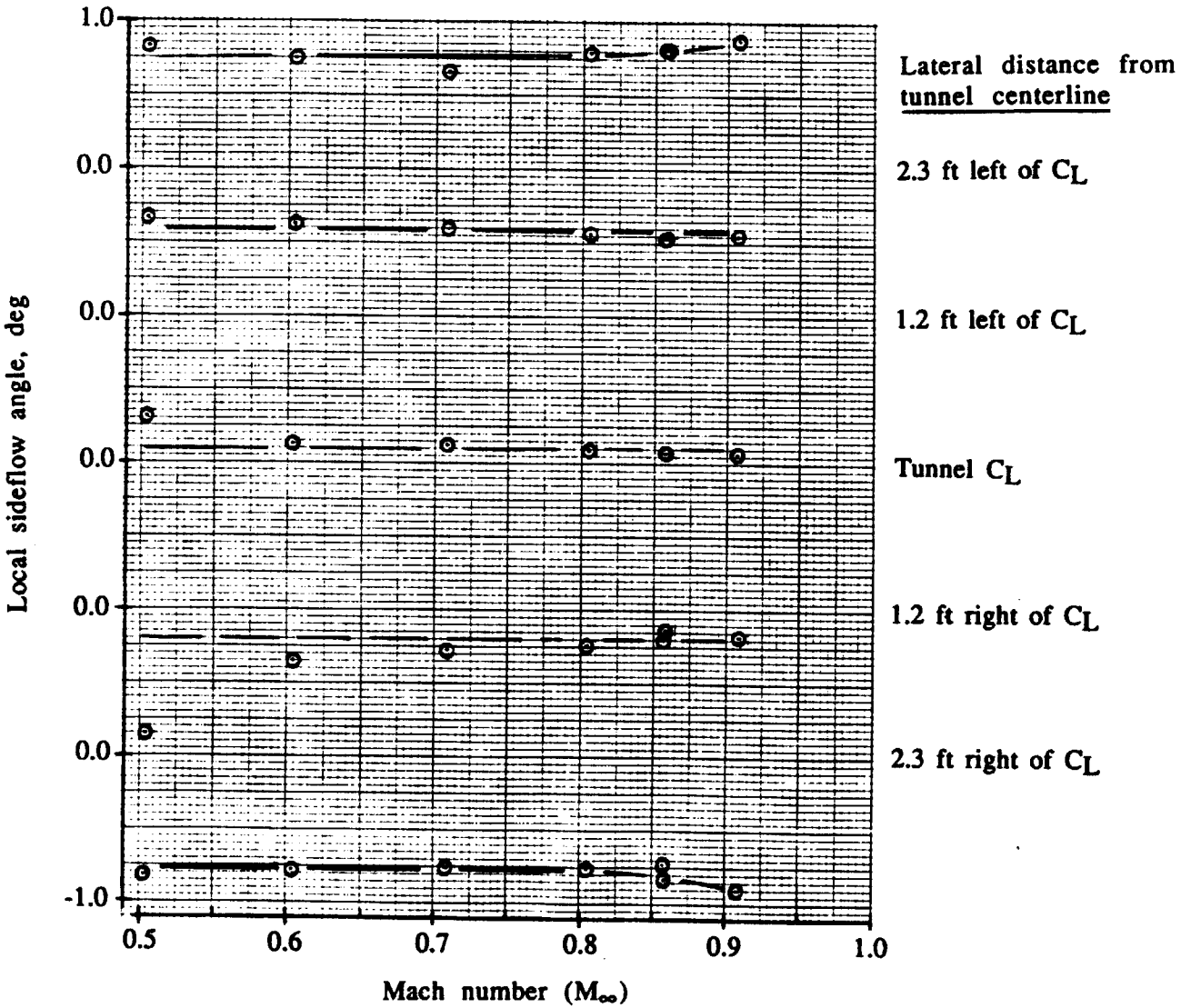

c.) Tunnel station 136.0.

Figure 31. - Concluded.

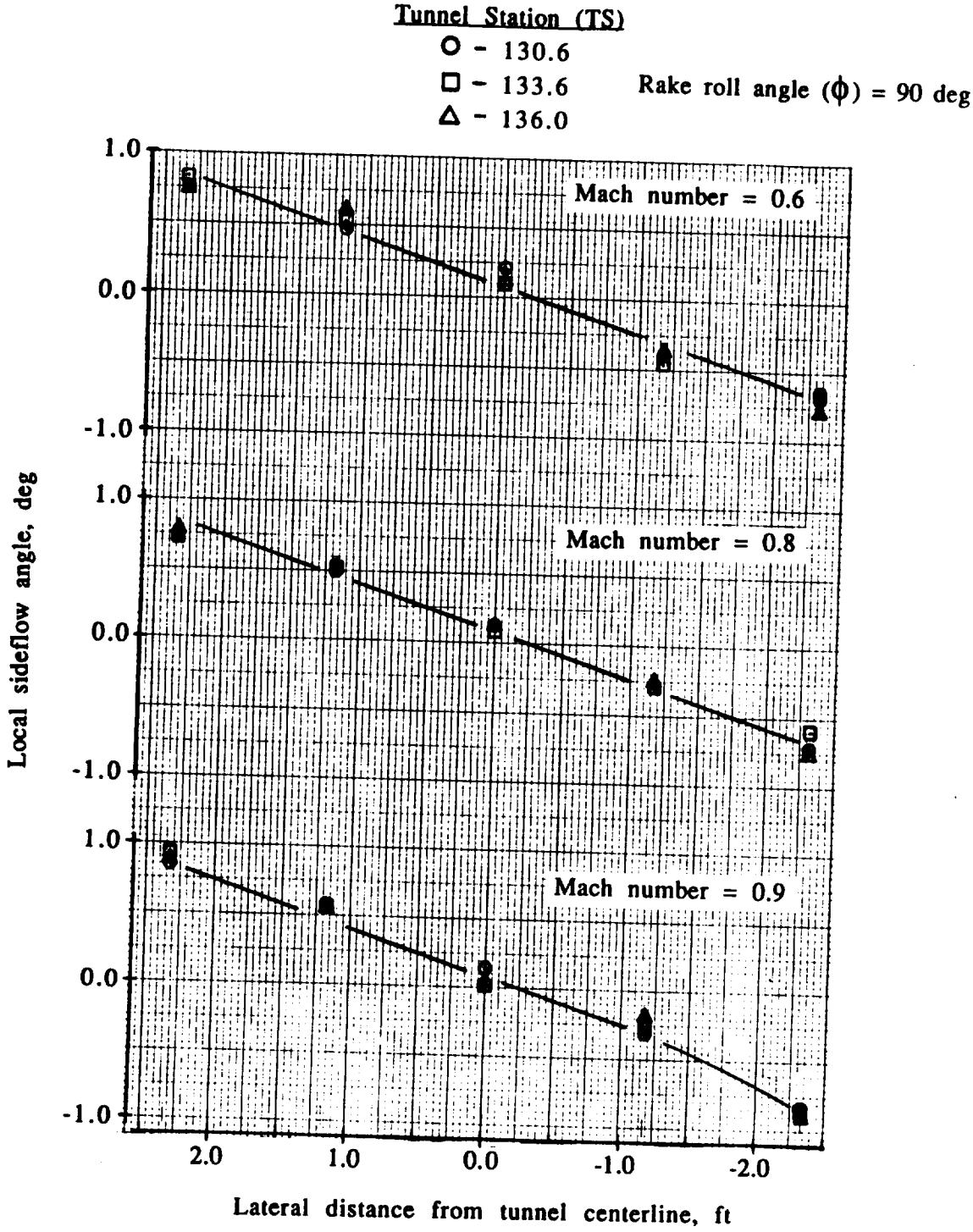

Figure 32. - Cross-plot of test section sideflow characteristics at tunnel stations 130.6, 133.6 and 136.0.

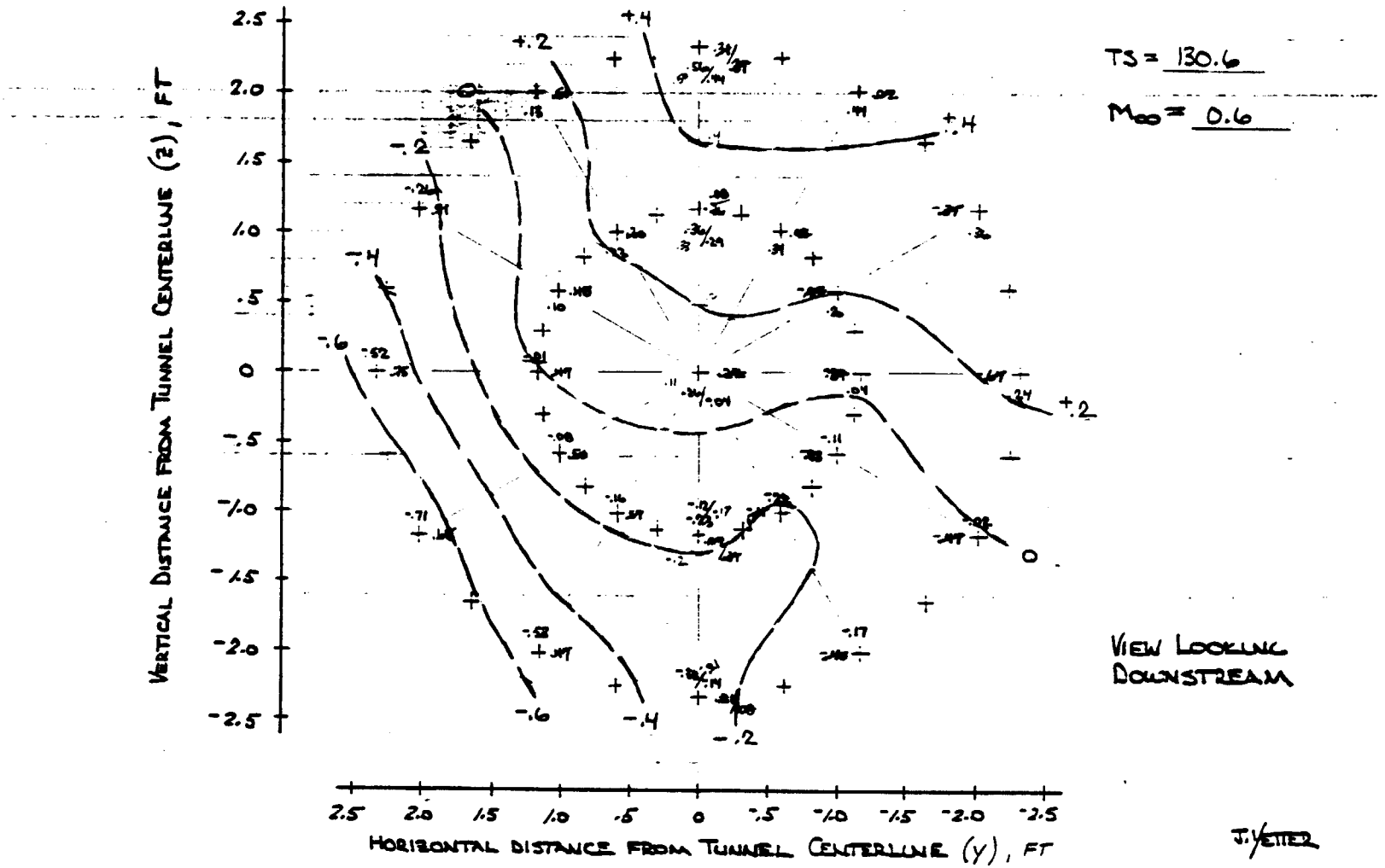

a. Upflow angle contours at Mach 0.6.

Figure 33. - Test section upflow and sideflow angle contours at TS 130.6.

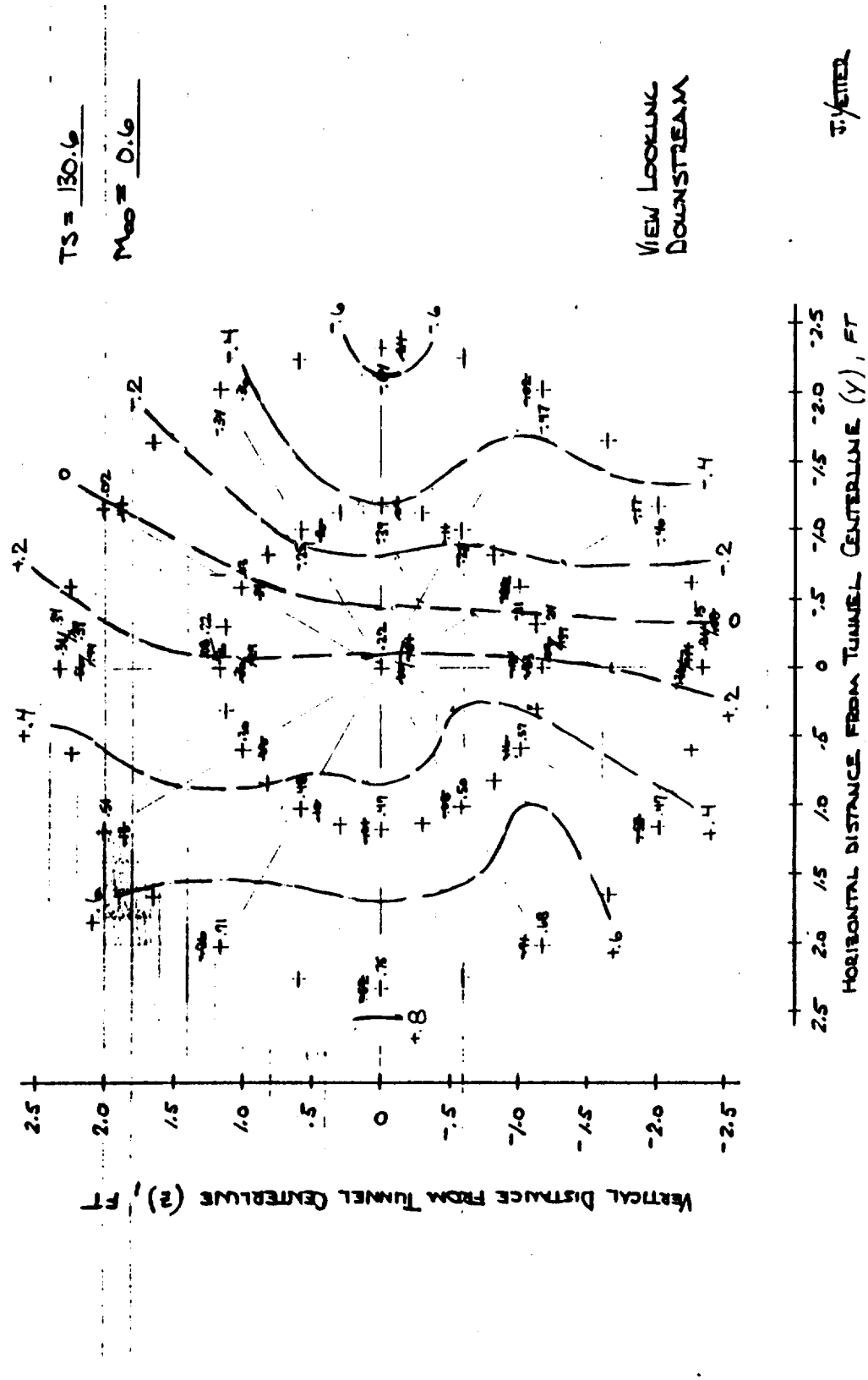

b. Sideflow angle contours at Mach 0.6.

Figure 33. - Continued.

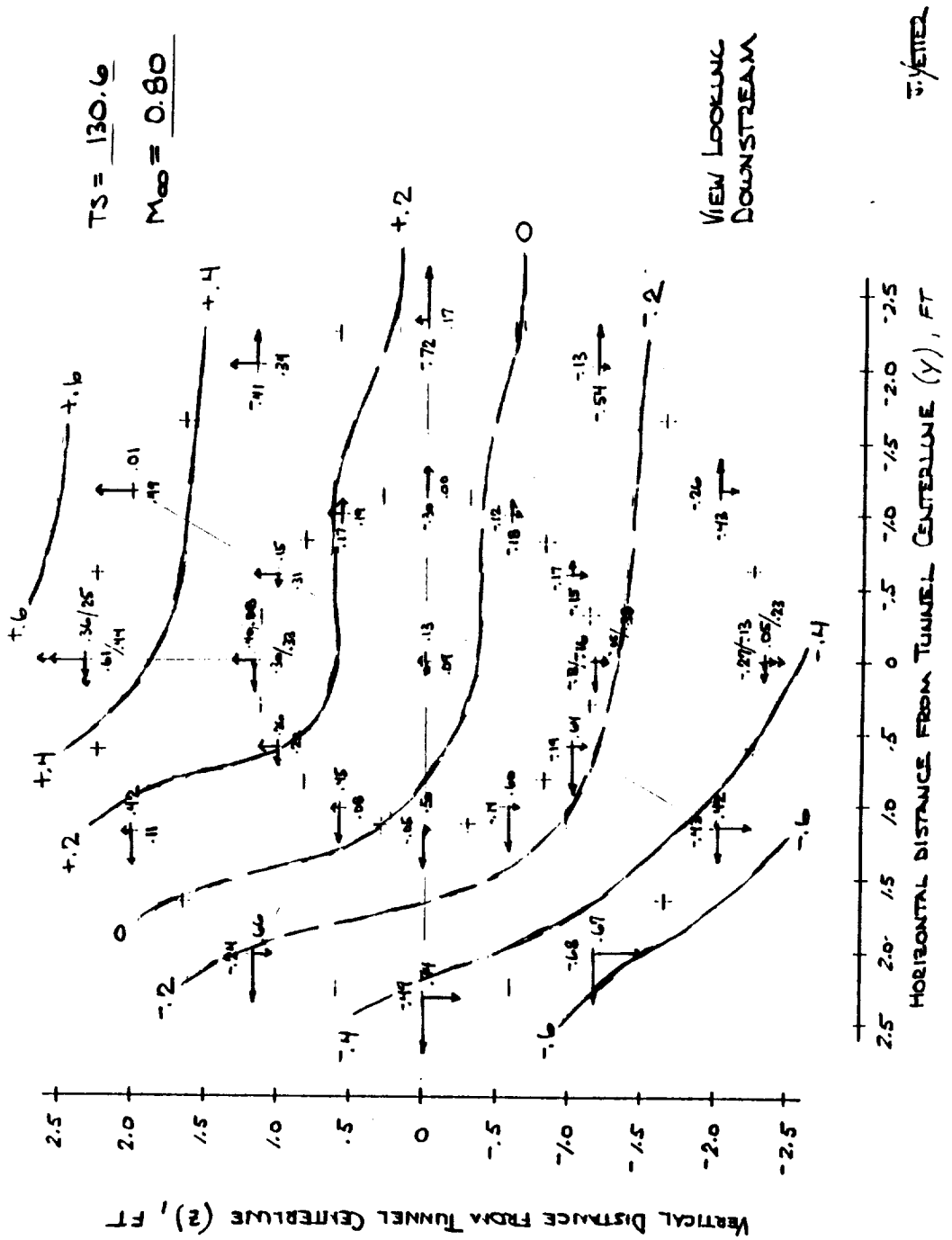

c. Upflow angle contours at Mach 0.8.

Figure 33. - Continued.

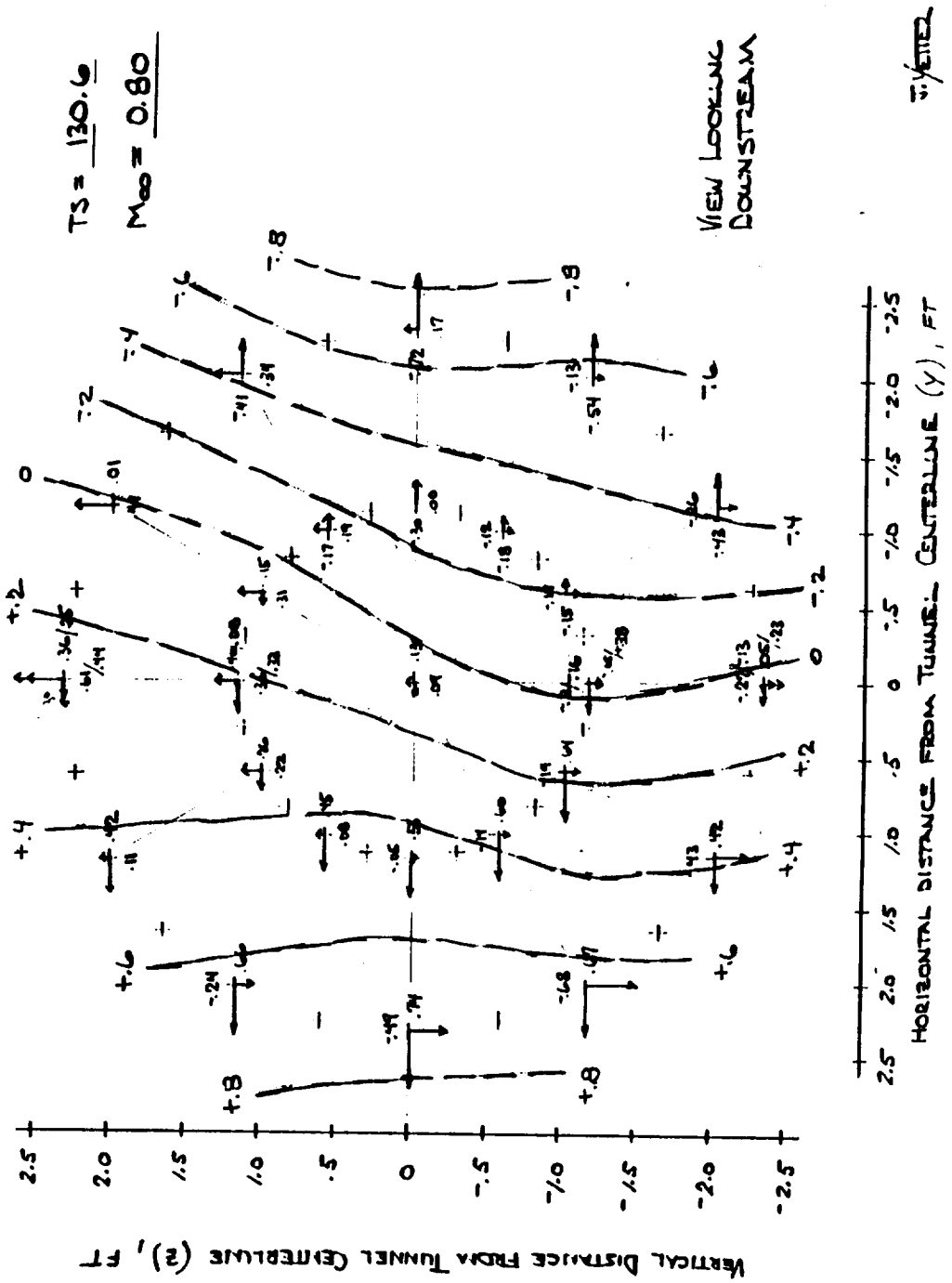

d. Sideflow angle contours at Mach 0.8.

Figure 33. - Continued.

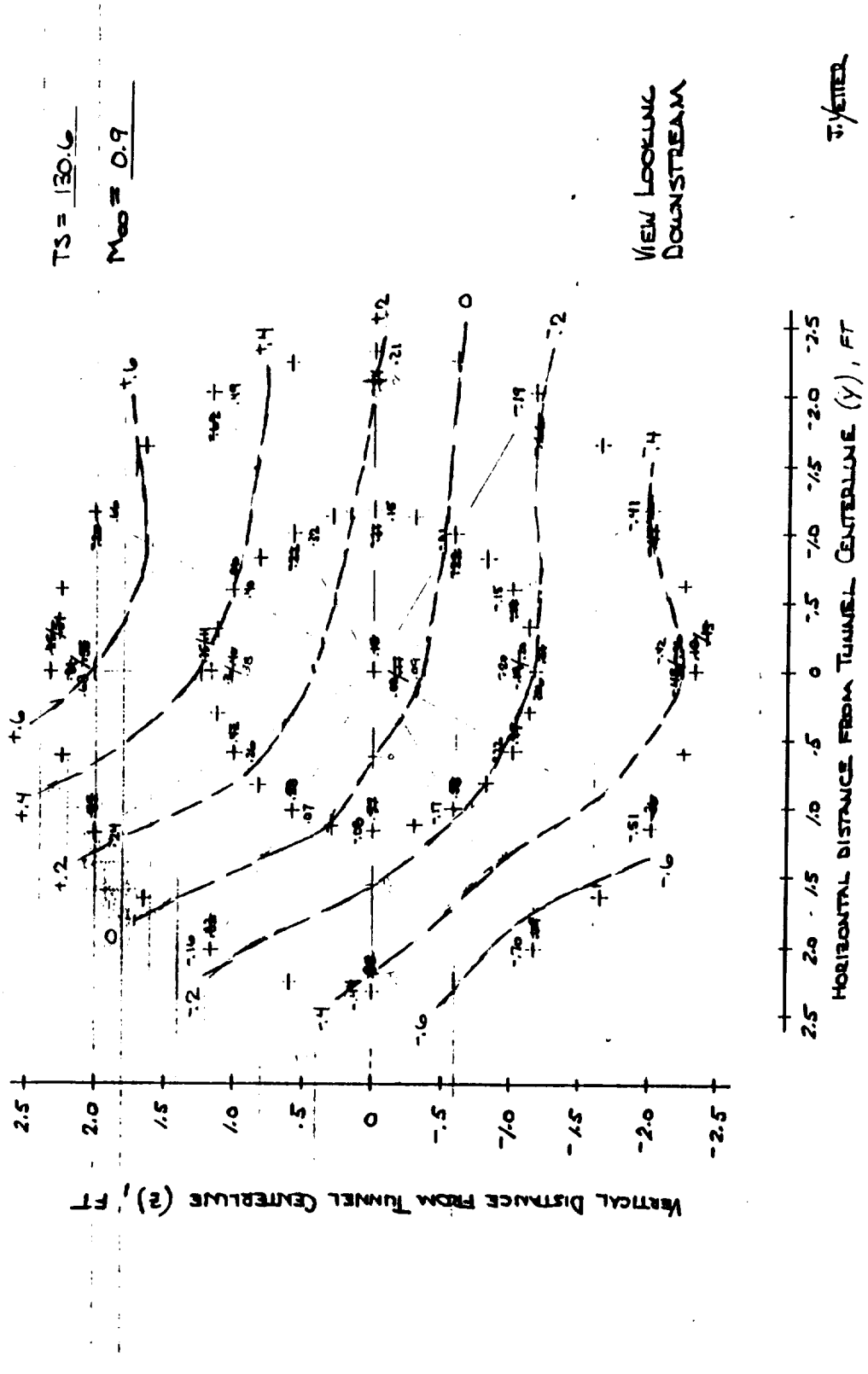

e. Upflow angle contours at Mach 0.9.

Figure 33. - Continued.

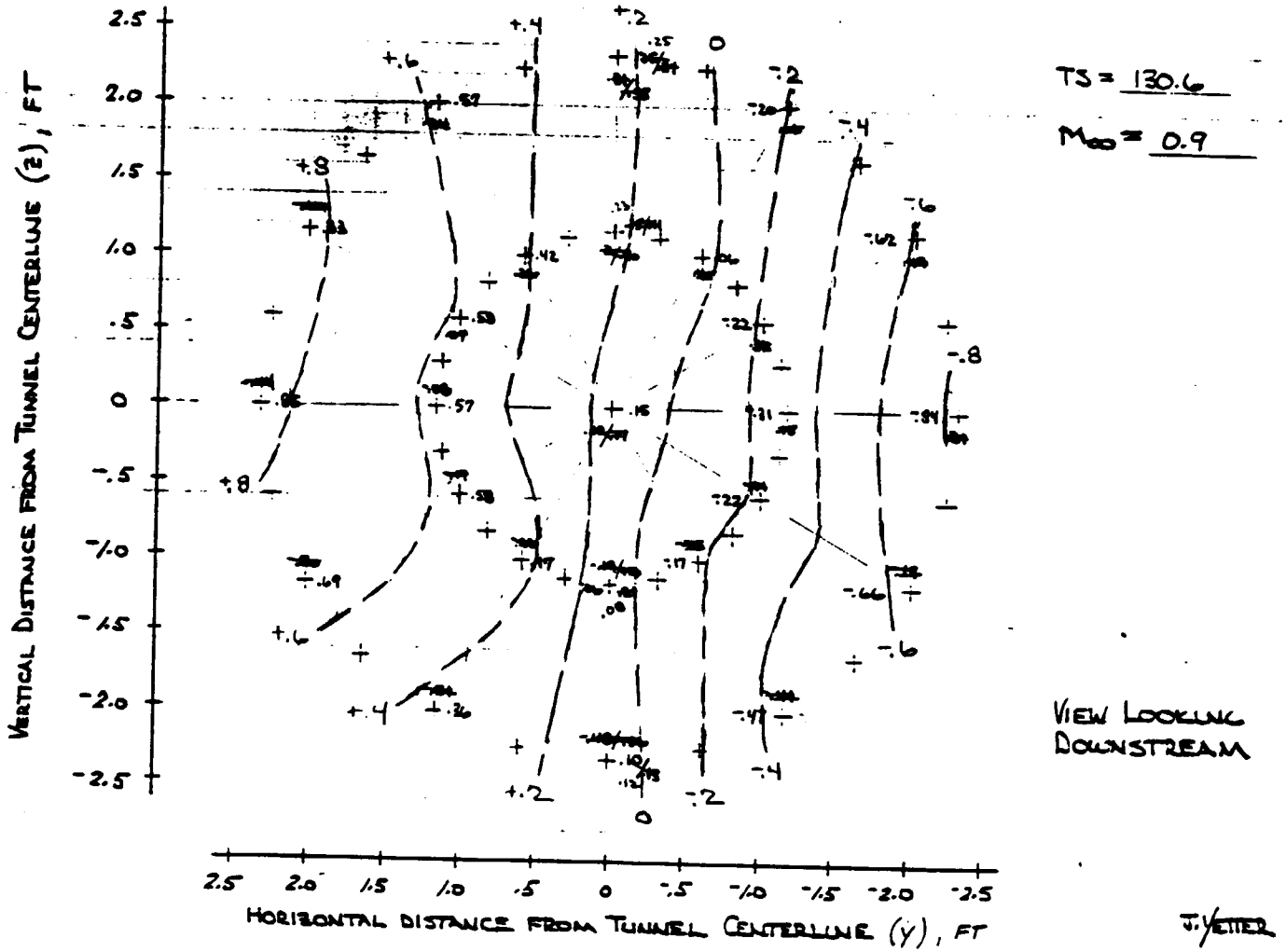

f. Sideflow angle contours at Mach 0.9.

Figure 33. - Concluded.

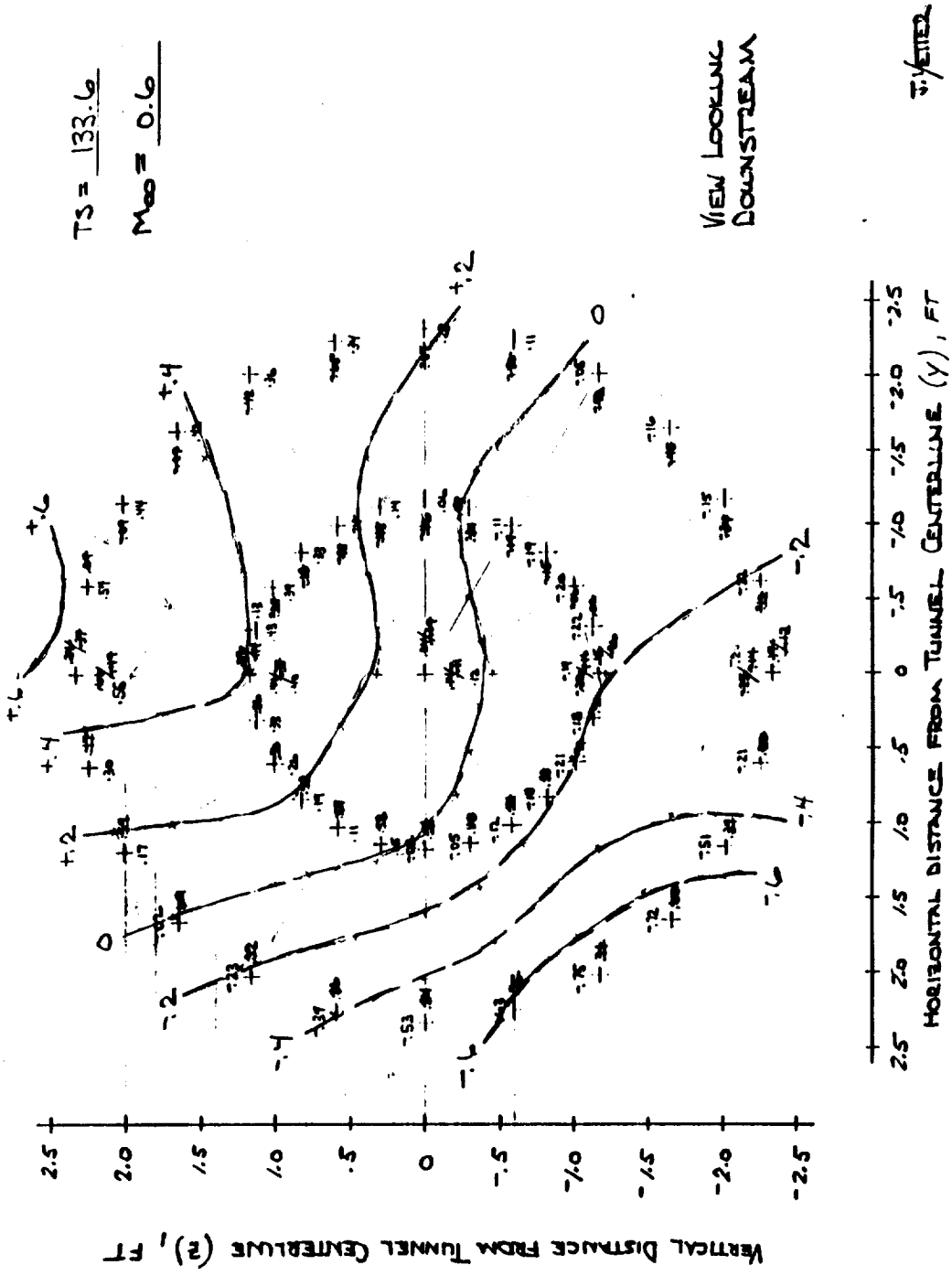

a. Upflow angle contours at Mach 0.6.

Figure 34. - Test section upflow and sideflow angle contours at TS 133.6.

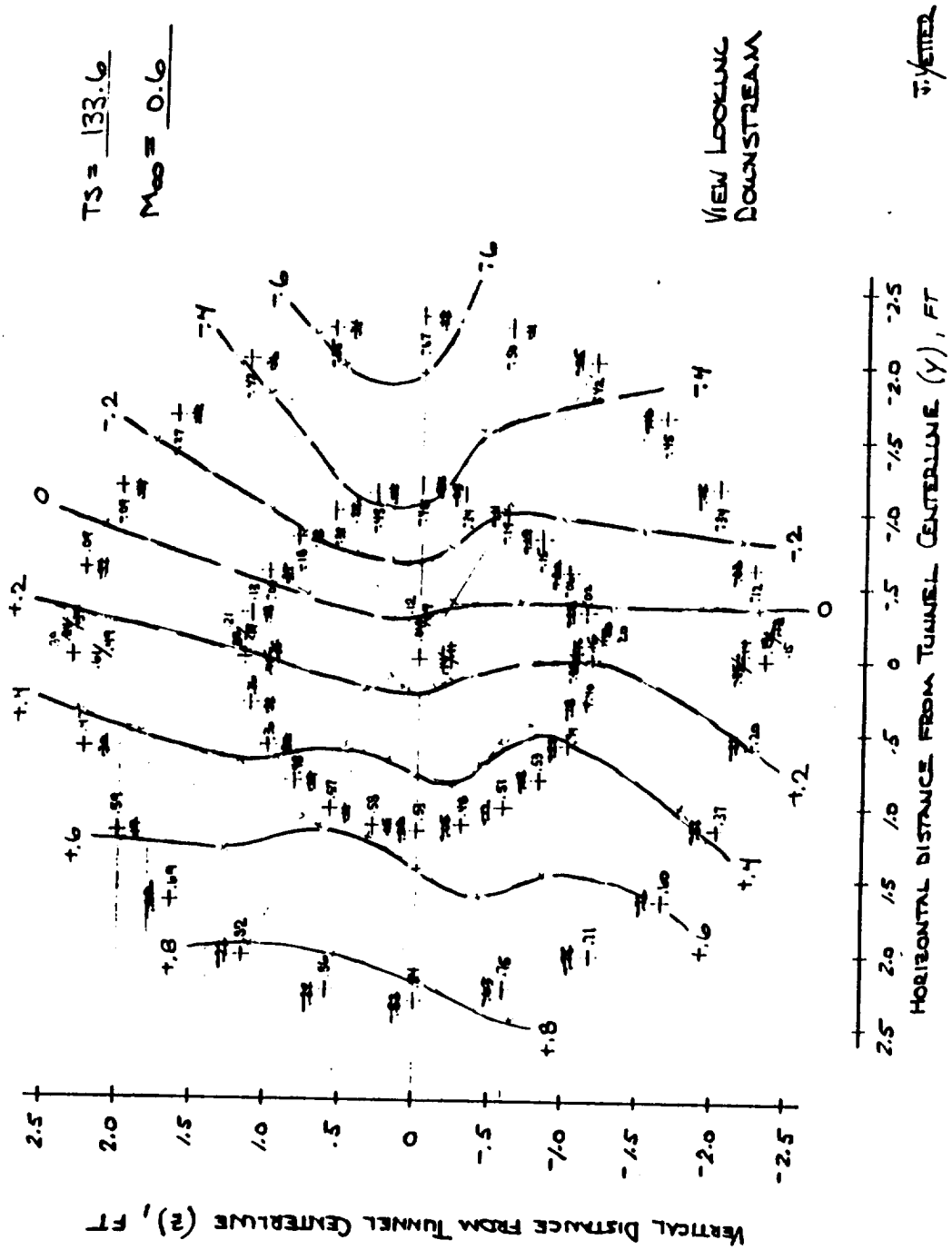

b. Sideflow angle contours at Mach 0.6.

Figure 34. - Continued.

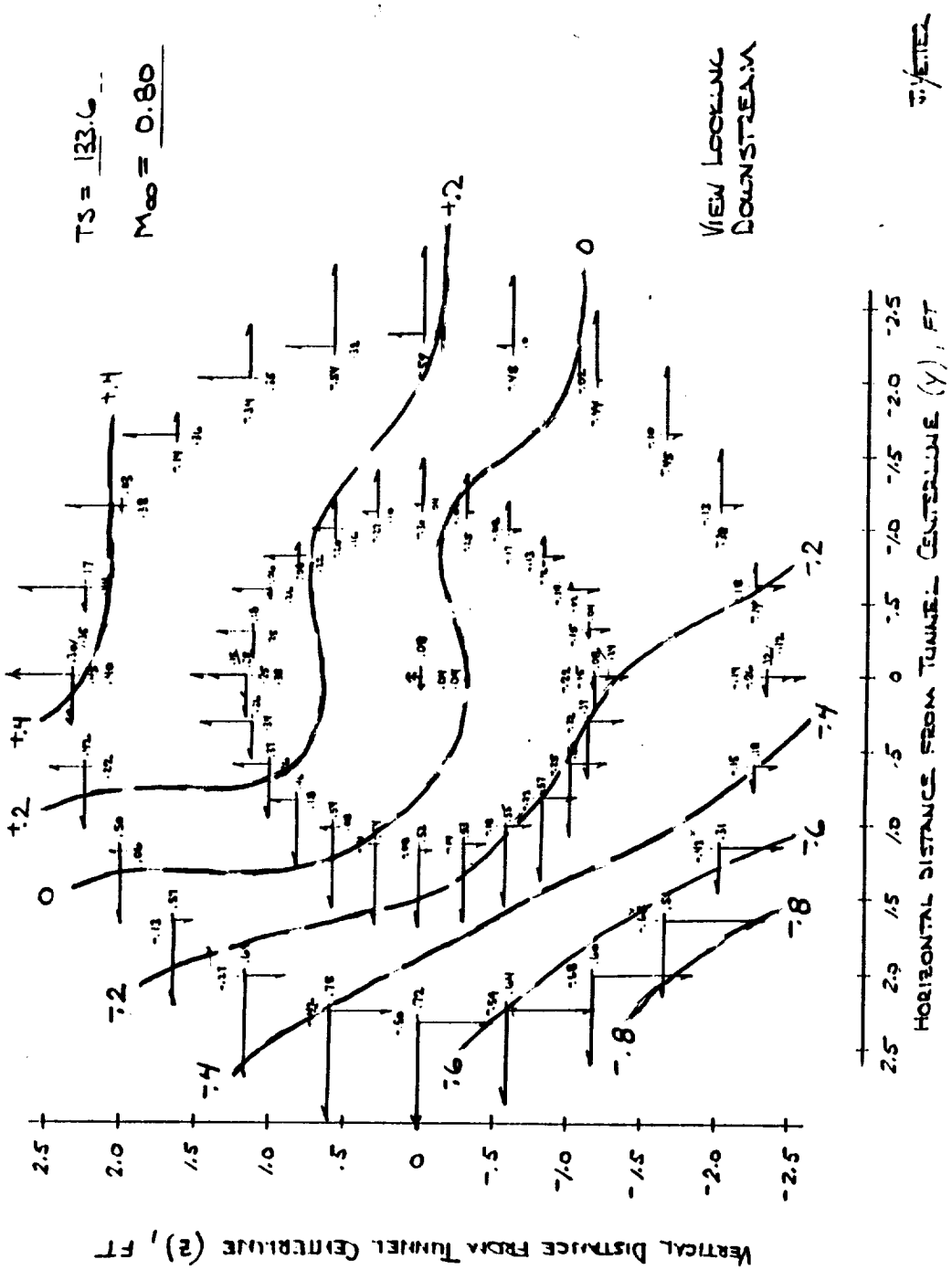

c. Upflow angle contours at Mach 0.8.

Figure 34. - Continued.

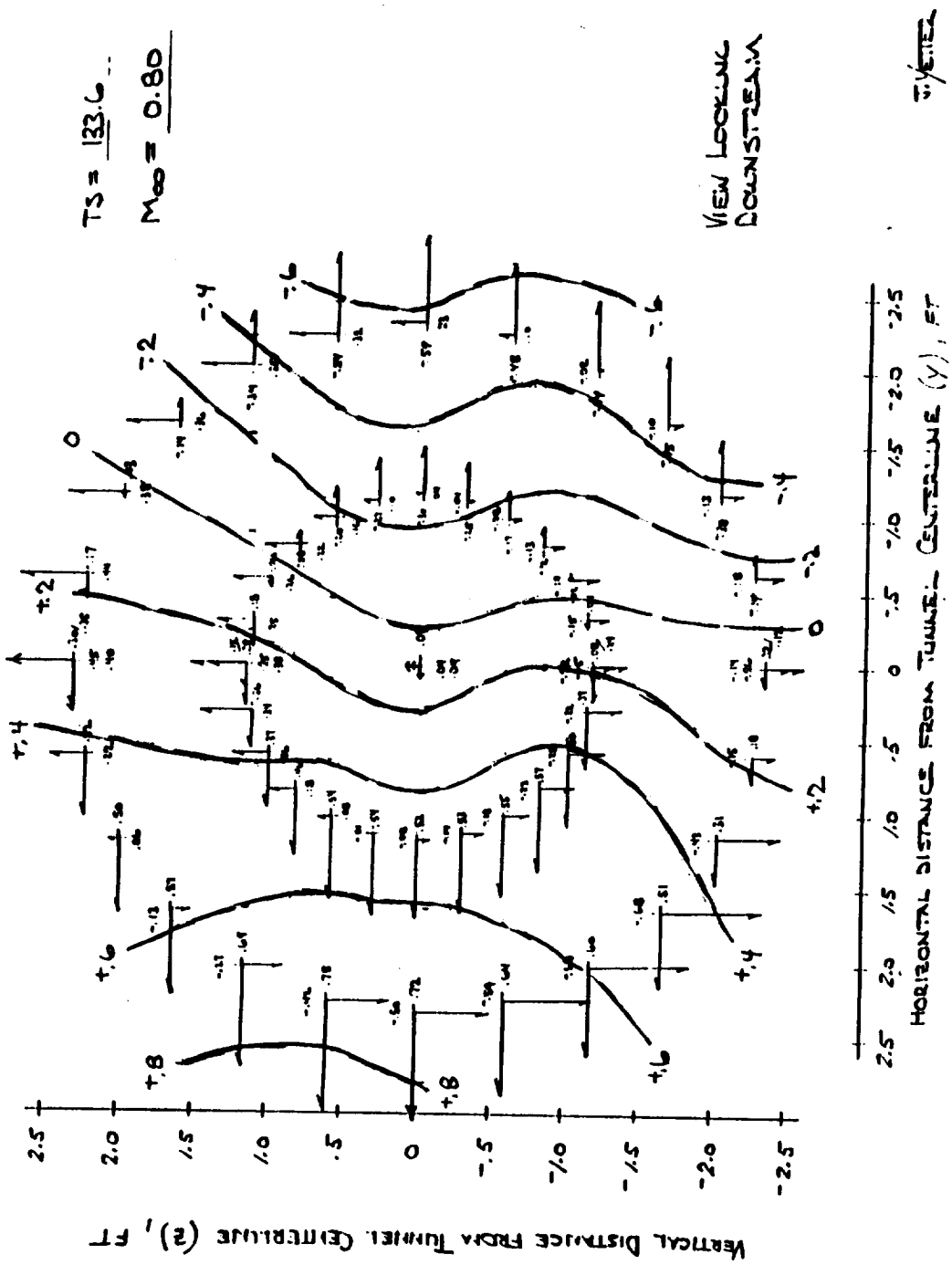

d. Sideflow angle contours at Mach 0.8.

Figure 34. - Continued.

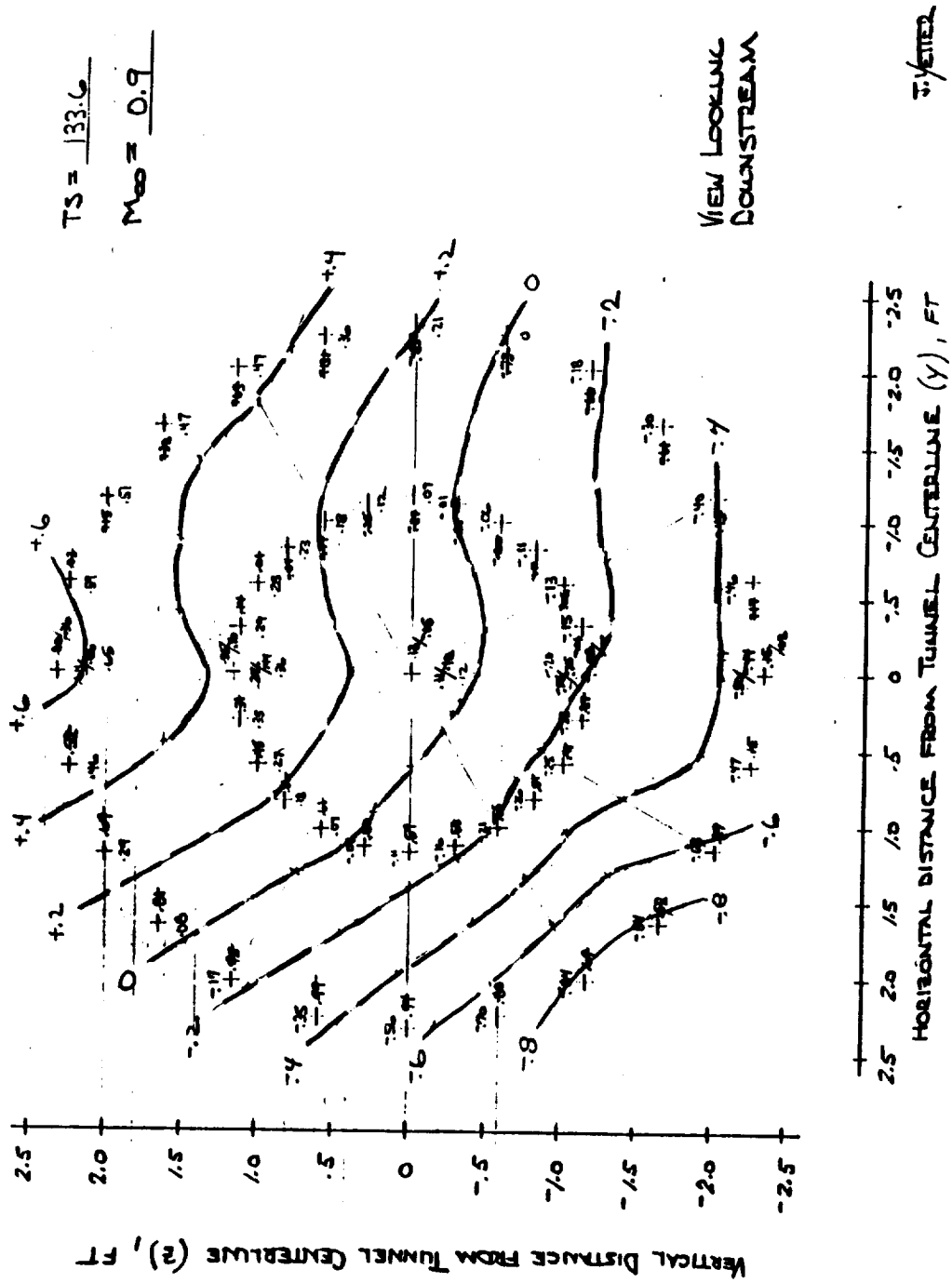

e. Upflow angle contours at Mach 0.9.

Figure 34. - Continued.

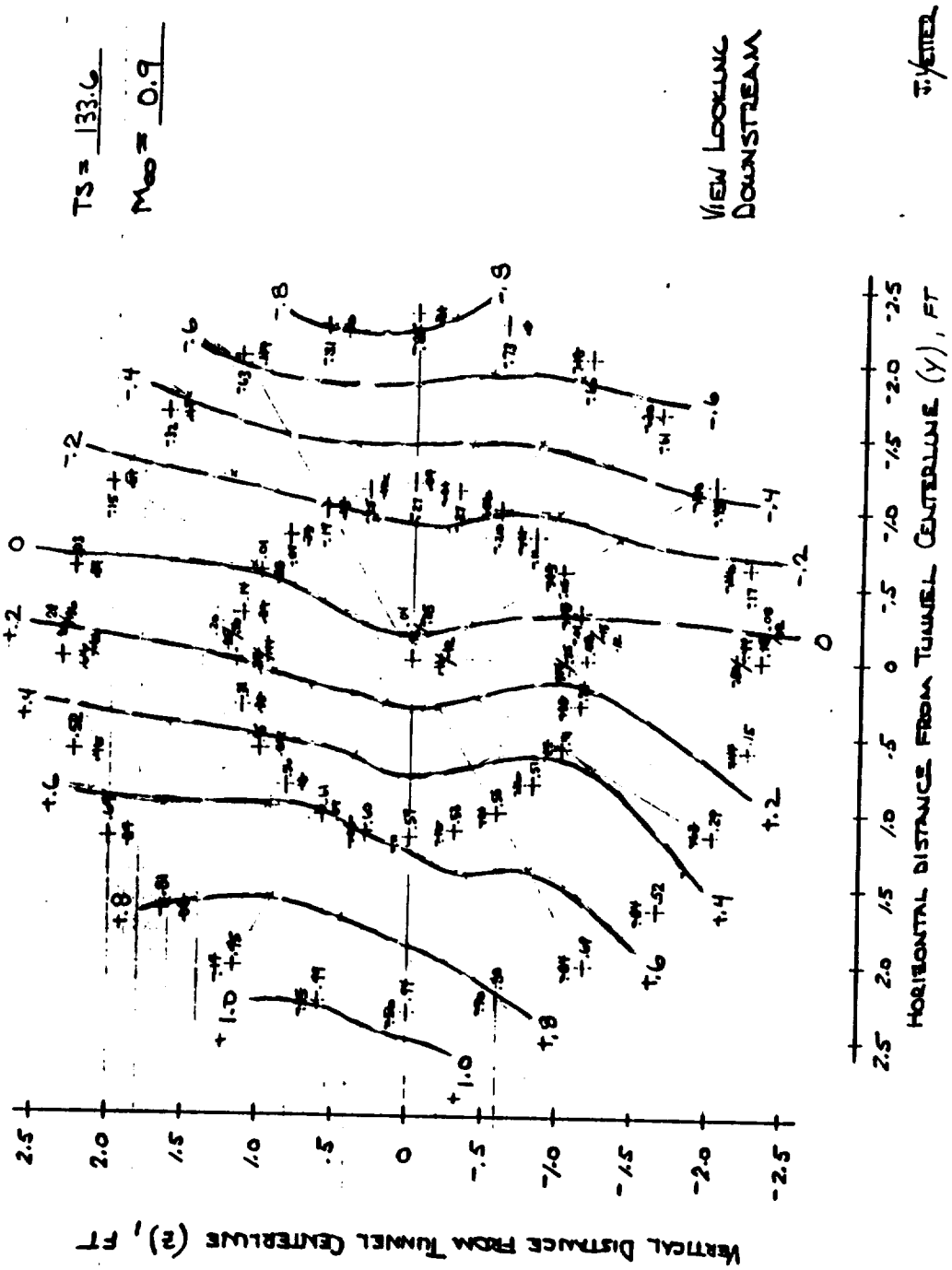

f. Sideflow angle contours at Mach 0.9.

Figure 34. - Concluded.

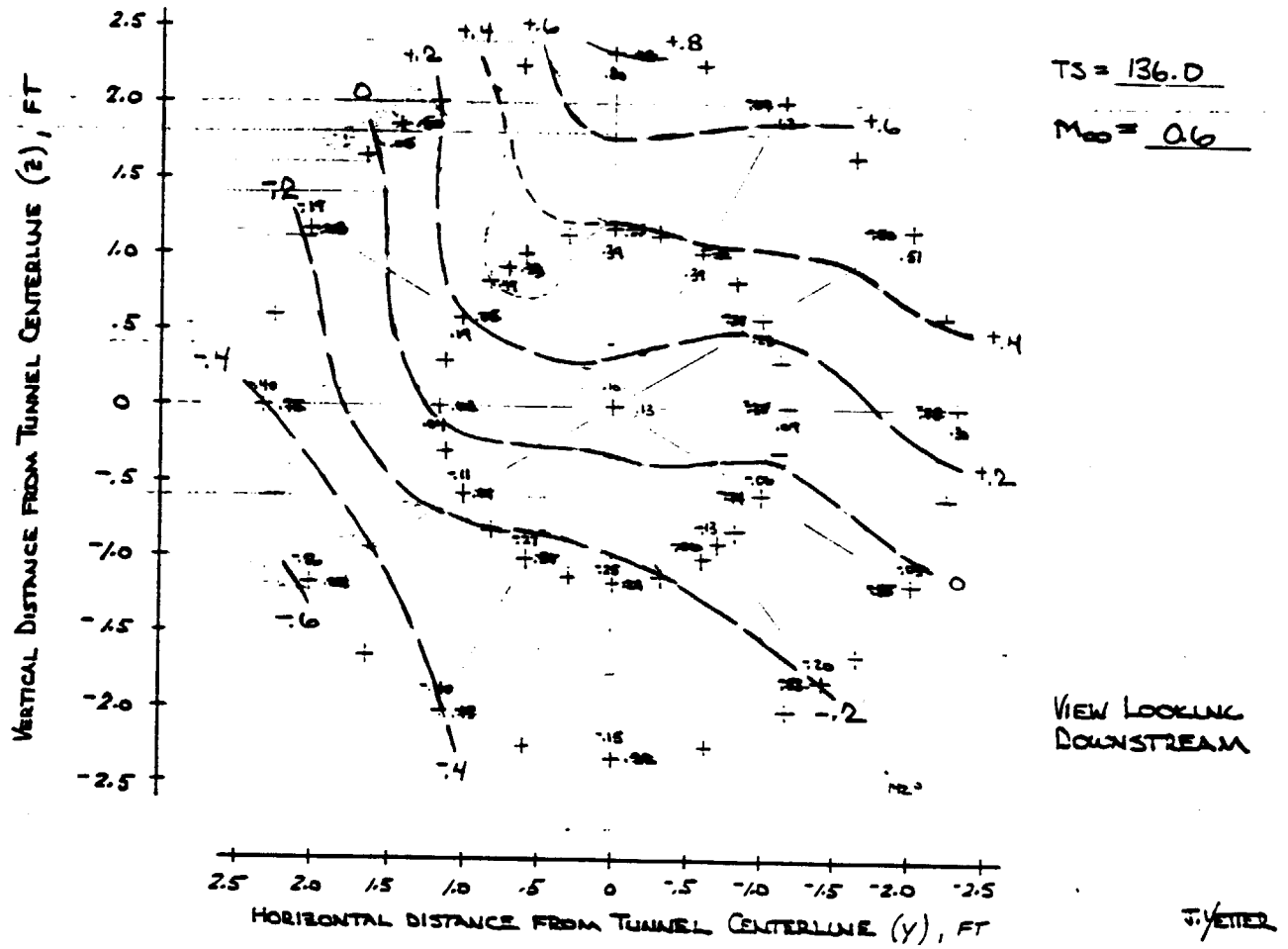

a. Upflow angle contours at Mach 0.6.

Figure 35. - Test section upflow and sideflow angle contours at TS 136.0.

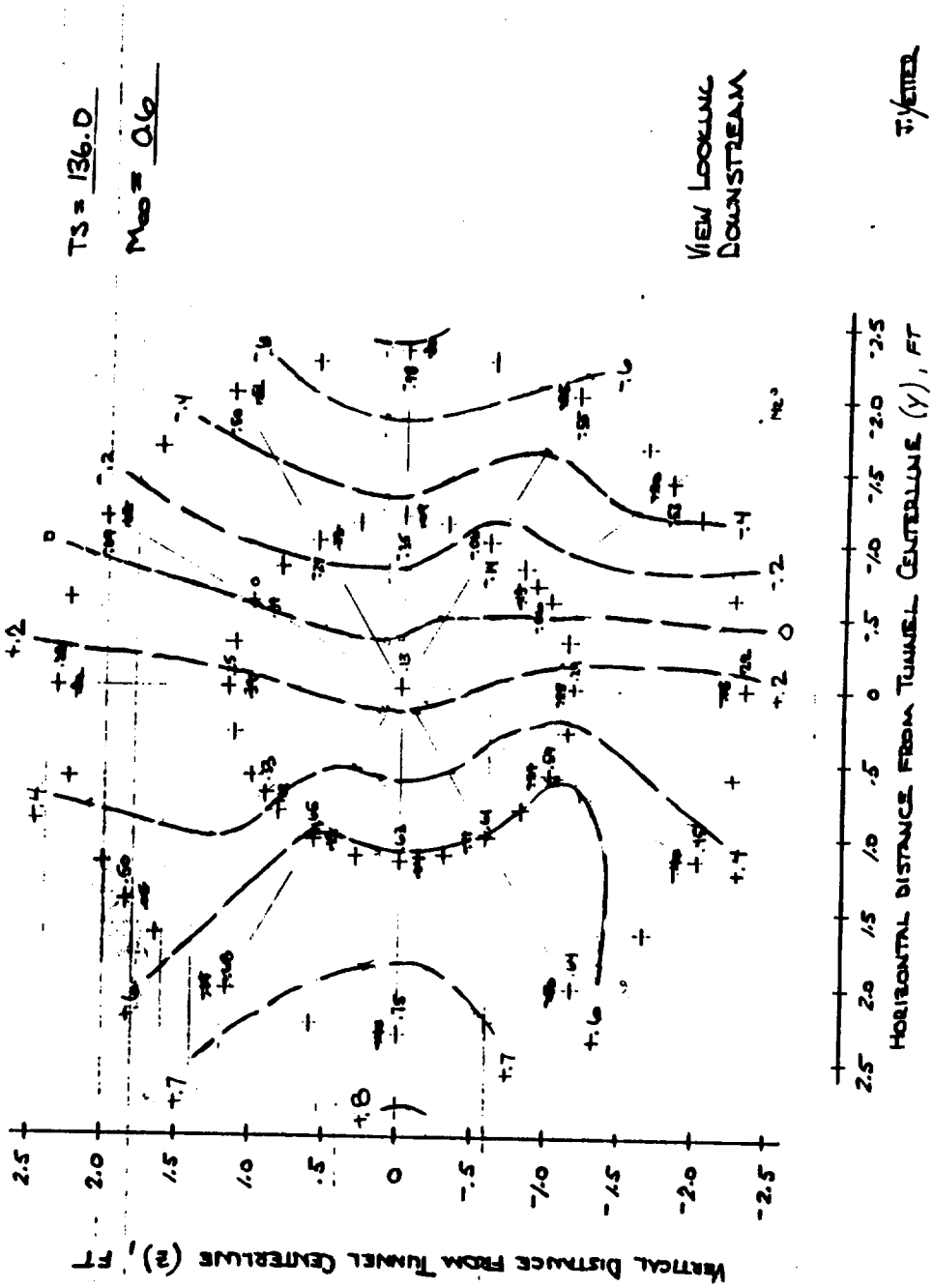

b. Sideflow angle contours at Mach 0.6.

Figure 35. - Continued.

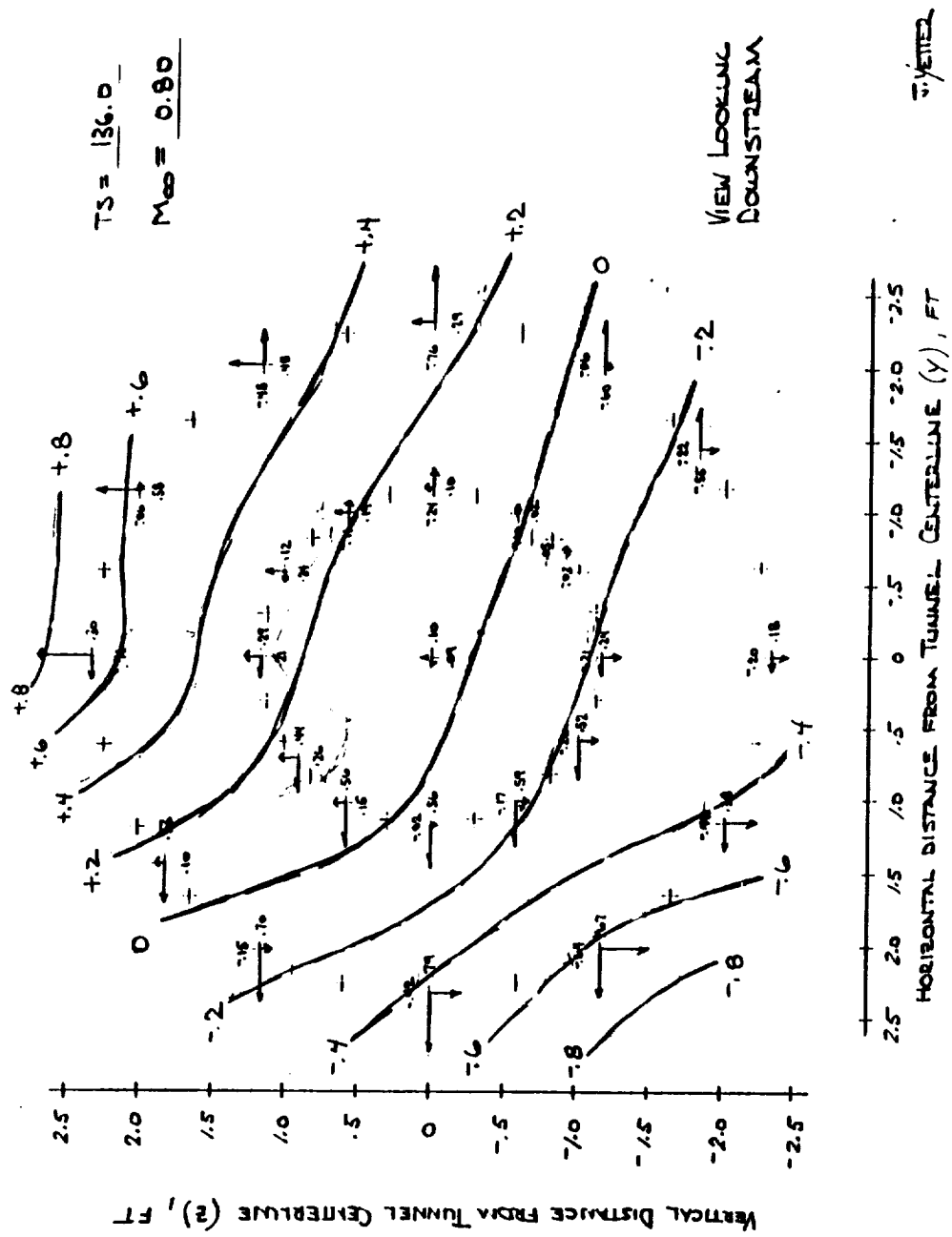

c. Upflow angle contours at Mach 0.8.

Figure 35. - Continued.

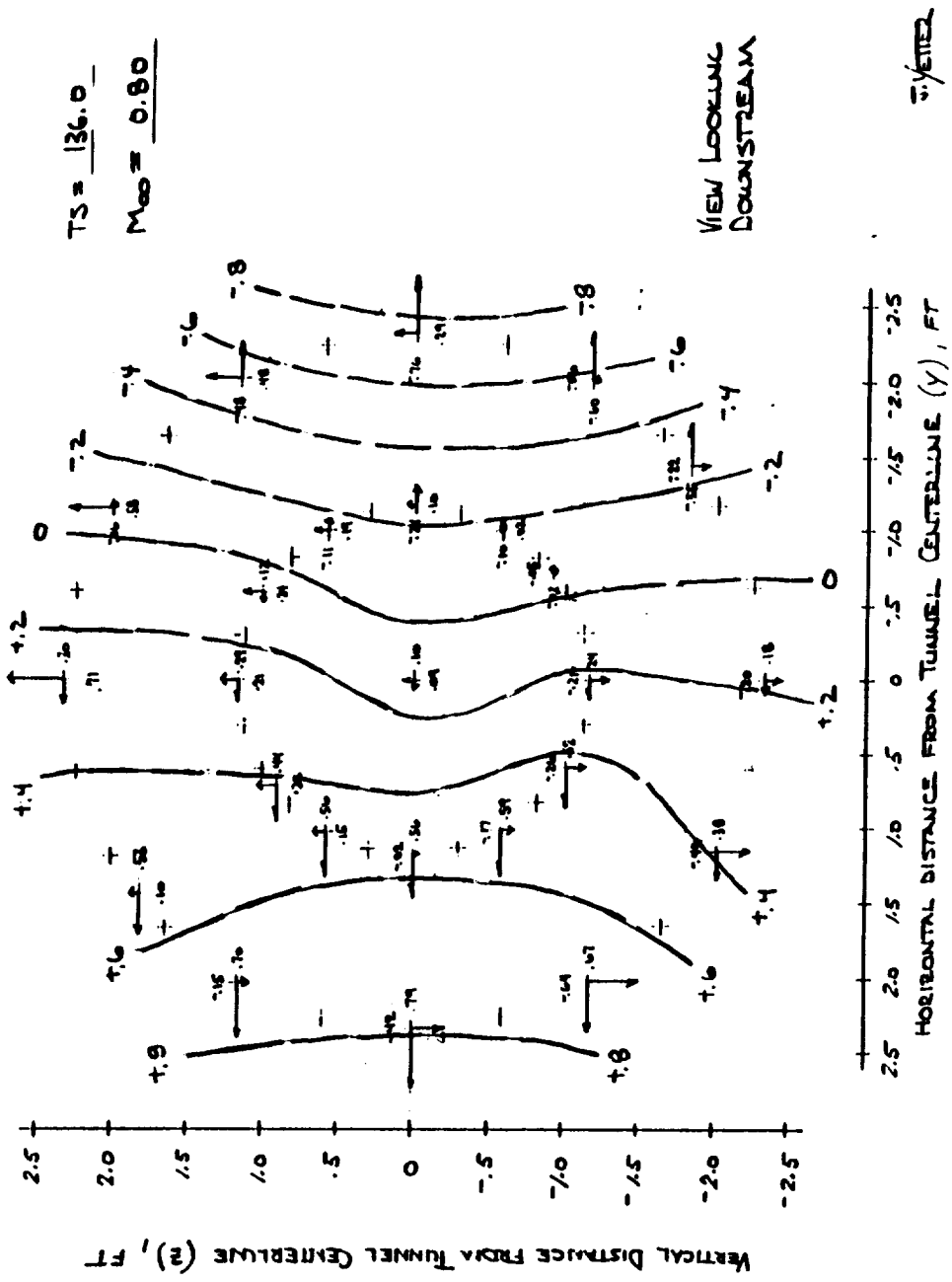

d. Sideflow angle contours, at Mach 0.8.

Figure 35. - Continued.

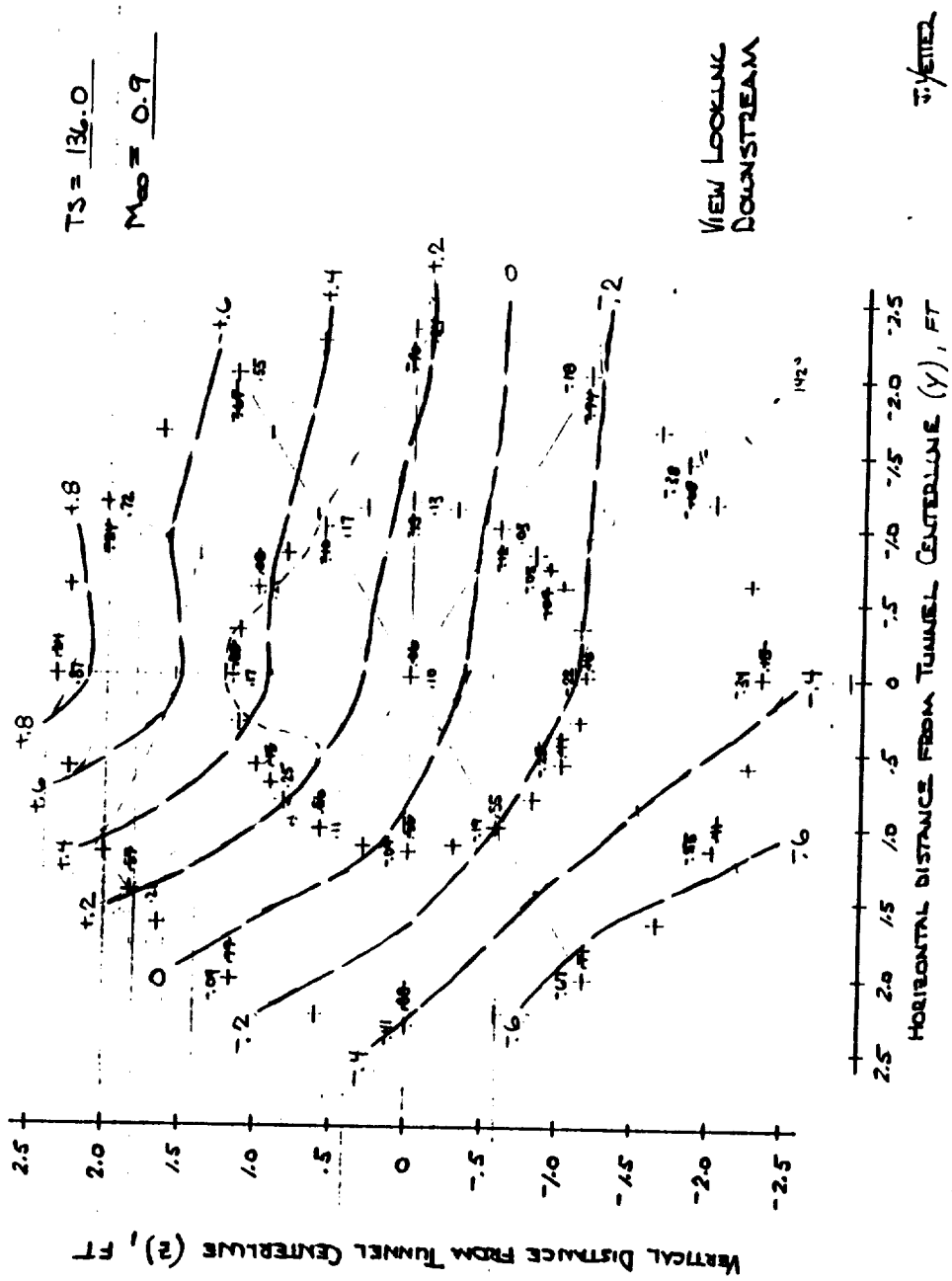

e. Upflow angle contours at Mach 0.9.

Figure 35. - Continued.

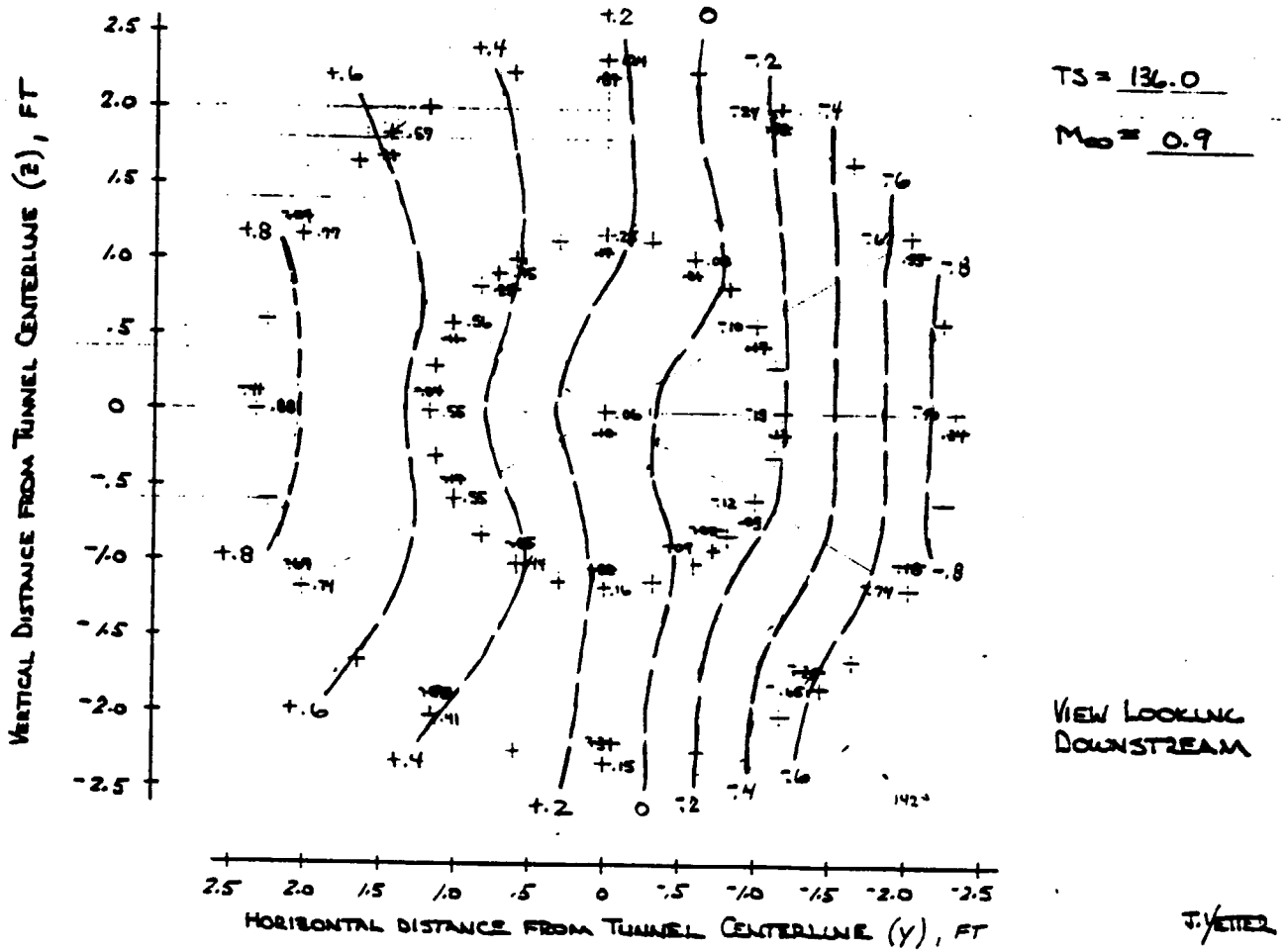

f. Sideflow angle contours at Mach 0.9.

Figure 35. - Concluded.

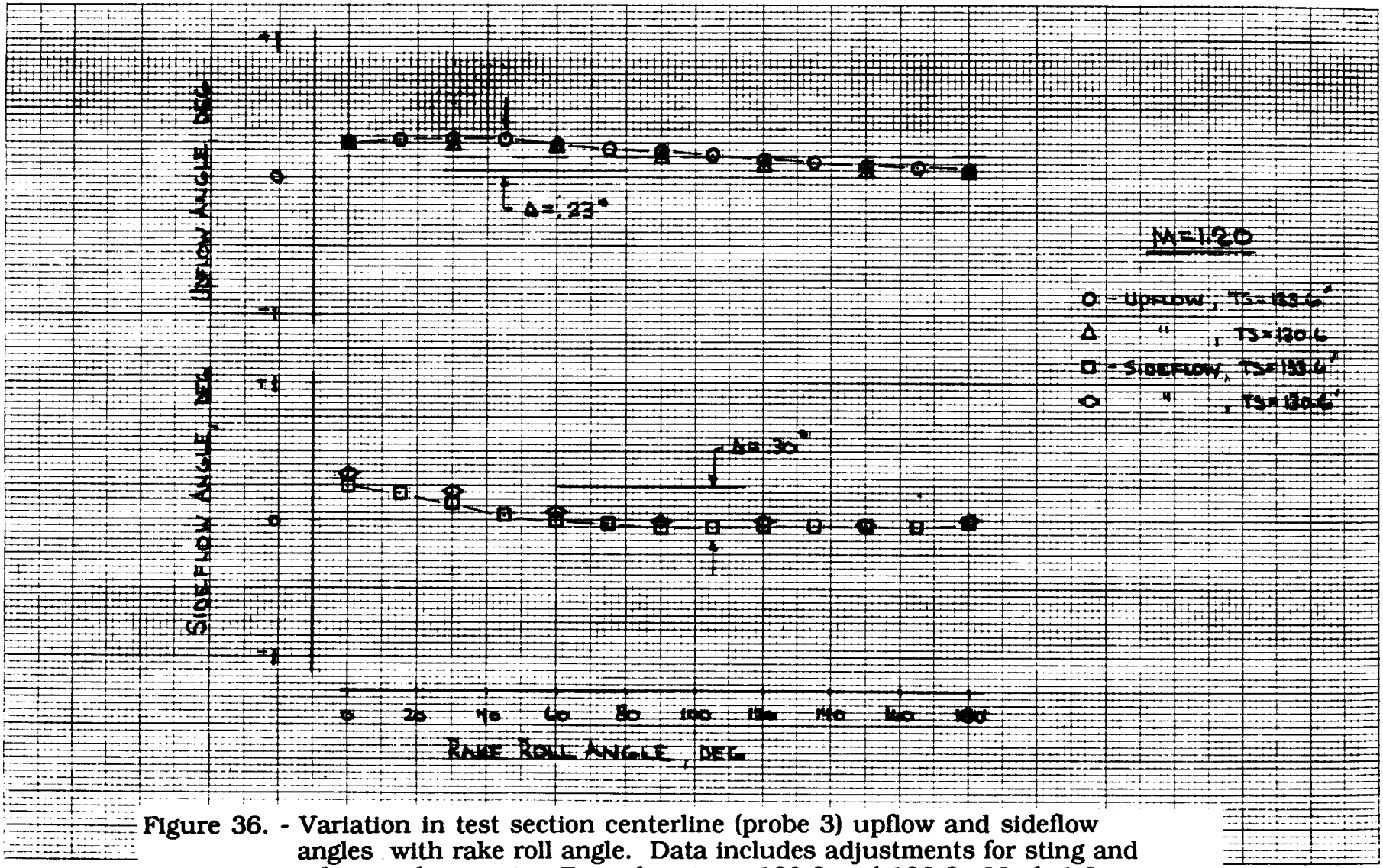

Figure 36. - Variation in test section centerline (probe 3) upflow and sideflow angles with rake roll angle. Data includes adjustments for sting and rake misalignments. Tunnel stations 130.6 and 133.6, Mach 1.2.

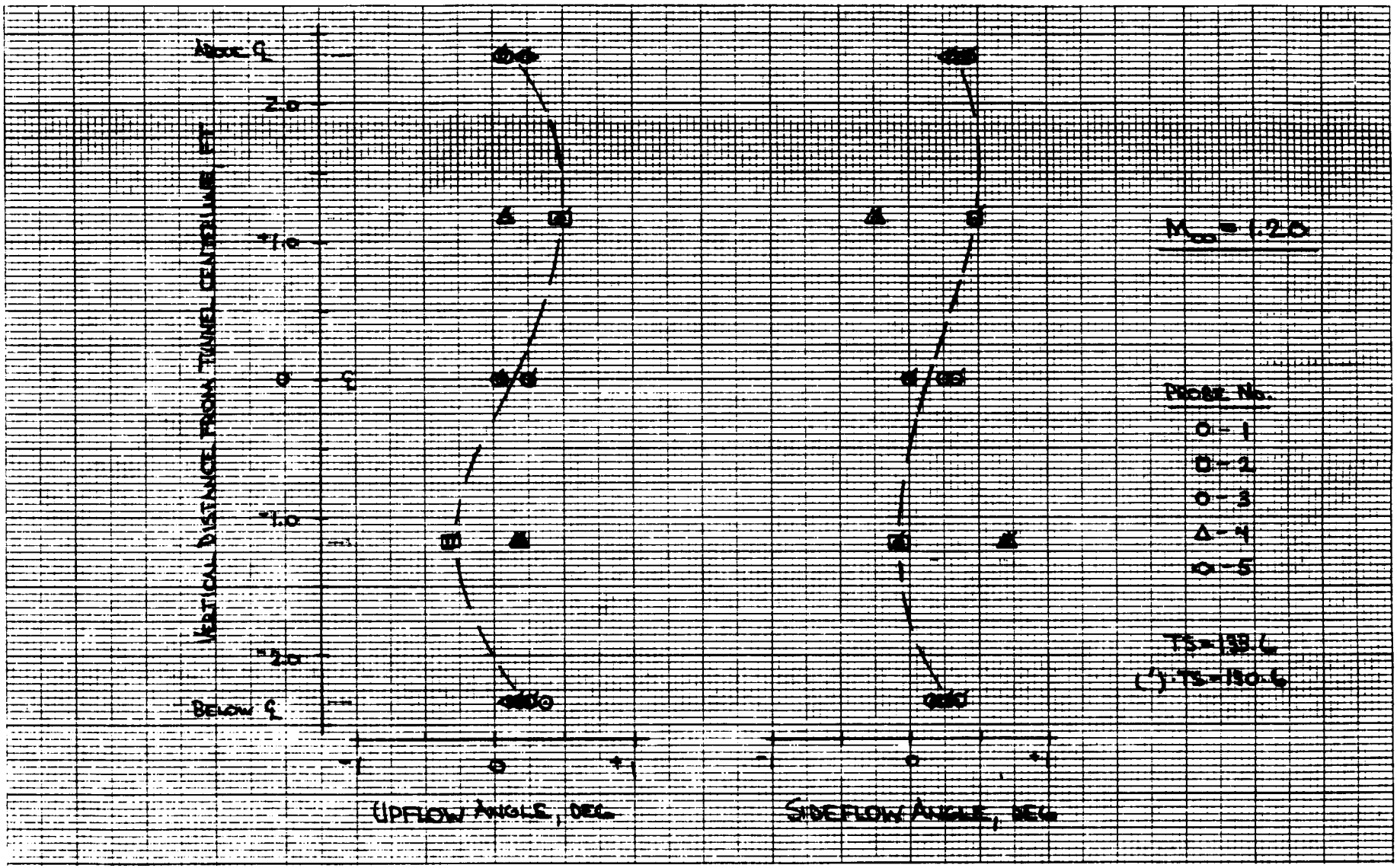

Figure 37. - Discrepancies in upflow and sideflow angles across vertical test section centerline at tunnel stations 130.6 and 133.6, and Mach 1.2.

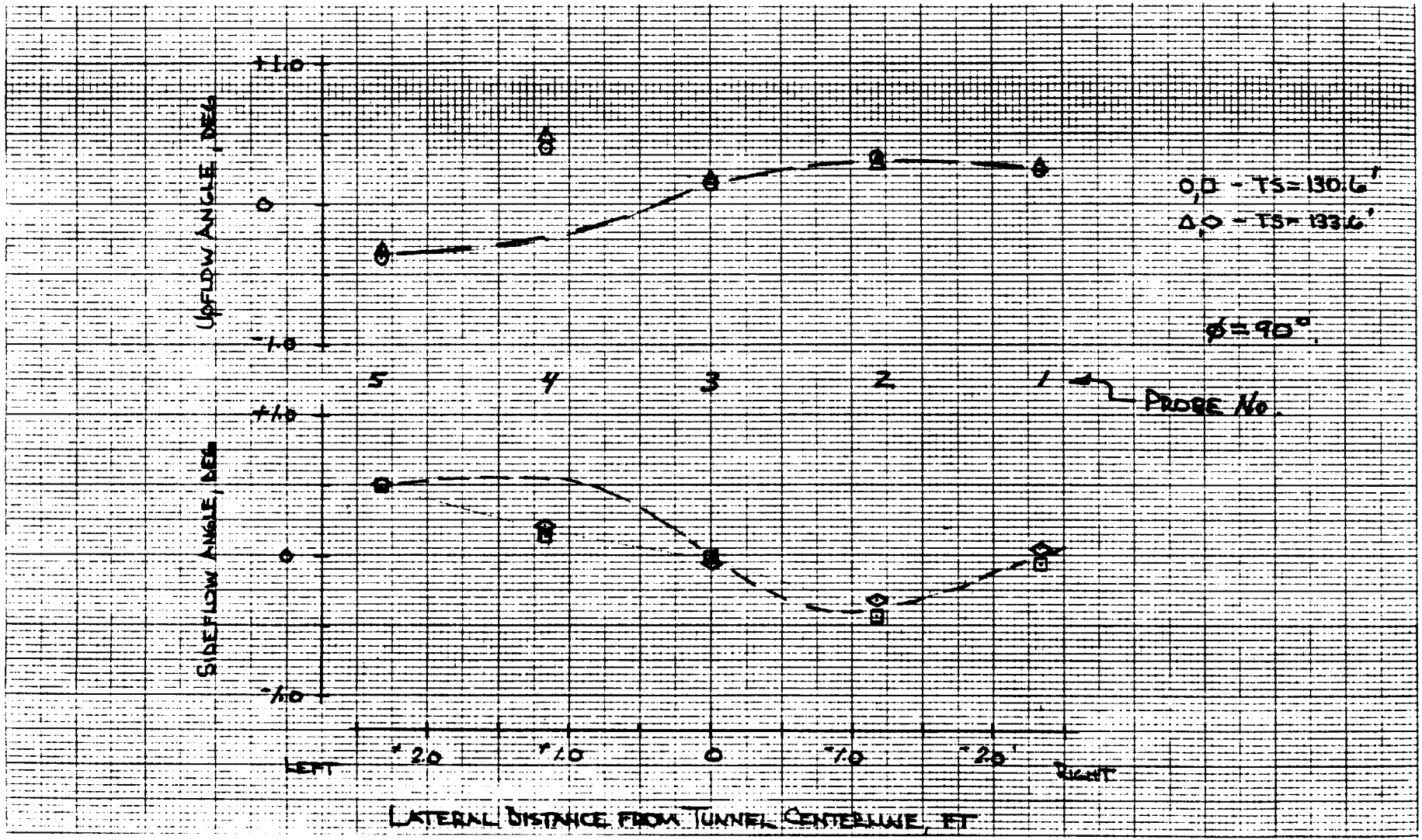

Figure 38. - Discrepancies in upflow and sideflow angles across horizontal test section centerline at tunnel stations 130.6 and 133.6, and Mach 1.2.

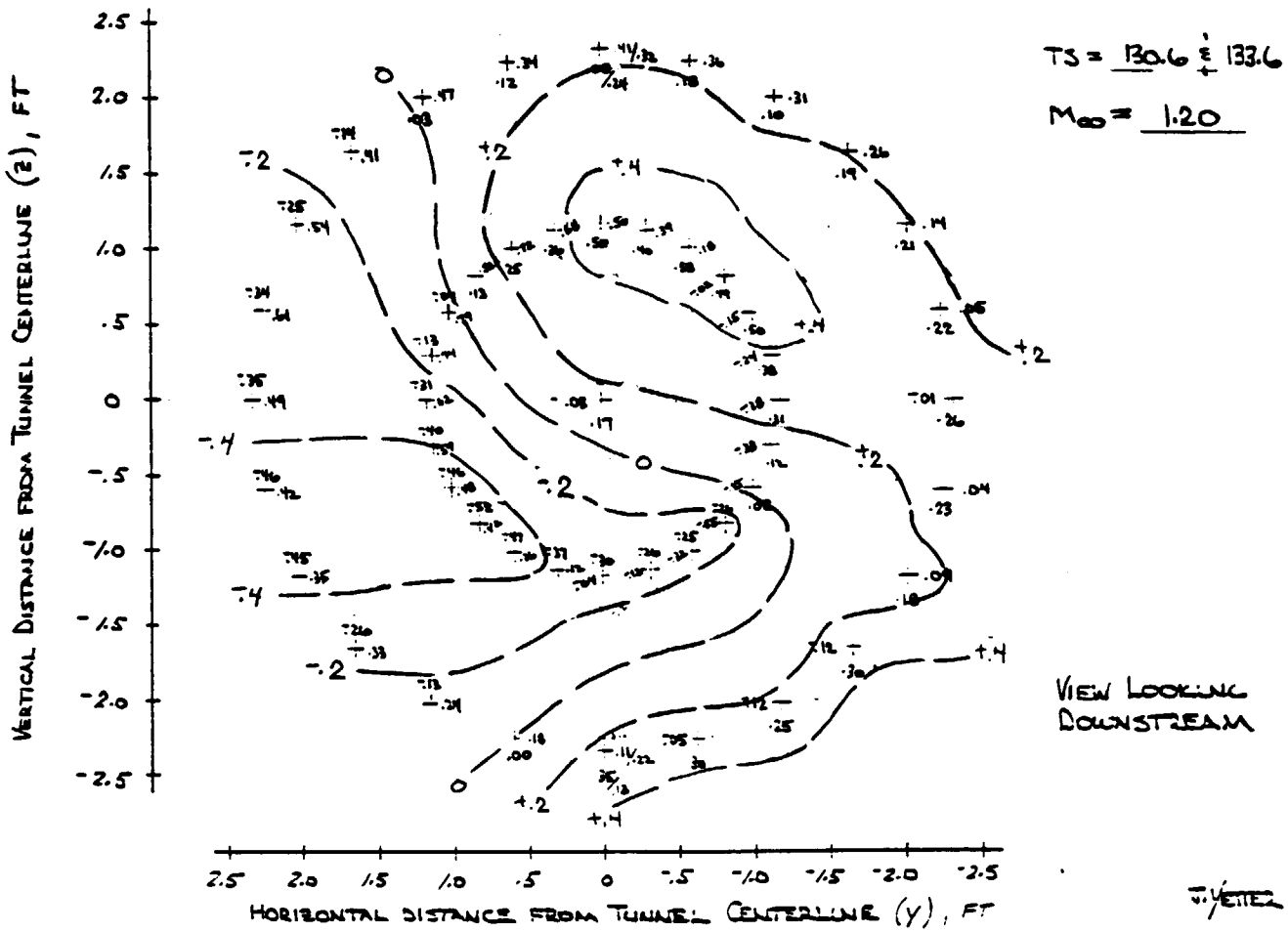

a. Upflow angle contours.

Figure 39. - Test section upflow and sideflow angle contours at Mach 1.2.

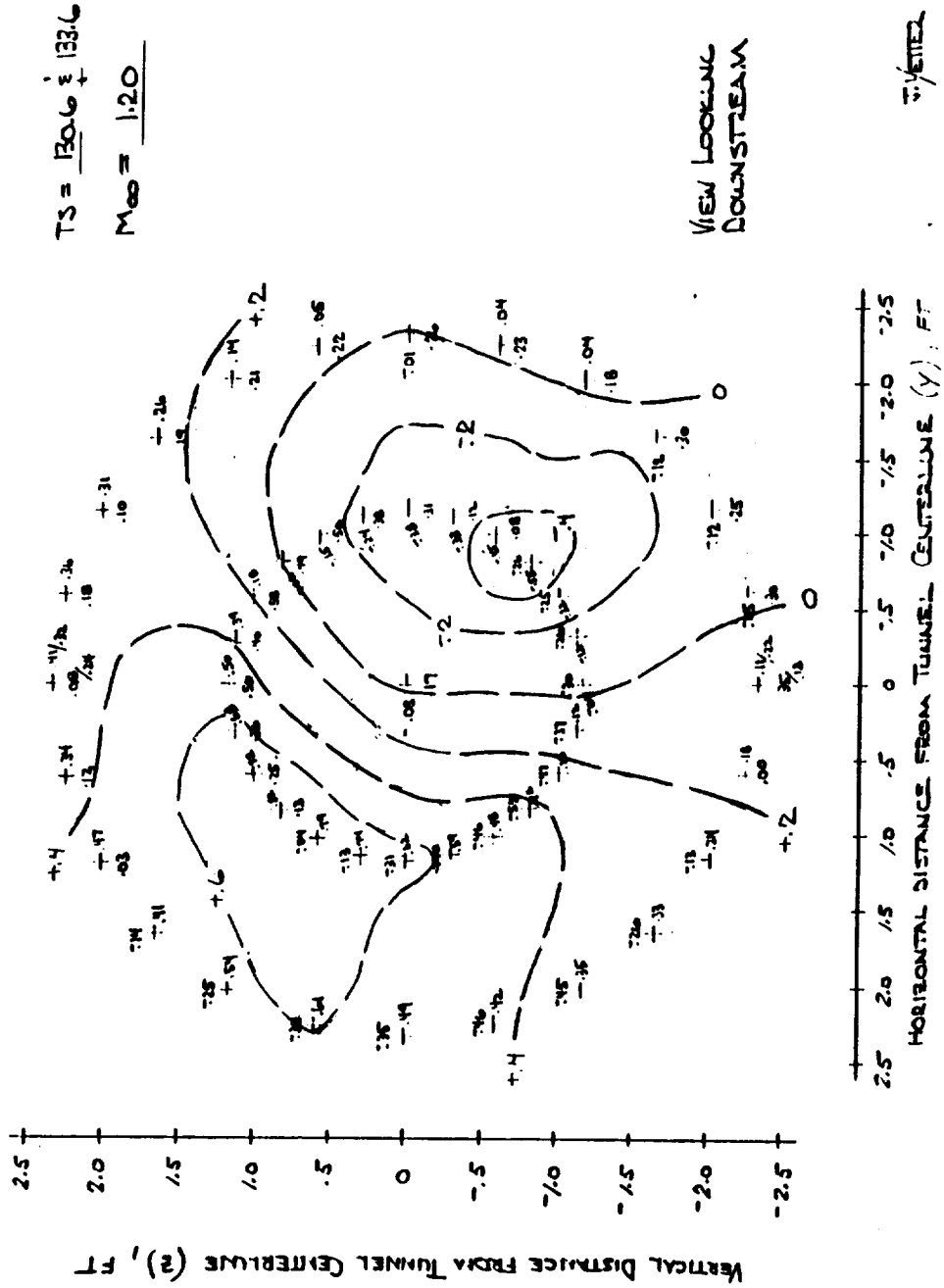

b. Sideflow angle contours.

Figure 39. - Concluded.

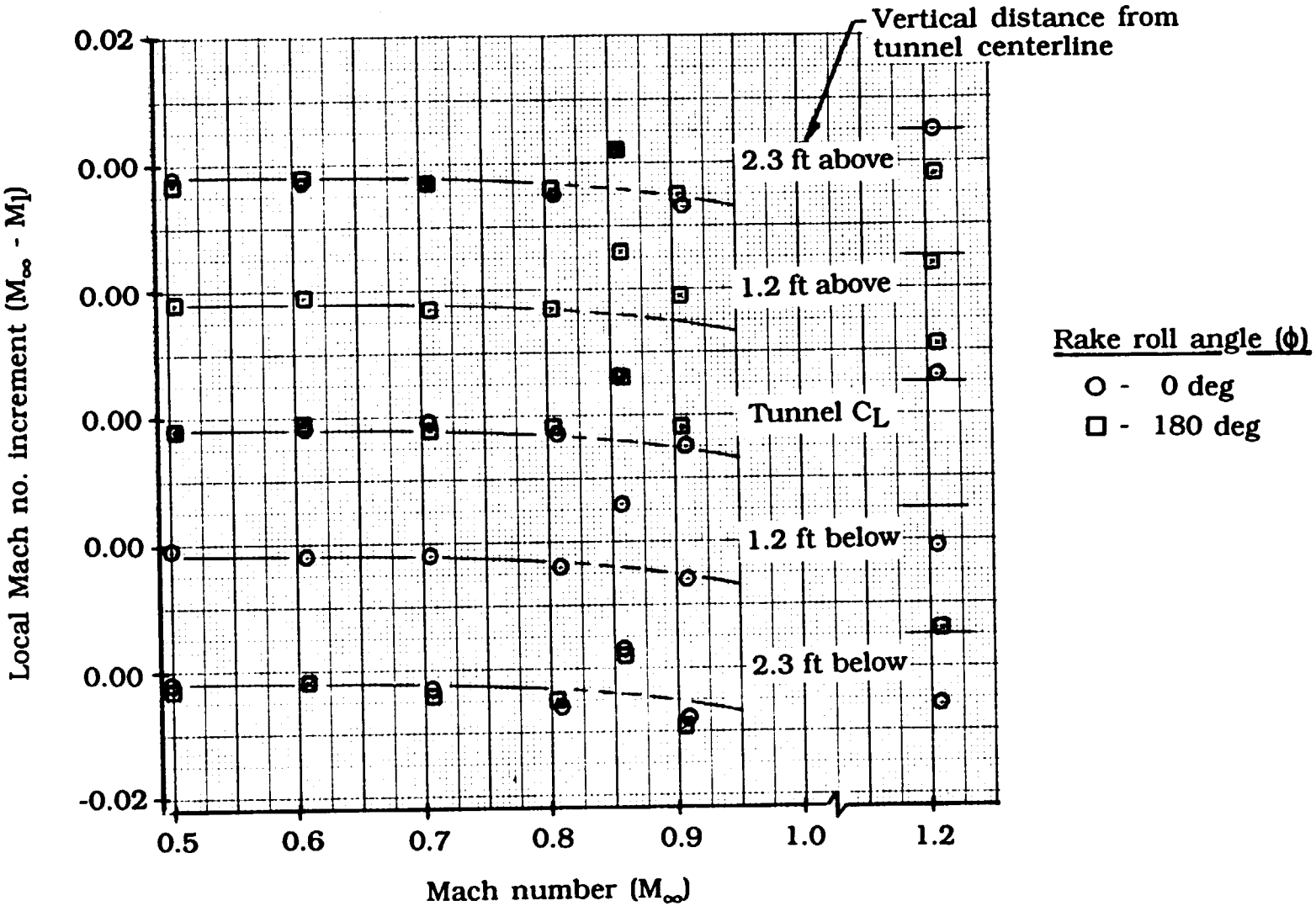

a.) Tunnel station 130.6

Figure 40. - Local test section Mach number increments across vertical plane containing tunnel centerline at tunnel stations 130.6, 133.6, and 136.0.

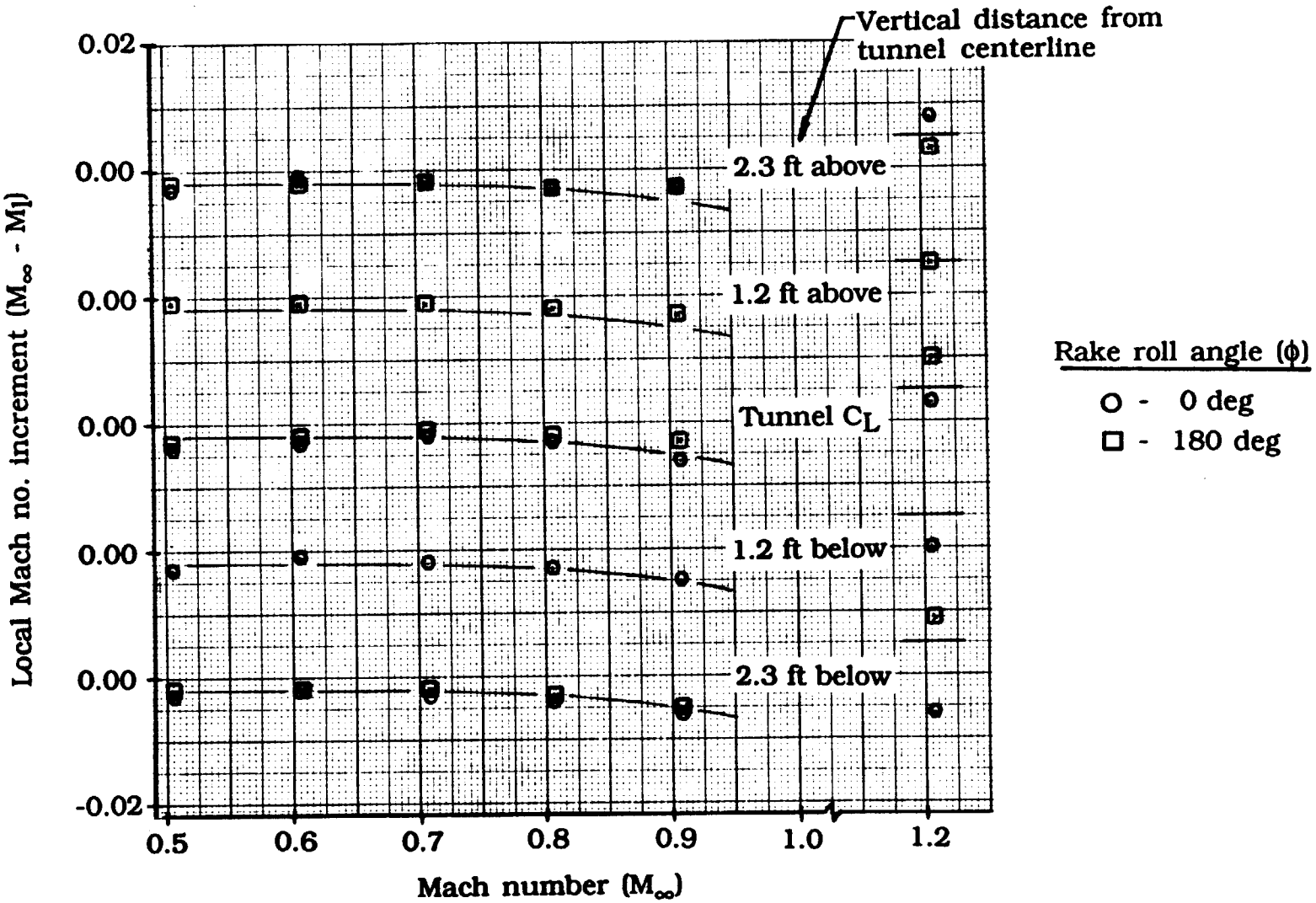

b.) Tunnel station 133.6

Figure 40. - Continued.

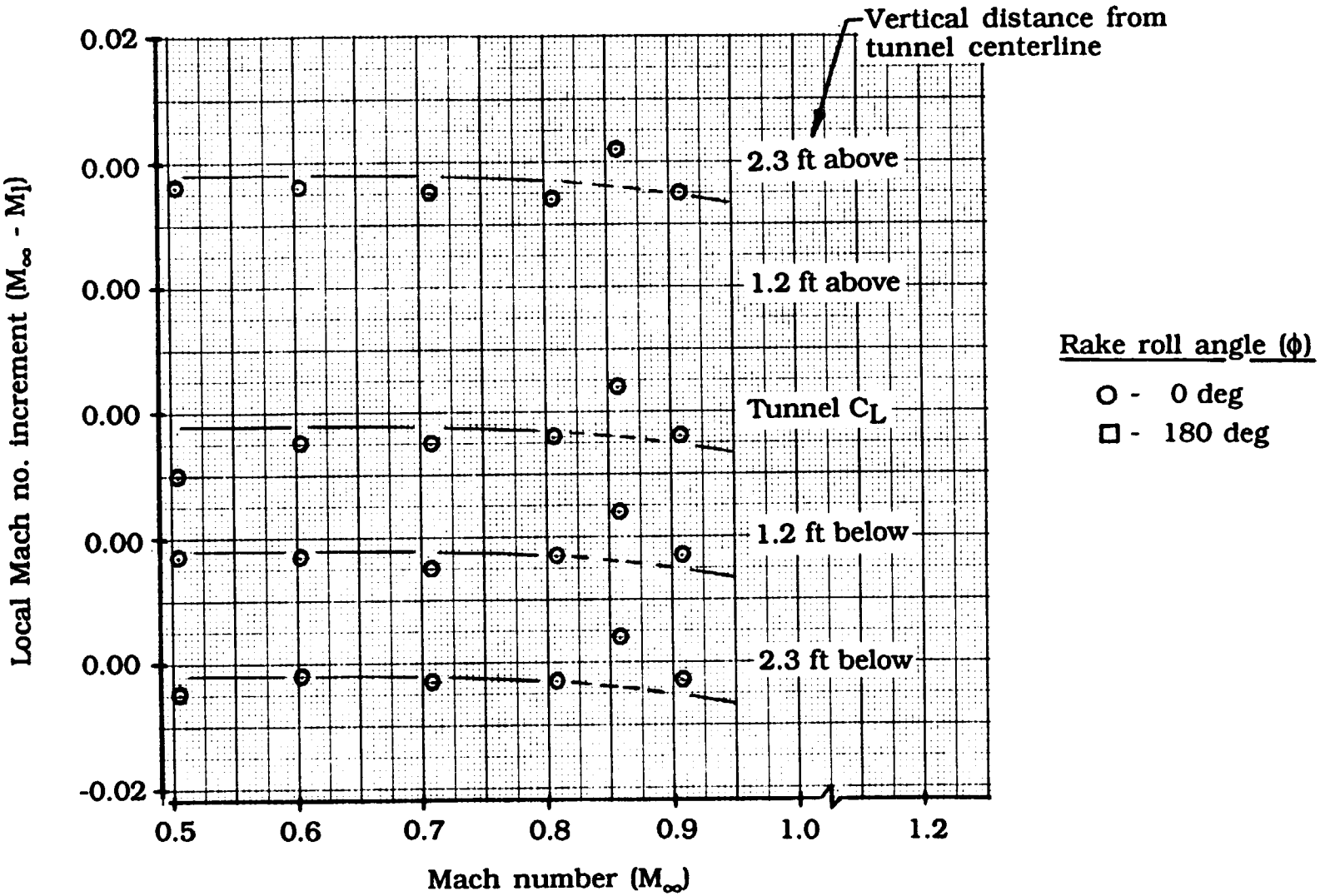

c.) Tunnel station 136.0

Figure 40. - Concluded.

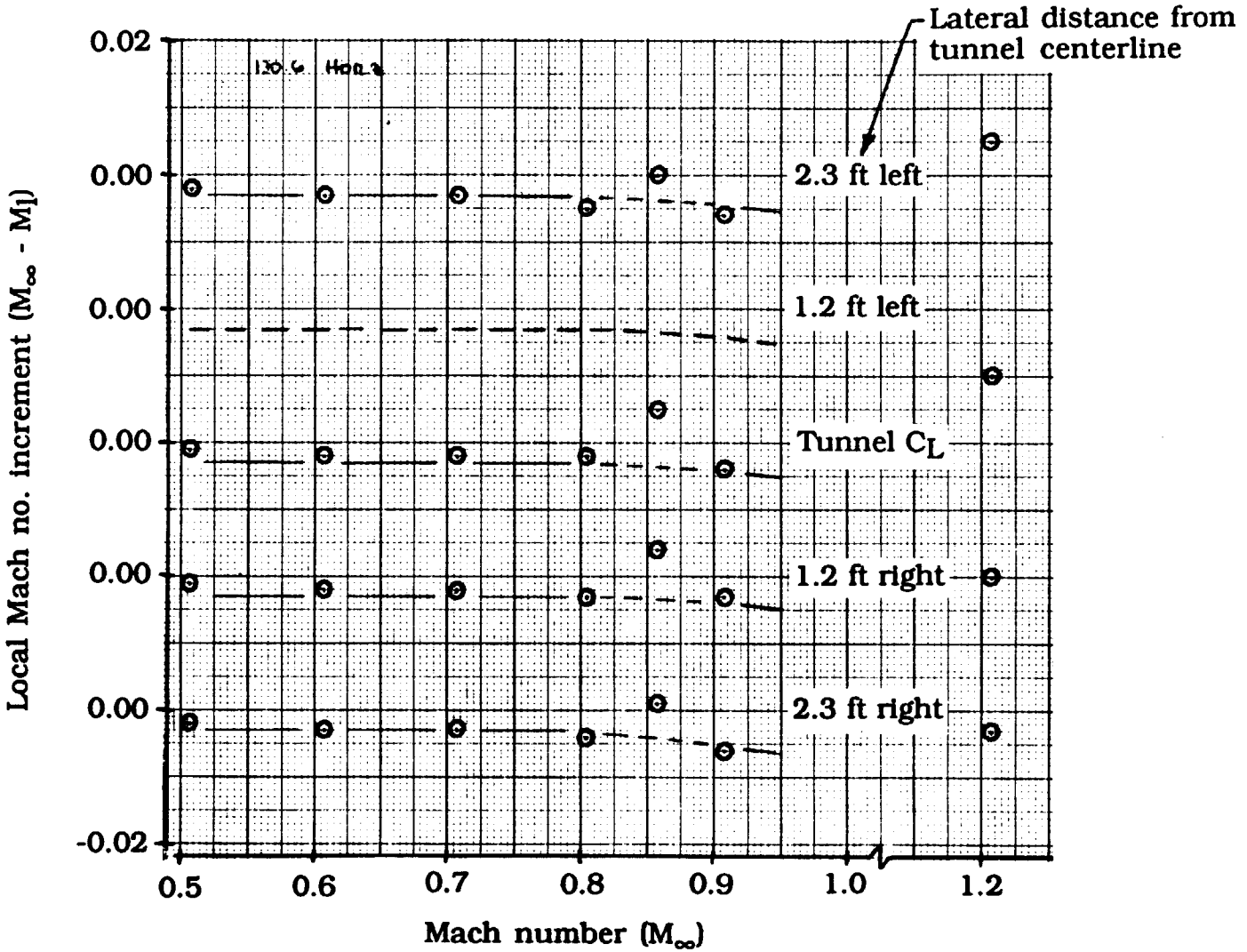

a.) Tunnel station 130.6

Figure 41. - Local test section Mach number increments across horizontal plane containing tunnel centerline at tunnel stations 130.6, 133.6, and 136.0. Data taken with rake rolled to horizontal (ϕ = 90 deg).

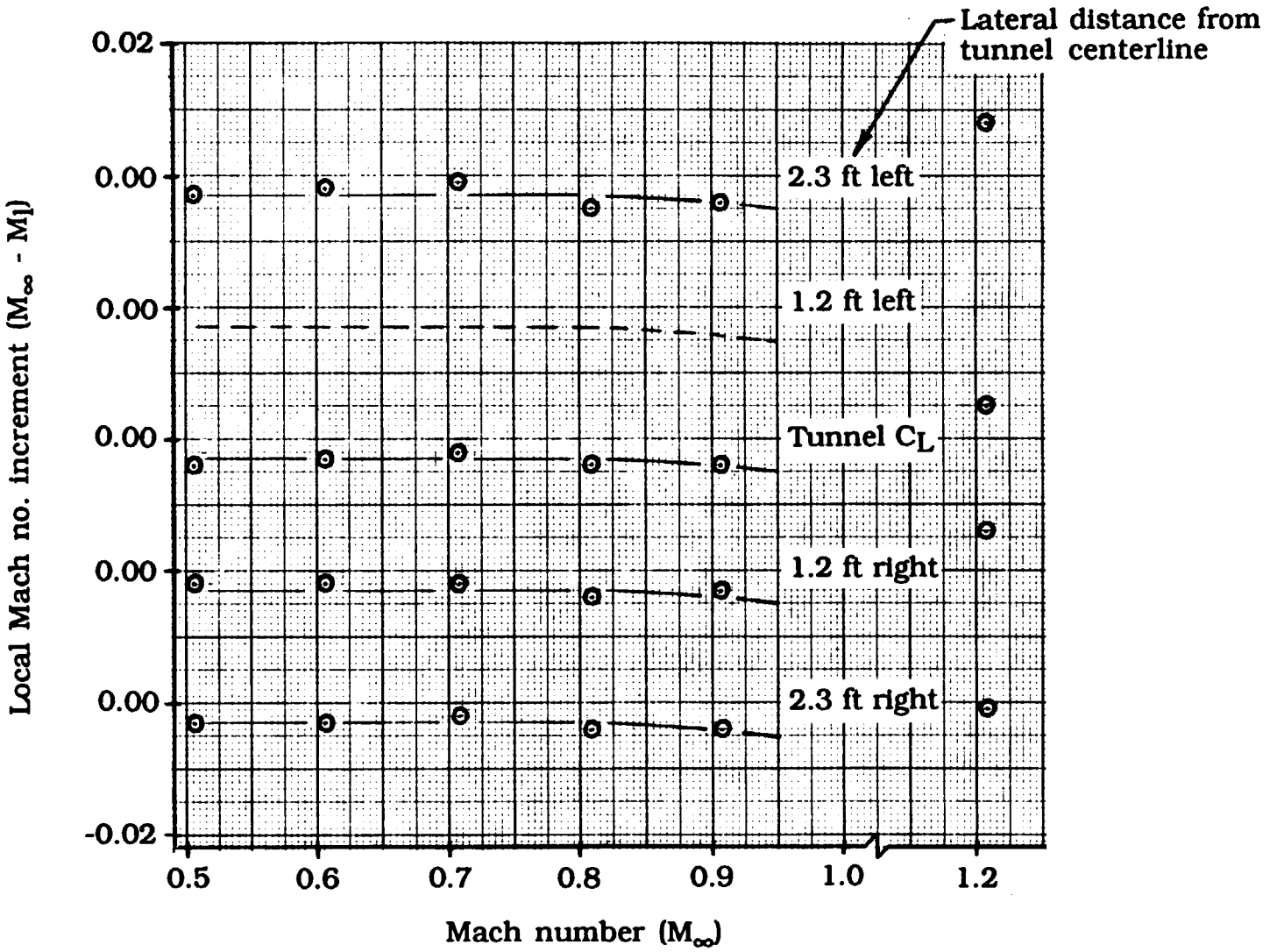

b.) Tunnel station 133.6

Figure 41. - Continued.

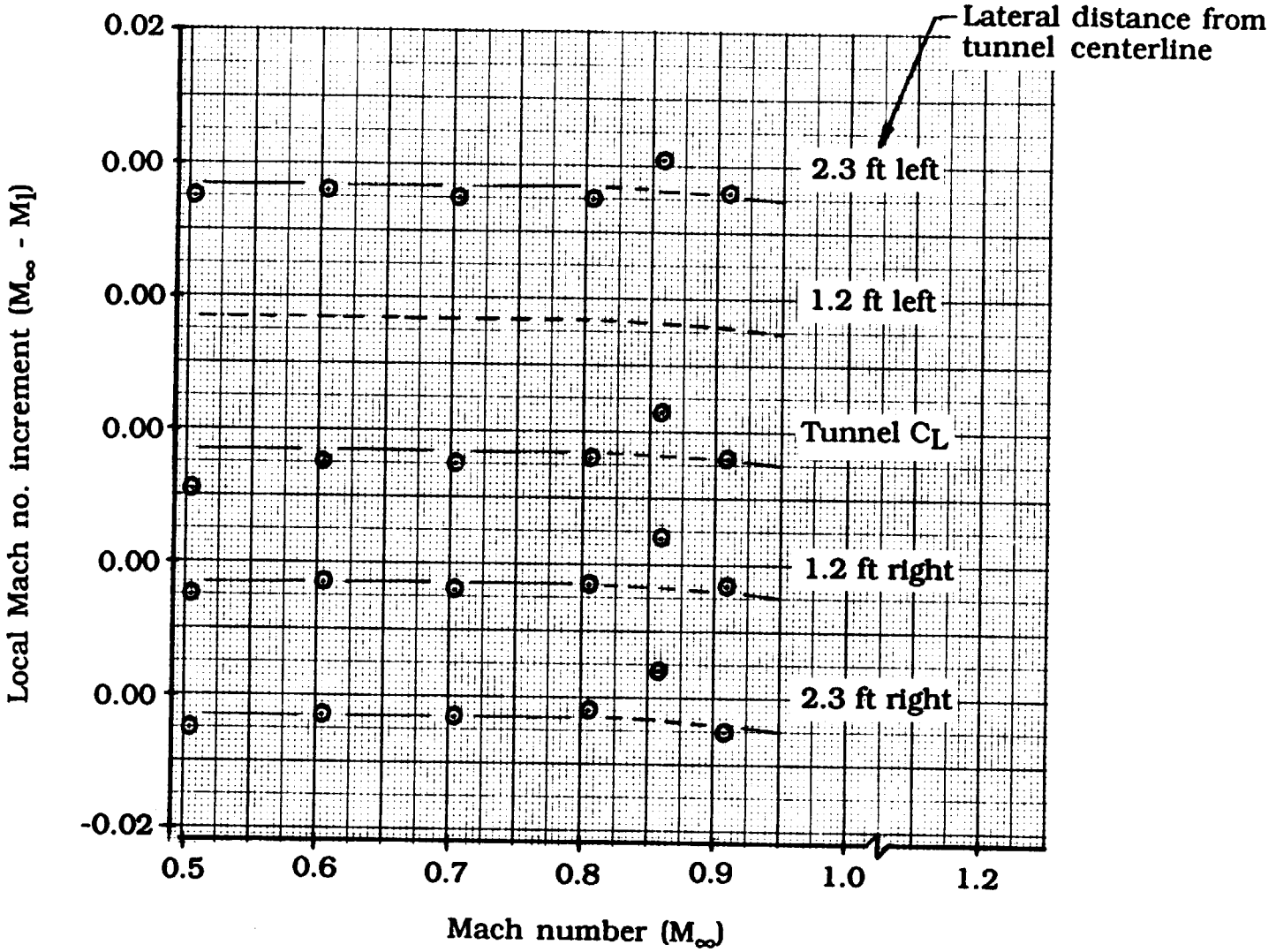

c.) Tunnel station 136.0

Figure 41. - Concluded.

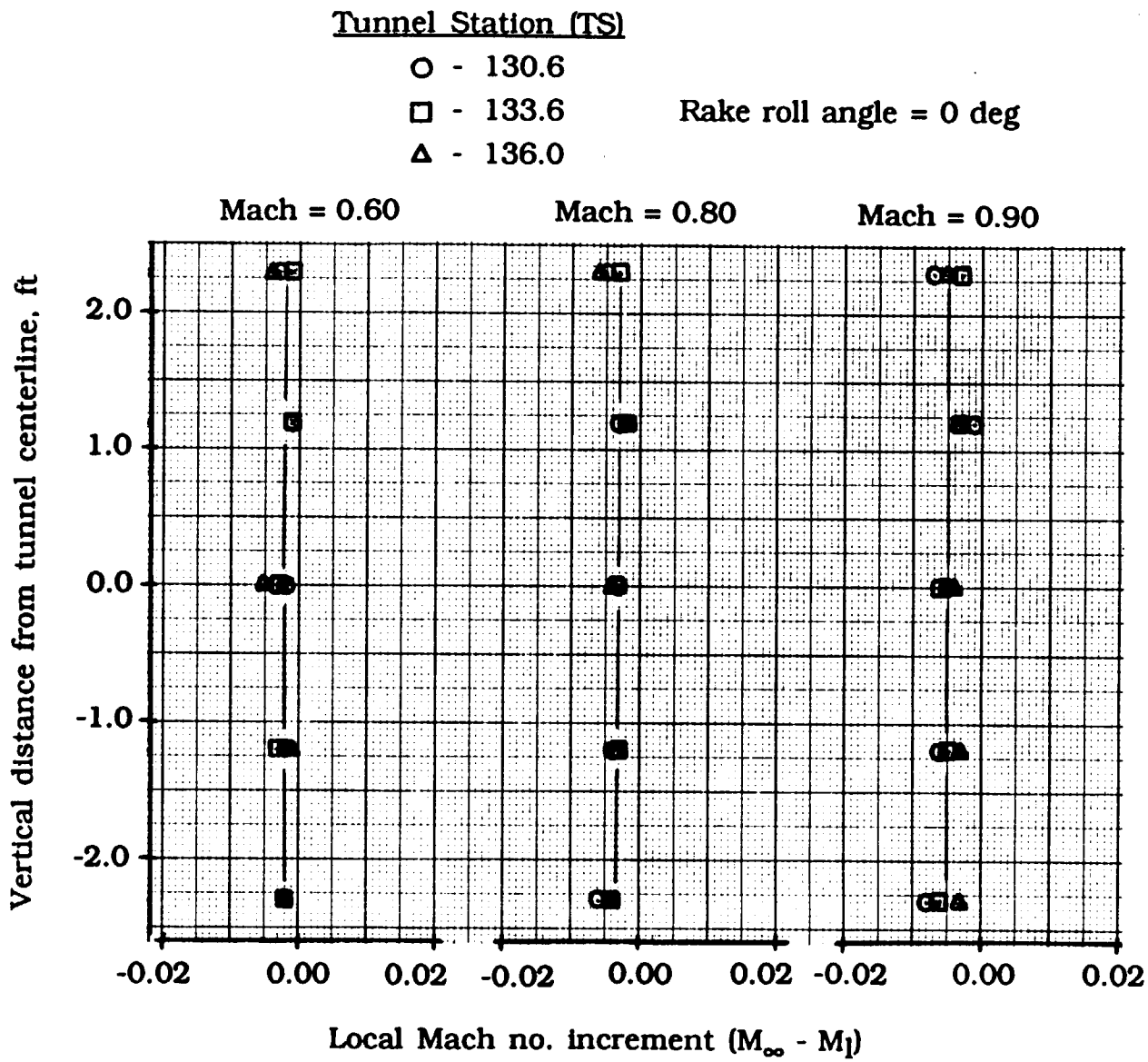

Figure 42. - Cross-plot of test section Mach number increments across the vertical centerline at tunnel stations 130.6, 133.6 and 136.0.

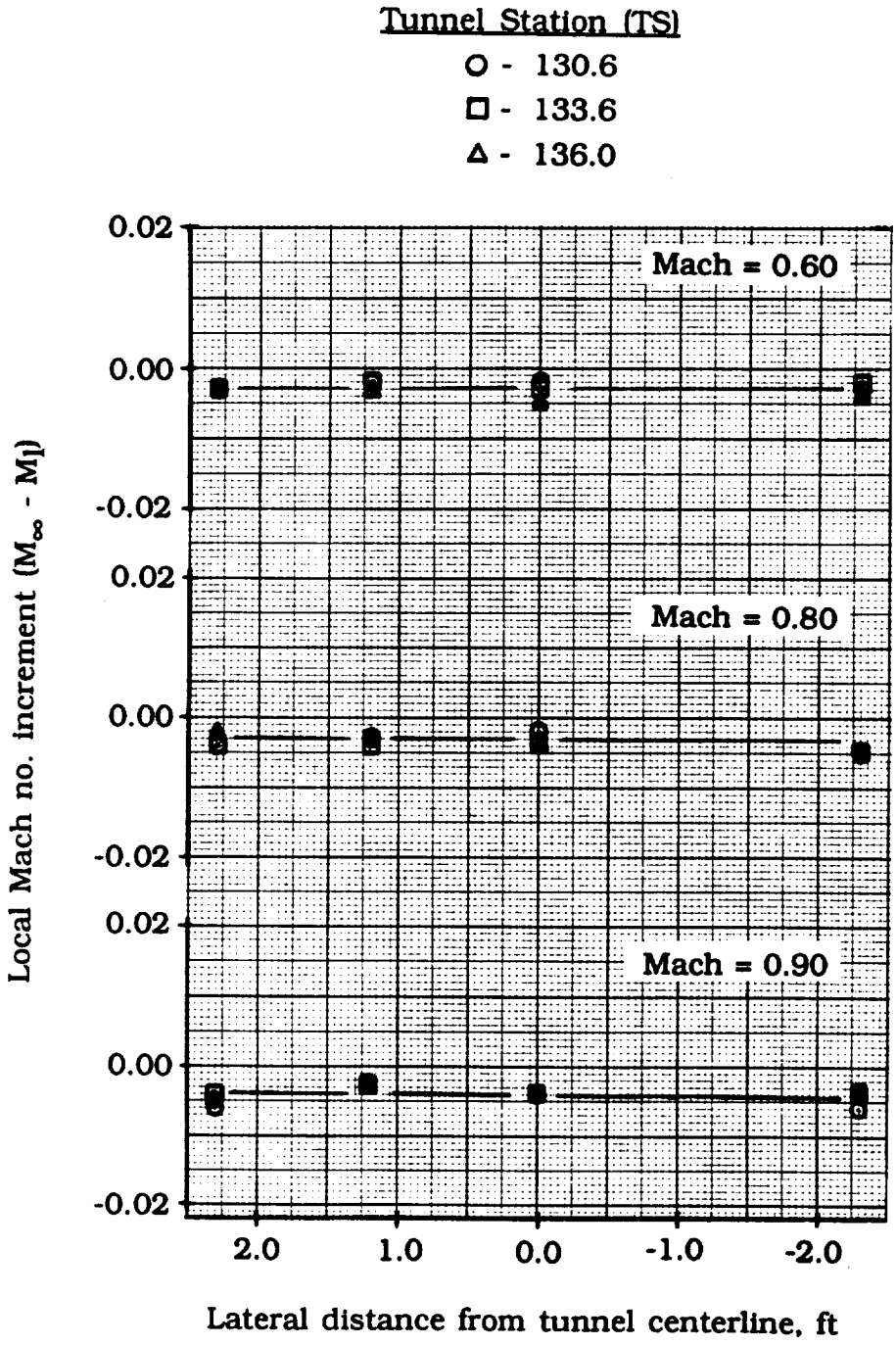

Figure 43. - Cross-plot of test section Mach number increments across the horizontal (lateral) centerline at tunnel stations 130.6, 133.6 and 136.0.

REPORT DOCUMENTATION PAGE

Form Approved
OMB No. 0704-0188

1. AGENCY USE ONLY (*Leave blank*)	2. REPORT DATE	3. REPORT TYPE AND DATES COVERED
	December 1994	Technical Memorandum

4. TITLE AND SUBTITLE
16-Foot Transonic Tunnel Test Section Flowfield Survey

5. FUNDING NUMBERS
WU 538-05-13-01

6. AUTHOR(S)
Jeffrey A. Yetter and William K. Abeyounis

7. PERFORMING ORGANIZATION NAME(S) AND ADDRESS(ES)
NASA Langley Research Center
Hampton, VA 23681-0001

8. PERFORMING ORGANIZATION REPORT NUMBER

9. SPONSORING / MONITORING AGENCY NAME(S) AND ADDRESS(ES)
National Aeronautics and Space Administration
Washington, DC 20546-0001

10. SPONSORING / MONITORING AGENCY REPORT NUMBER
NASA TM-109157

11. SUPPLEMENTARY NOTES

12a. DISTRIBUTION / AVAILABILITY STATEMENT
Unclassified - Unlimited

Subject Category 09

12b. DISTRIBUTION CODE

13. ABSTRACT (*Maximum 200 words*)

A flow survey has been made of the test section of the NASA Langley Research Center 16-Foot Transonic Tunnel at subsonic and supersonic speeds. The survey was performed using five five-hole pyramid-head probes mounted at 14 inch intervals on a survey rake. Probes were calibrated at freestream Mach numbers from 0.50 to 0.95 and from 1.18 to 1.23. Flowfield surveys were made at Mach numbers from 0.50 to 0.90 and at Mach 1.20. The surveys were made at tunnel stations 130.6, 133.6, and 136.0. By rotating the survey rake through 180 degrees, a cylindrical volume of the test section 4.7 feet in diameter and 5.4 feet long centered about the tunnel centerline was surveyed. Survey results showing the measured test section upflow and sideflow characteristics and local Mach number distributions are presented. The report documents the survey probe calibration techniques used, summarizes the procedural problems encountered during testing, and identifies the data discrepancies observed during the post-test data analysis.

14. SUBJECT TERMS	15. NUMBER OF PAGES
LaRC 16-Foot Tunnel and Flowfield Survey.	91
	16. PRICE CODE: A05

17. SECURITY CLASSIFICATION OF REPORT	18. SECURITY CLASSIFICATION OF THIS PAGE	19. SECURITY CLASSIFICATION OF ABSTRACT	20. LIMITATION OF ABSTRACT
Unclassified	Unclassified	Unclassified	